GiD 2006
3rd Conference on Advances and Applications of GiD

M. Pasenau, R. Ribó, E. Escolano
J. Suit and A. Coll (Eds.)

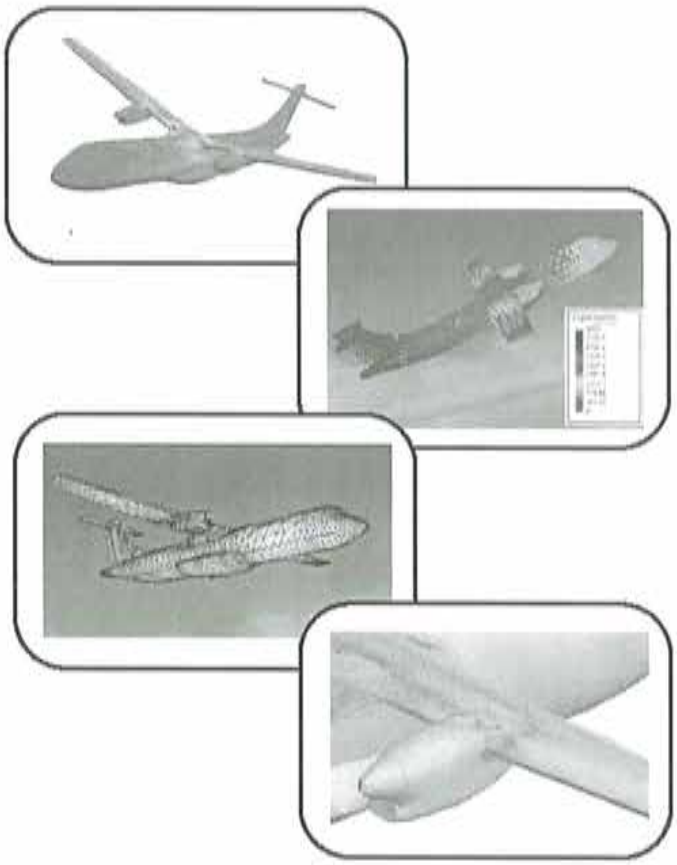

Monograph CIMNE Nº-94, March 2006

GiD 2006
3rd Conference on Advances and Applications of GiD

M. Pasenau, R. Ribó, E. Escolano
J. Suit and A. Coll (Eds.)

Monograph CIMNE Nº-94, March 2006

INTERNATIONAL CENTER FOR NUMERICAL METHODS IN ENGINEERING
Gran Capitán s/n, 08034 Barcelona, Spain

INTERNACIONAL CENTER FOR NUMERICAL METHODS IN ENGINEERING
Edificio C1, Campus Norte UPC
Gran Capitán s/n
08034 Barcelona, Spain
www.cimne.upc.es

First edition: March 2006

GID 2006, 3rd Conference on Advances and Applications of GID
Monograph CIMNE M94

ISBN: 84-95999-90-0

Depósito legal: B-14312-2006

3rd Conference on Advances and Applications of GiD Index

Keynote Lectures

Contributed Papers

Keynote Lectures

RECENT ADVANCES IN UNSTRUCTURED MESH AND OBJECT GENERATION

R. Löhner

School of Computational Sciences
M.S. 4C7, George Mason University, Fairfax, VA 22030-4444, USA

SUMMARY: Recent developments in mesh and point generation are reviewed. These include: minimal input meshing, fast meshing for very large problems, volume-to-surface meshing and the generation of clouds of arbitrary objects. Several examples are included to illustrate the effectiveness of the developed techniques.

KEYWORDS: Unstructured Grid Generation, Volume-to-Surface Meshing, Point and Object Generation

1. INTRODUCTION

Field solvers based on unstructured grids play an ever increasing role in physics and engineering. Presently, all of the large-scale commercial software packages in Computational Structural Dynamics (CSD), Computational Fluid Dynamics (CFD) and Computational Thermodynamics (CTD) are based on finite element or finite volume methods operating on unstructured grids. The relentless advance in the physical complexity that may be modeled by these codes, together with increases in algorithmic efficiency and computer power, have placed a premium on minimum-input, reliable, automatic generation of grids for complex geometries that are suitable for the problem at hand. The present paper reviews some recent developments in this direction. The first topic discussed is minimal input meshing, a subject that has come to the forefront as the geometries modeled become ever more complex. The second topic is concerned with fast meshing for very large problems, focusing on optimal space-filling tetrahedra and so-called stencil meshing. The third topic describes some recent developments in volume-to-surface meshing. Finally, as a fourth topic, the generation of clouds of arbitrary objects is discussed.

2. MINIMAL INPUT MESHING

The ability to generate unstructured grids with arbitrary element size distributions in space immediately places the burden of specifying the desired element size on the user. This freedom of being able to specify and arbitrary element size can, for many complex-geometry cases, become an onerous, labour-intensive task. Ideally, the elements should conform to the geometrical complexity of the surfaces **without** leading to overall grid sizes that are impossible to handle by the solvers. Manual input options for element size commonly used (and provided by pre-processors) include background grids, sources,

and element size linked to CAD entities (points, lines, surfaces, bodies, domains, ...) [Löh01a]. Adaptive background grid refinement may be employed in order to reduce the amount of user intervention to a minimum. As with any other mesh refinement scheme, one has to define **where** to refine and **how** to refine.

2.1 Cloud of Points

Assuming that we do not have any previous knowledge about the physics of the problem at hand, the only criteria for mesh size are based on resolving the geometry at hand. The two main aspects to this general question are:

- Resolution of Surface Curvature; and
- Resolution of Gaps.

Several techniques have been proposed to define the desired element size in space [Löh01a]. The simplest approach is to obtain a surface mesh, measure the element size vis a vis surface curvature and gaps, and then define a new, desired element size based on the actual versus desired values. This is done repeatedly in an iterative loop, until the actual and desired resolutions coincide.

One can avoid the iterative loop by using a relatively fine cloud of points generated for each surface. At each point, the desired element size is defined based on the surface curvature and gaps.

2.2 Background Mesh Refinement

Because of its very high speed, classic h-refinement [Löh92] is used to subdivide background grid elements. The selection as to where to refine the background mesh is made with the following assumptions:

a) Points have already been generated;

b) At each of these points, a value for the characteristic or desired element size δ is given;

c) For each of these points, the background grid element containing it is known;

d) A desired increase factor c_i between elements is known.

The refinement selection is then made in two passes (see Figure 2.1):

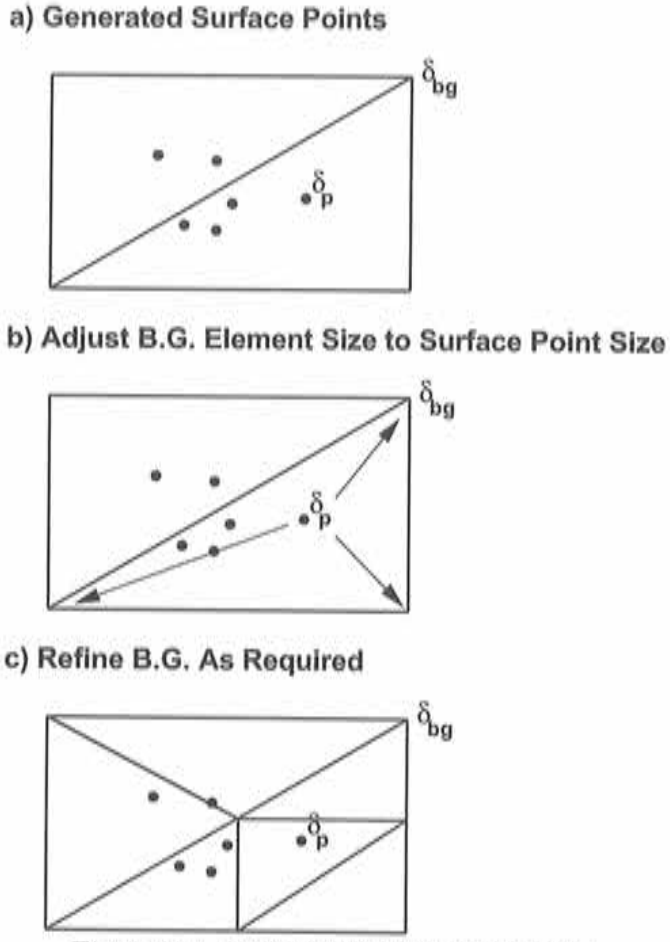

Figure 2.1 Background Grid Refinement

Pass 1: Background Grid Adjustment

Suppose a background grid element has very large element sizes defined at its nodes. If it contains a generated point with characteristic length that is much smaller, an incompatibility is present. The aim of this first pass is to prevent these incompatibilities by comparing lengths. Given a set of two points with coordinates $\mathbf{x}_1, \mathbf{x}_2$, as well as an element length parameter δ_1, the maximum allowable element length at the second point may be determined from the geometric progression formula:

$$s_n = |\mathbf{x}_2 - \mathbf{x}_1| = \delta_1 \frac{c_i^{n+1} - 1}{c_i - 1} \tag{2.1}$$

implying

$$\delta_2^* = \delta_1 c_i^n = \frac{s_n(c_i - 1) + \delta_1}{c_i} \tag{2.2}$$

Given this constraint, one compares the characteristic length of each of the generated points with the element size defined at each of the background grid nodes of the background grid element containing it:

$$\delta_{bg} = \min\left(\delta_{bg}, \delta_p^*(\mathbf{x}_{bg} - \mathbf{x}_p)\right) \quad . \tag{2.3}$$

Pass 2: Selection of Elements to be Refined

After the element lengths at the points of the background grid have been made compatible with the lengths of the actual points, the next step is to decide where to refine the background grid. The argument used here is that if there is a significant difference between the element size at generated points and the points of the background grid, the element should be refined. This simple criterion is expressed as:

$$\min_{a,b,c,d}(\delta_{bg}) > c_f \delta_p \quad \Rightarrow \quad refine \tag{2.4}$$

where, typically, $1.5 \leq c_f \leq 3$. All elements flagged by this last criterion are subdivided further via classic h-refinement [Löh92], and the background grid variables are interpolated linearly for the newly introduced points.

Adaptive background grids combine a number of advantages:
- Possible use in combination with CAD-based element size specification and/or background sources;
- Automatic gridding to specified surface deviation tolerance;
- Automatic gridding to specified number of elements in gaps;
- Smooth transition between surface-faces of different size;
- Smooth transition from surface-faces to volume-elements.

Thus, they may be used to arrive at automatic, minimal-input grid generators.

2.3 Aneurysm: Aneurysm rupture can have devastating consequences. In order to answer the fundamental questions: "Who should be treated", and "Which treament ?" the aneurysms of more than 100 patients have been analyzed by Castro, Cebral and Putnam [Ceb05a, Ceb05b, Cas06]. Figure 2.2a shows a bilateral aneurysm located in the anterior communicating artery. The surface definition is discrete, i.e. a triangulation obtained via image segmentation and merging [Ceb01, Cas05]. The background grid was automatically adapted based on the surface curvature. Figures 2.2b-d show the surface grids obtained for different parts of the overall geometry. Note that in all cases the surface grid accurately represents the geometry. Without automatic background grid refinement/adaption, the user would have had to spend many hours specifying sources to obtain an appropriate distribution of element size in space.

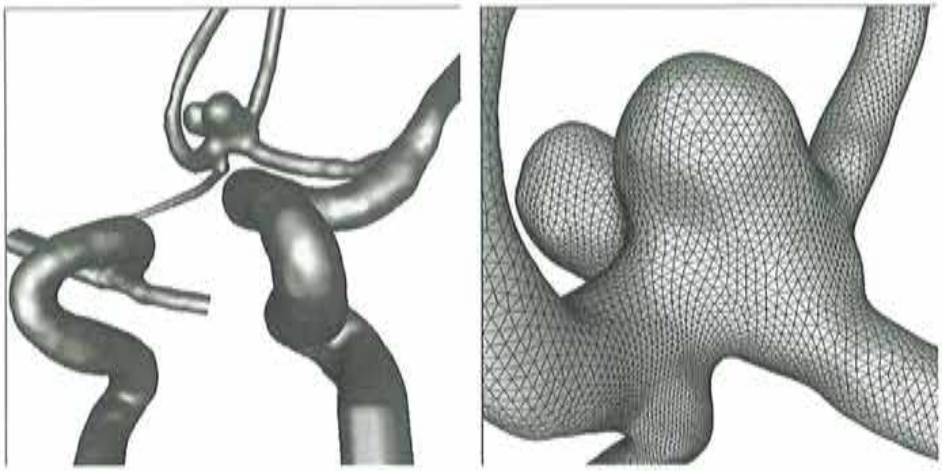

Figures 2.2a,b: Aneurysm: Overall Geometry and Surface Mesh Detail

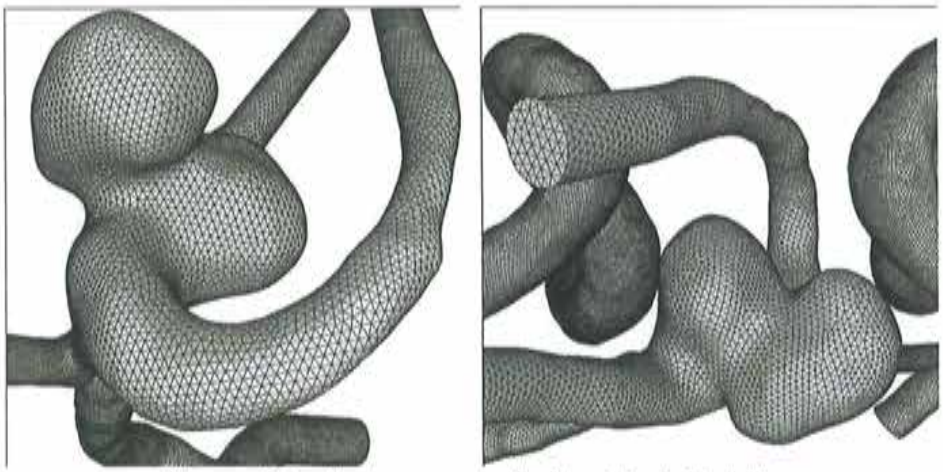

Figures 2.2c,d: Aneurysm: Surface Mesh Details

3. FAST MESHING FOR VERY LARGE PROBLEMS

Large grids occur when the size of the smallest features resolved (physics (e.g. vortices), geometries (e.g. buildings)) are small in comparison to the overall domain size. Current projections are that grids in excess of 10^{13} elements will be required for flight Reynolds-number large-eddy simulation (LES) calculations. Similar, if not larger, grids are expected for contaminant transport in cities, as well as high frequency aeroacoustics and electromagnetics. An obvious way to speed up the grid generation process is via parallel meshing techniques [Löh01b, Chr05]. The results, to date, have not lived up to expectations: while for simple cases scalability is not an issue, for truly general geometries the achievable parallelism has remained in the order of 16-32 processors. Fortunately, many of the problems mentioned above require large regions of uniformly

fine grids. This opens the way to so-called stencil meshing, which is orders of magnitude faster than general unstructured gridding techniques.

3.1 Optimal Space-Filling Tetrahedra

Unlike the optimal (equilateral) triangle, the optimal (equilateral) tetrahedron shown in Figure 3.1 is not space-filling. All the edge-angles have $\alpha = 70.52^0$, a fact that does not permit an integer division of the 360^o required to surround any given edge. Naturally, the question arises as to which is the optimal space-filling tetrahedron [Fuc98], [Bri05].

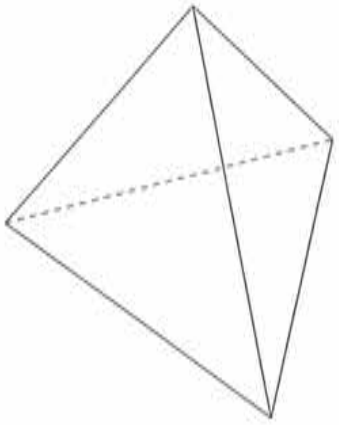

Figure 3.1: Ideal (Equilateral) Tetrahedron

The answer may be obtained by invoking the argument that any space-filling tetradron must be self-similar when refined. In this way, the tetrahedron can be regarded as coming from a previously refined tetrahedron, thus filling space. If we consider the refinement configuration shown in Figure 3.2, the displacements in x, y of point 3 and the displacements in x, y, z of point 4 may be regarded as the design variables, and the problem may be cast as an optimization problem. Typical quality criteria include: equidistance of sides, maximization of the minimum angle, equalization of all angles and George's $h_{min}Area/Volume$ criterion.

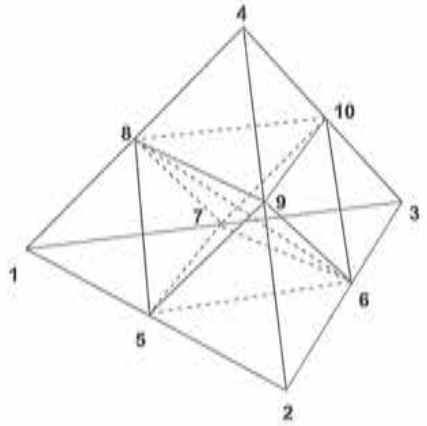

Figure 3.2: H-Refinement of Tetrahedron

The optimization yields the optimal space-filling tetraheron, given by: $l_{min} = 1.0$, $l_{max} = 1.157$, $\alpha_1 = \alpha_2 = \alpha_3 = \alpha_4 = 60.00^o$ and $\alpha_5 = \alpha_6 = 90.00^o$. One can show that this tetrahedron corresponds to the Delaunay triangulation (tetrahedrization) of the points of a body-centered cubic lattice [Bri05].

3.2 Grids With Uniform Cores

The possibility to create near-optimal space-filling tetrahedra allows the generation of grids where the major portion of the volume is composed of such near-perfect elements, and the approximation to a complex geometry is accomplished by a relatively small number of 'truly unstructured' elements. These types of grids are highly suitable for wave or vortex propagation problems (acoustics, electromagnetics, LES), where mesh isotropy is required to obtain accurate results. The generation of such grids is shown in Figure 3.3.

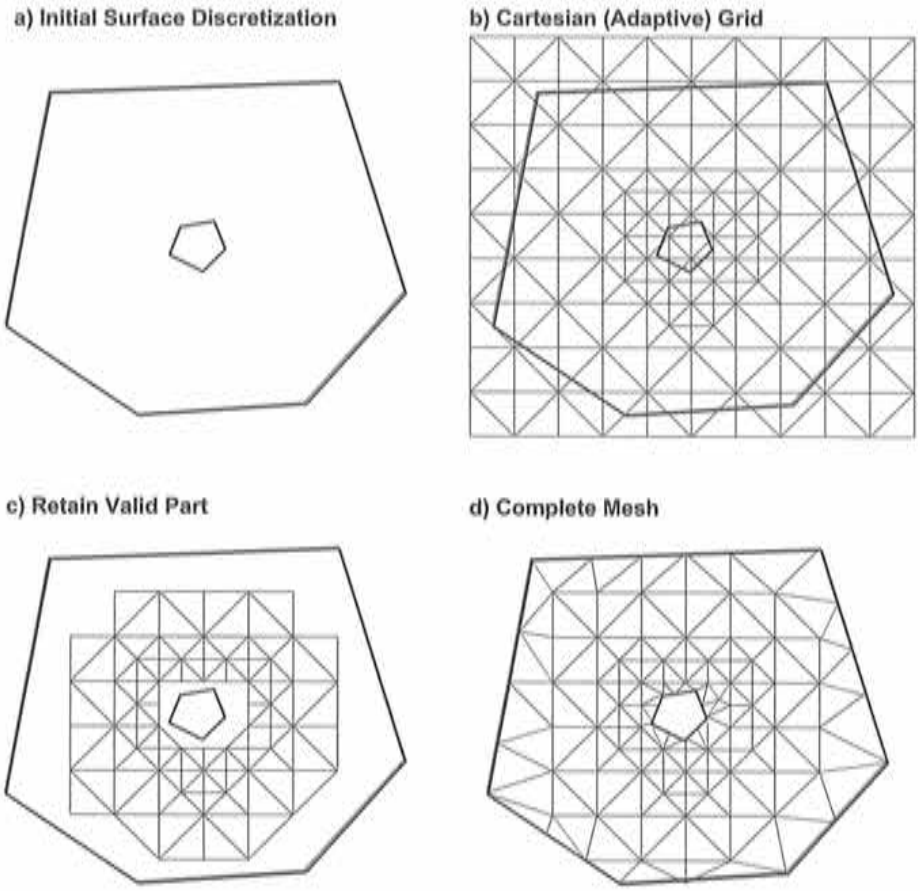

Figure 3.3: Mesh Generation With Adaptive Cartesian Core

In a first step the surface of the computational domain is discretized with triangles of a size prescribed by the user (or automatically, see above). In a second step a mesh of space-filling tetrahedra (or even a cartesian mesh subdivided into tetrahedra) that has the element size of the largest element desired in the volume is superimposed on the volume. From this point onwards this 'core mesh' is treated as an unstructured mesh. This mesh is then adaptively refined locally in order to obtain the element size distribution prescribed by the user. Once the adaptive core mesh is obtained, the elements that are outside the domain to be gridded are removed. A number of techniques have been tried to make this step both robust and fast. One such technique uses a fine, uniform voxel (bin, cartesian) mesh that covers the entire computational domain. All voxels that are crossed by the surface triangulation are marked. A marching cube (advancing layers) technique is then used to mark all the voxels that are inside/outside the computational domain. Any element of the adaptive cartesian mesh that covers a voxel marked as either crossed by the surface triangulation or outside the computa-

tional domain is removed. This yields an additional list of faces, which, together with the surface discretization, form the initial front of the as yet ungridded portion of the domain. One can then use any unstructured grid generation technique to mesh this portion of the domain. The capability to mesh core regions with space-filling tetrahedra only requires a small change within an unstructured grid generator. The core meshing is done in an independent module whose main role is to supply an additional list of triangles for the initial front. Meshing the core region is extremely fast, so that overall CPU requirements for large grids decrease considerably. A preliminary version of such a procedure (without the adaptive refinement of the cartesian core) was proposed by Darve [Dar97]. Other techniques that generate unstructured grids with Cartesian cores are all those that use point distributions from regular Cartesian grids [Bak87] or Octrees [She91], [Kal92].

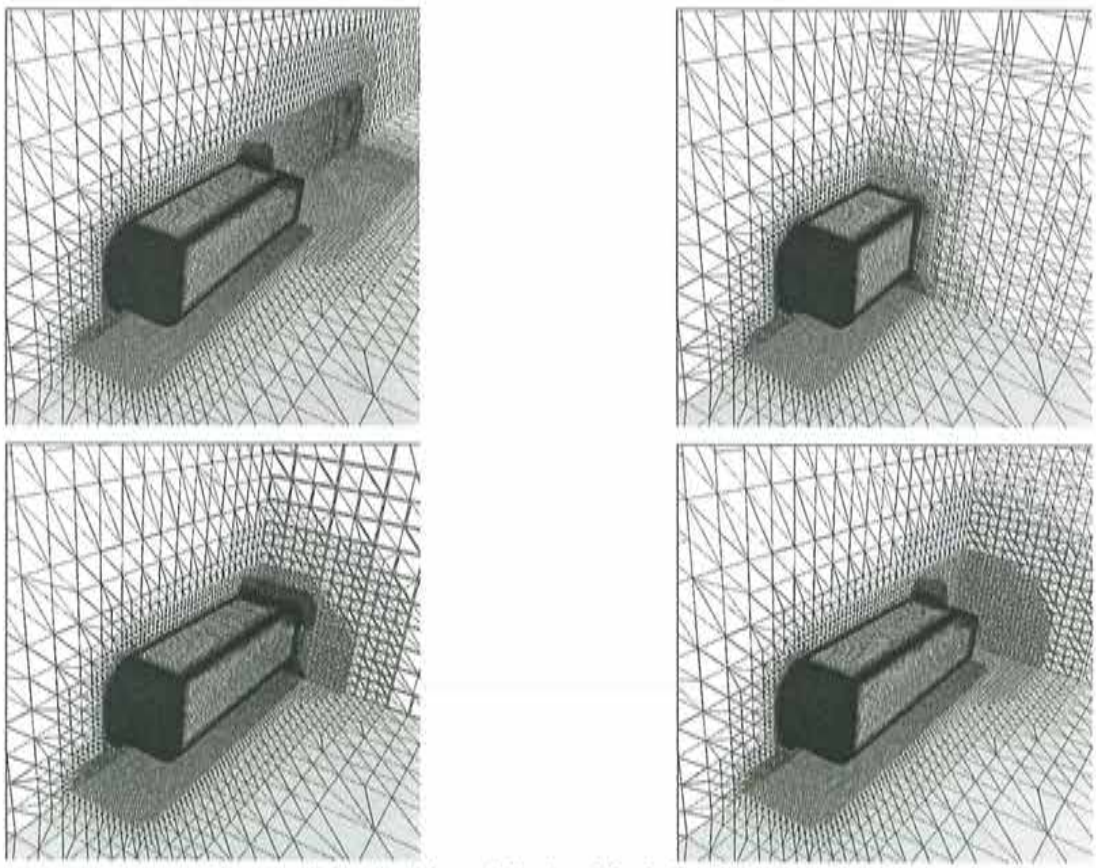

Figures 3.4a-d: Ahmed Body: Mesh in Different Cuts

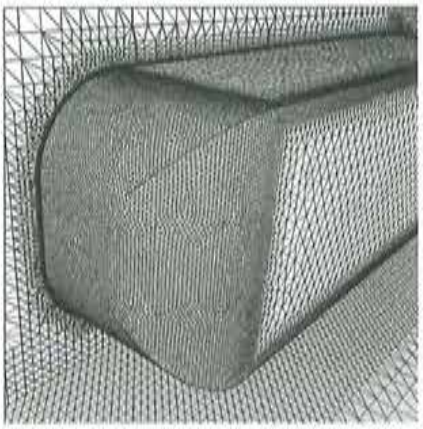
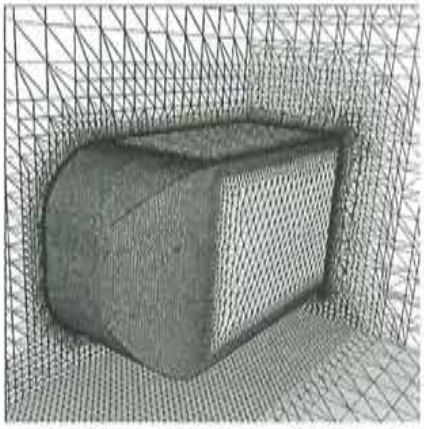

Figures 3.4e,f: Ahmed Body: Details of Mesh

3.3 Ahmed Car Body: This example demonstrates the use of boundary layer gridding techniques, as well as tetrahedra obtained from cartesian cores for the field. The geometry and discretization used are shown in Figures 3.4a-f. One can clearly see the RANS grid, the adaptively refined Cartesian cores of the flow domain, as well as the transition to an unstructured grid between these two zones. The number of elements in the RANS region is `nelns=1,302K`, in the cartesian core region `necrt=820K` and in the remaining unstructured grid region `nelun=415K`.

4. SURFACE TO VOLUME MESHING

The transition from a general CAD description or image (e.g. medical [Ceb01] or remote sensing data) of an arbitrary object to a clean, watertight surface that can be used by a body-conforming unstructured grid generator can represent weeks of labour-intensive, dull work. Faced with the need to provide quick results for such 'dirty' geometries, so-called immersed, embedded, fictitious domain or Cartesian methods have been developed. All of these employ grids that are not body-conforming and impose the required kinetic or kinematic boundary conditions at the surface of the embedded surfaces or bodies (and in some cases inside) [Cla85, Zee91, Mel93, Qui94, Kar95, Pem95, Lan97, Lev99, Aft00, Fad00, Pin01, Dad02, Pes02, Mur03a, Mur03b, Gil05]. An embedded technique for adaptive unstructured grids was proposed in [Löh04a] and used successfully for complex fluid-structure interaction cases [Bau03], as well as some external aerodynamics cases [Löh04a]. The essential elements of this technique may be summarized as follows:

- The key modification of the original, body fitted edge-based solver was the removal of all geometry-parameters (essentially the area normals) belonging to edges cut by embedded surface faces;
- Higher-order boundary conditions are achieved by duplicating crossed edges and their endpoints, or by extrapolating values and gradients from inside the domains to the surface;

- Geometric resolution and solution accuracy may be enhanced by adaptive mesh refinement that is based on the proximity to or the curvature of the embedded CSD surfaces;

- In order to save work, user-defined or automatic deactivation for regions inside immersed solid bodies is employed.

One of the main attractions of the embedded approach is its ability to effortlessly handle complex, 'dirty' and non-watertight geometries. On the other hand, our experience indicates that for the same element size, body-fitted grids yield more accurate results. It seemed only natural, then, to explore the possibility of obtaining a body-fitted grid by post-processing the volume grid obtained via the adaptive embedded approach. The embedded approach yields a volume mesh suitable for the problem at hand. This volume mesh covers the inside and outside of the flow domain. Once this volume mesh is obtained, the volume mesh is modified in two steps:

a) The points close to the surface are moved towards the surface, and the mesh in the neighbourhood of these points is smoothed;

b) The elements that are exterior to the flow domain are removed, leaving a new surface mesh/definition.

This approach to body-fitted grid generation via 'volume to surface meshing' has been used extensively for the generation of all-hex grids [Sch95], [Wie98].

4.1 Generic Car: A more realistic case of the 'volume to surface' meshing option is shown in Figure 4.1. The starting point for this run is a non-watertight triangulation with approximately 350 Ktria. This triangulation was introduced into a box, and a coarse unstructured grid of approximately 800 Kels was generated. This mesh was subsequently refined based on edges crossed by the triangulation of the car geometry. The final embedded mesh had approximately 9.5 Mtet. The points inside the car were then removed, and the points close to the surface were placed on the triangulation. This yielded a mesh of approximately 6.3 Mtet with the associated surface triangulation shown in Figures 4.1a. One can see that more work is required to simultaneously obey edges and avoid negative/distorted elements, but that the results are promising.

Figure 4.1a: Generic Car: Surface Obtained

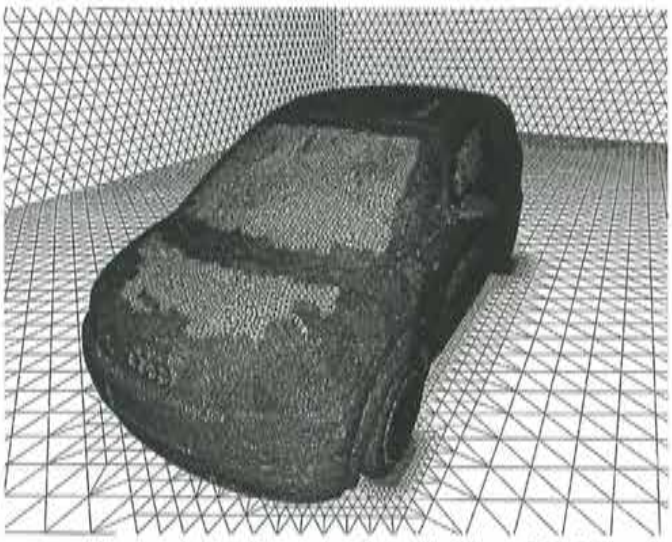

Figure 4.1b: Generic Car: Surface Mesh

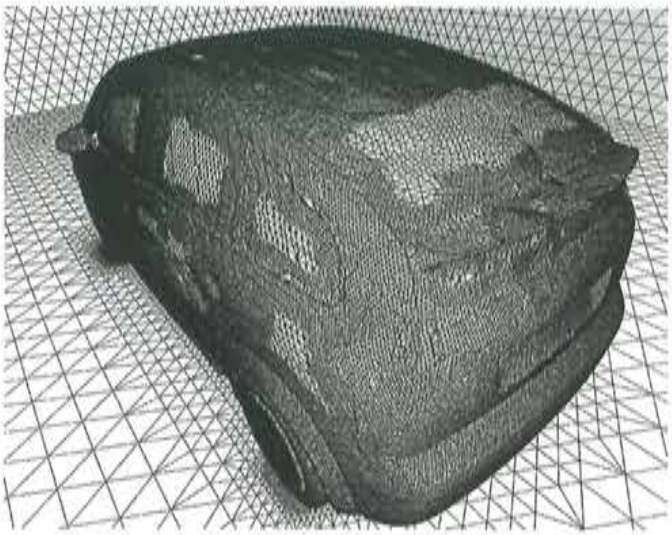

Figure 4.1c: Generic Car: Surface Mesh

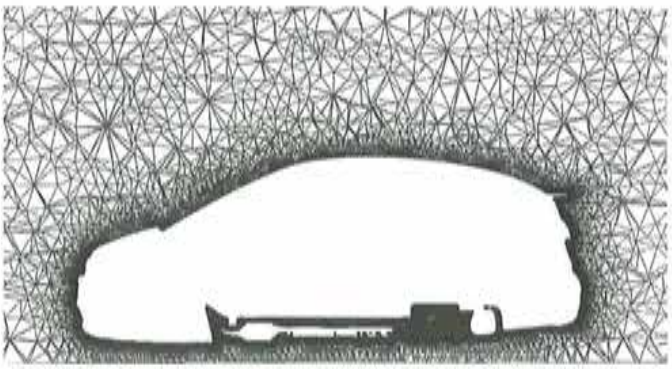

Figure 4.1d: Generic Car: Mesh in Cut Plane

5. GENERATING CLOUDS OF ARBITRARY OBJECTS

Many simulation techniques in computational mechanics require a space-filling cloud of arbitrary objects. For the case of 'gridless' or 'mesh free' partial differential equation (PDE) solvers (see [Nay72], [Bat93], [Bel94], [Dua95], [Gin83], [Oña96a,b], [Liu96], [Löh02]) these are simply points. For discrete element methods (see [Cun79], [Cun88], [Cle98], [Sak02]), these could be spheres, ellipsoids, polyhedra, or any other arbitrary

shape. The task is therefore to fill a prescribed volume with these objects so that they are close but do not overlap in an automatic way.

Several techniques have been used to place these objects in space. The so-called 'fill and expand' or 'popcorn' technique [Sak02] starts by first generating a coarse mesh for the volume to be filled. This subdivision of the volume into large, simple polyhedra (elements), is in most cases performed with hexahedra. The objects required (points, spheres, ellipsoids, polyhedra, etc.) are then placed randomly in each of these elements. These are then expanded in size until contact occurs or the desired fill-ratio has been achieved. An obvious drawback of this technique is the requirement of a mesh generator to initiate the process. A second class of techniques are the 'advancing front' or 'depositional' methods [Löh98], [Fen02]. Starting from the surface, objects are added where empty space still exists. In contrast to the 'fill and expand' procedures, the objects are packed as close as required during introduction. Depending on how the objects are introduced, one can mimic gravitational or magnetic deposition, layer growing, or size-based growth. Furthermore, so-called radius growing can be achieved by first generating a coarse cloud of objects, and then growing more objects around each of these. In this way, one can simulate granules or stone.

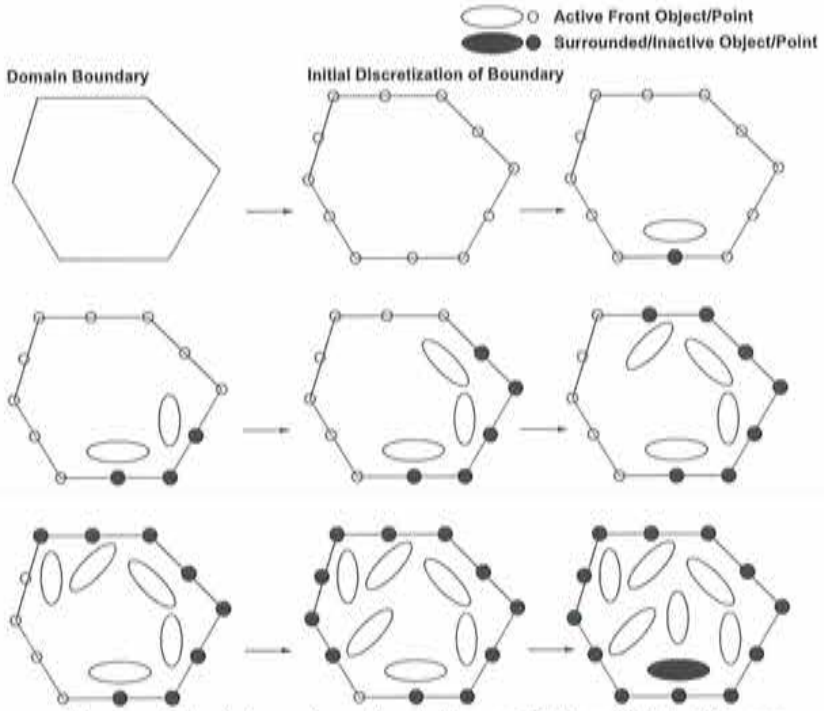

Figure 5.1: Advancing Front Space-Filling With Ellipses

In the present section, we consider a scheme that allows for the direct generation of clouds of arbitrary objects with the same degree of flexibility as advanced unstructured mesh generators. The mean distance between objects (or, equivalently, the material

density) is specified by means of background grids, sources and density attached to CAD-entities. In order not to generate objects outside the computational domain, an initial triangulation of the surface that is compatible with the desired mean distance between objects specified by the user is generated. Starting from this initial 'front' of objects, new objects are added, until no further objects can be introduced. Whereas the advancing front technique for the generation of volume grids removes one face at a time to generate elements, the present scheme removes one object at a time, attempting to introduce as many objects as possible in its immediate neighbourhood.

5.1 The Algorithm

Assume as given:

- A specification of the desired mean distance between objects in space, as well as the mean size of these objects. This can be done through a combination of background grids, sources and mean distance to neighbours attached to CAD-data (see above).
- An initial triangulation of the surface, with the face normals pointing towards the interior of the domain to be filled with points.

With reference to Figure 5.1, which shows the filling of a simple 2-D domain with ellipsoids, the complete advancing front space-filling algorithm may be summarized as follows:

- Determine the required mean point distance for the points of the triangulation;
- `while`: there are active objects in the front:
- Remove the object `ioout` with the smallest specified mean distance to neighbours from the front;
- With the specified mean object distance: determine the coordinates of `nposs` possible new neighbours. This is done using a stencil, some of which are shown in Figure 5.2;
- Find all existing objects in the neighbourhood of `ioout`;
- Find all boundary faces in the neighbourhood of `ioout`;
- `do`: For each one of the possible new neighbour objects `ionew`:
  - If there exists an object closer than a minimum distance `dminp` from `ionew`, or if the objects are penetrating each other:
    ⇒ skip `ionew`;
  - If the object `ionew` crosses existing faces:
    ⇒ skip `ionew`;
  - If the line connecting `ioout` and `ionew` crosses existing faces:
    ⇒ skip `ionew`;
  - Determine the required mean point distance for `ionew`;
  - Increment the number of objects by one;
  - Introduce `ionew` to the list of coordinates and store its attributes;
  - Introduce `ionew` to the list of active front objects;

  `enddo`
- `endwhile`

The main search operations required are:

- Finding the active object with the smallest mean distance to neighbours;
- Finding the existing objects in the neighbourhood of `ioout`;
- Finding the boundary faces in the neighbourhood of `ioout`.

These three search operations are performed efficiently using heap-lists, octrees and linked lists respectively (see chapter 2 and the present chapter).

5.2 Point/Object Placement Stencils

A number of different stencils may be contemplated. Each one of these corresponds to a particular space-filling point/object configuration. The simplest possible stencil is the one that only considers the 6 nearest neighbours on a Cartesian grid (see Figure 5.2a). It is easy to see that this stencil, when applied recursively with the present advancing front algorithm, will fill a 3-D volume completely. Other Cartesian stencils, which include nearest neighbours with distances $\sqrt{2}$ and $\sqrt{3}$ from `ioout` are shown in Figures 5.2b,c. The 'tetrahedral' stencil shown in Figure 5.2d represents another possibility. Furthermore, one can contemplate the use of random stencils, i.e. the use of n randomly selected directions to place new objects close to an existing one. For the generation of points and spheres, it was found that the 8-point stencil leads to the smallest amount of rejections and unnecessary testing [Löh98].

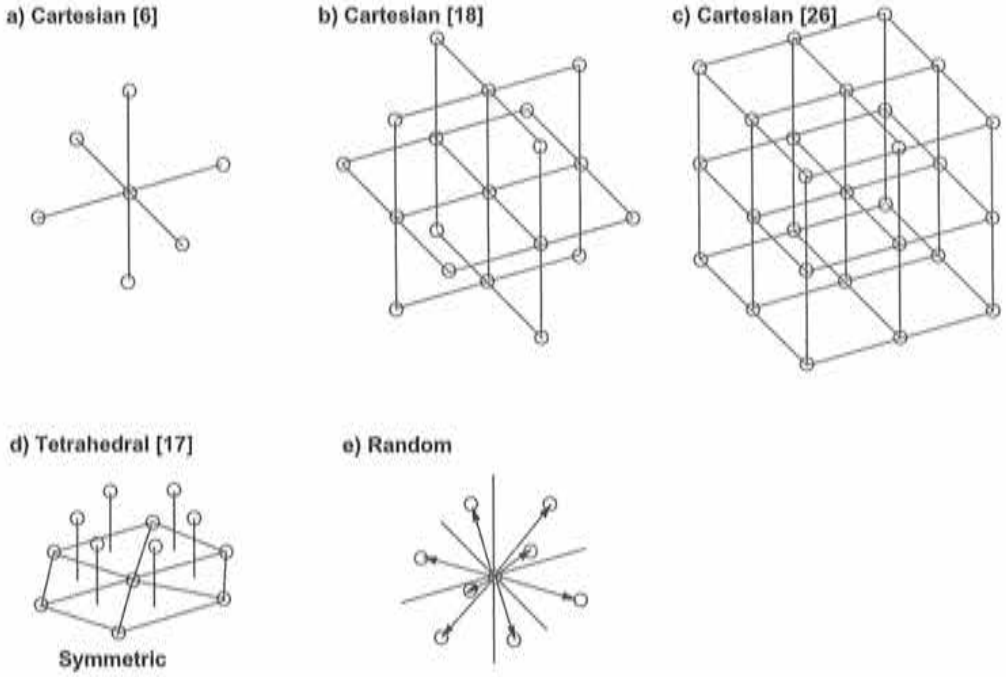

Figure 5.2: Point Stencils

In many instances, it is advisable to generate 'body conforming' clouds of points in the vicinity of surfaces. In particular, Finite Point or SPH techniques may require these

'boundary layer point distributions'. Such point distributions can be achieved by evaluating the average point-normals for the initial triangulation. When creating new points, the stencil used is rotated in the direction of the normal. The newly created points inherit the normal from the point `ioout` they originated from. Algorithmic details, in particular the boundary consistency checks, maximum compaction techniques, closest object placement, move/enlarge post-processing, approximation of arbitrary objects by spheres and deposition patterns have been described in [Löh04b].

5.3 Hopper Filled With Beans/Ellipsoids: Granular materials that require simulation include grains, ground stone, woodchips, and many other materials [Cun79], [Cle98]. Bridging in silos and hoppers can cause severe structural damage, and has always been a concern. Figure 5.3 shows a hopper configuration with bean-like objects composed of four spheres each. The total number of beans is 2,124, i.e. 8,496 spheres, and took 7 seconds to generate (2.8GHz ITP4, Linux OS). Figure 5.4 shows the same configuration filled with ellipsoidal objects composed of five spheres each. The total number of ellipsoids is 2,794, i.e. 13,970 spheres, and took 10 seconds to generate.

5.4 Semi-Autonomous Gravity Mill: Semi-autonomous gravity (SAG) mills are common in the mineral industry. The grinding action is relegated to large steel spheres that fall under the influence of gravity, demolishing the other ores in the mill. Some of these mills consume copious amounts of power, which immediately raises the question of how to optimize loads, number of spheres and speed. Figure 5.5 shows a typical large SAG mill configuration. The number of large steel spheres ($r = 0.1\ m$) is approximately 70. The ore is simulated by approximately 74K small spheres (($r = 0.01\ m$). The colouring is according to the absolute value of the particle velocity.

6. CONCLUSIONS AND OUTLOOK

Unstructured grid generation continues to be an important area of research. The present paper has reviewed some recent developments in minimal input meshing, fast meshing for very large problems, volume-to-surface meshing and the generation of clouds of arbitrary objects. Each one of these areas has seen advances.

As with any development of technology, the list of possible improvements is never ending. Among the areas of research in unstructured grid generation requiring immediate attention we mention:

- Scaling of parallel gridding to large numbers of processors (> 100);
- Improved RANS gridding, especially for separated, transient wake regions; and
- Robust volume-to-surface meshing.

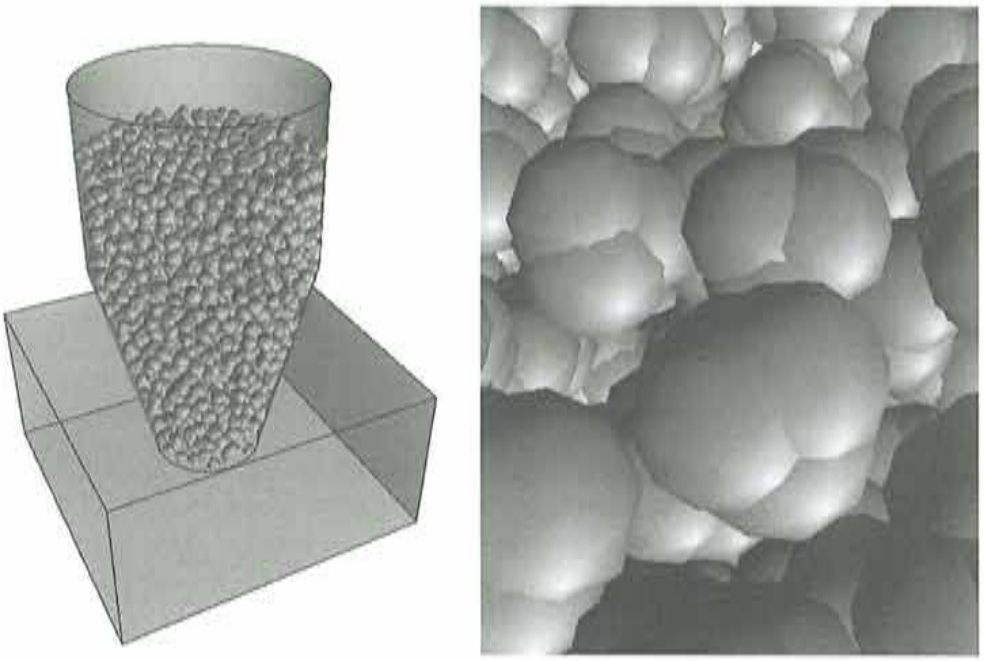

Figure 5.3: Hopper Filled With Beans

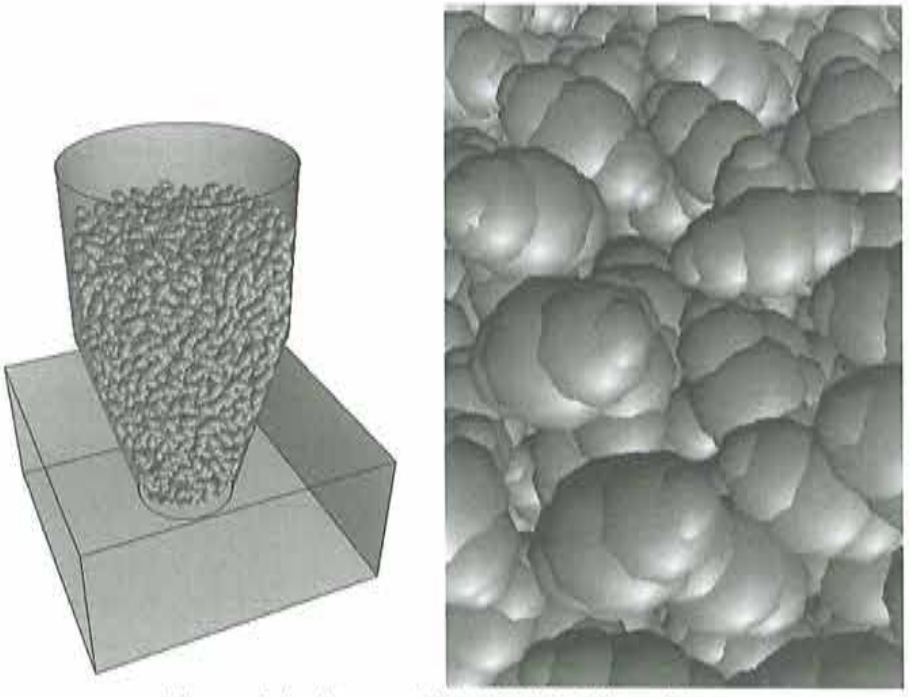

Figure 5.4: Hopper Filled With Ellipsoids

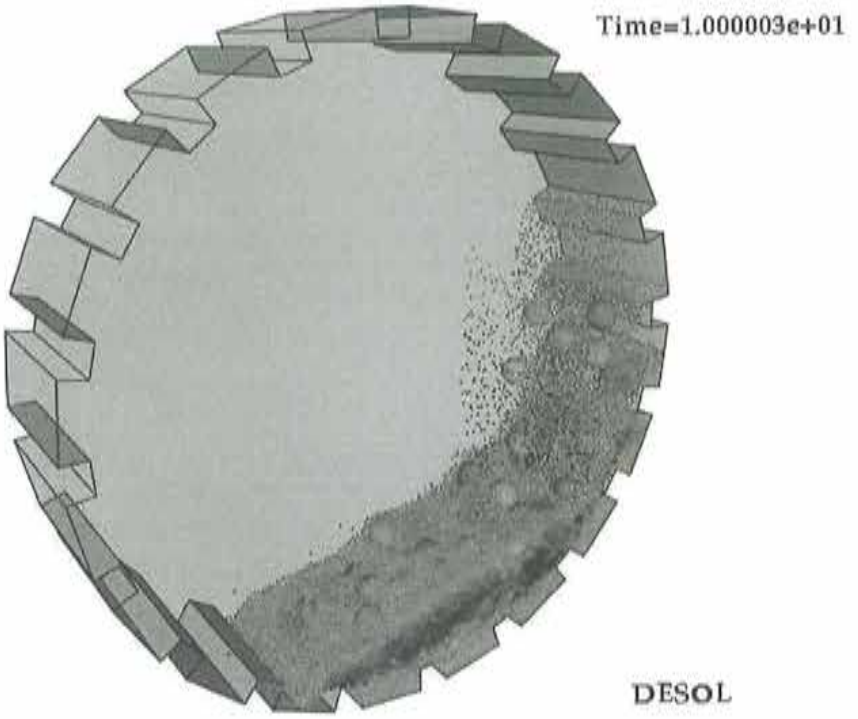

Figure 5.5: SAG Mill (70 Large, 74K Small Spheres)

7. ACKNOWLEDGEMENTS

This work was partially supported by DTRA and NRL. The technical monitors were Drs. Michael Giltrud, Young Sohn, Ali Amini and William Sandberg.

8. REFERENCES

[Aft00] M.J. Aftosmis, M.J. Berger and G. Adomavicius - A Parallel Multilevel Method for Adaptively Refined Cartesian Grids with Embedded Boundaries; *AIAA*-00-0808 (2000).

[Bak87] T.J. Baker - Three-Dimensional Mesh Generation by Triangulation of Arbitrary point Sets; *AIAA-CP*-87-1124, 8th CFD Conf., Hawaii (1987).

[Bat93] J. Batina - A Gridless Euler/Navier-Stokes Solution Algorithm for Complex Aircraft Configurations; *AIAA*-93-0333 (1993).

[Bau03] J.D. Baum, E. Mestreau, H. Luo, R. Löhner, D. Pelessone and Ch. Charman - Modeling Structural Response to Blast Loading Using a Coupled CFD/CSD Methodology; *Proc. Des. An. Prot. Struct. Impact/ Impulsive/ Shock Loads (DAPSIL)*, Tokyo, Japan, December (2003).

[Bel94] T. Belytschko, Y. Lu and L. Gu - Element Free Galerkin Methods; *Int. J. Num. Meth. Eng.* 37, 229-256 (1994).

[Bri05] R. Bridson, J. Teran, N. Molino and R. Fedkiw - Adaptive Physics Based Tetrahedral Mesh Generation Using Level Sets; *Engineering with Computers* (2005).

[Cas05] M.A. Castro, C.M. Putman and J. R. Cebral - Computational Modeling of Cerebral Aneurysms in Arterial Networks Reconstructed from Multiple 3D Rotational Angiography Images; *Medical Imaging 2005: Physics of Medical Imaging* 5746, 233-244 (2005).

[Cas06] M.A. Castro, C.M. Putman and J.R. Cebral - A Study of the Hemodynamics of Anterior Cerebral Artery Aneurysms *Medical Imaging 2006: Physics of Medical Imaging Image Reconstruction*, 6142 (2006).

[Ceb01] J.R. Cebral and R. Löhner - From Medical Images to Anatomically Accurate Finite Element Grids; *Int. J. Num. Meth. Eng.* 51, 985-1008 (2001).

[Ceb05a] J.R. Cebral, M.A. Castro, S. Appanaboyina, C. Putman, D. Millan and A. Frangi; Efficient Pipeline for Image-Based Patient-Specific Analysis of Cerebral Aneurysms Hemodynamics: Technique and Sensitivity *IEEE TMI Transactions on Medical Imaging; Special Issue on Vascular Imaging* 24(4), 457-467 (2005).

[Ceb05b] J.R. Cebral, M.A. Castro, J.E. Burgess, R. Pergolizzi and C.M. Putman - Characterization of Cerebral Aneurysm Hemodynamics for Assessing Risk of Rupture Using Patient-Specific Computational Models; *Am. J. Neuroradiol.* 26, 2550-2559, (2005).

[Chr05] N. Chrisochoides - A Survey of Parallel Mesh Generation Methods; *Brown-SC-2005-09* (2005).

[Cla85] D.K. Clarke, H.A. Hassan and M.D. Salas - Euler Calculations for Multielement Airfoils Using Cartesian Grids; *AIAA*-85-0291 (1985).

[Cle98] P.W. Cleary - Discrete Element Modeling of Industrial Granular Flow Applications; *TASK. Quarterly - Scientific Bulletin* 2, 385-416 (1998).

[Coo02] B.K. Cook and R.P. Jensen (eds.) - *Discrete Element Methods*; ASCE (2002).

[Cun79] P.A. Cundall and O.D.L. Stack - A Discrete Numerical Model for Granular Assemblies; *Geotechnique* 29 (1), 47-65 (1979).

[Cun88] P.A. Cundall - Formulation of a Three-Dimensional Distinct Element Model - Part I: A Scheme to Detect and Represent Contacts in a System Composed of Many Polyhedral Blocks; *Int. J. Rock Mech. Min. Sci.* 25, 107-116 (1988).

[Dad02] A. Dadone and B. Grossman - An Immersed Boundary Methodology for Inviscid Flows on Cartesian Grids; *AIAA*-02-1059 (2002).

[Dar97] E. Darve and R. Löhner - Advanced Structured-Unstructured Solver for Electromagnetic Scattering from Multimaterial Objects; *AIAA*-97-0863 (1997).

[Dua95] C.A. Duarte and J.T. Oden - H_p Clouds - A Meshless Method to Solve Boundary-Value Problems; *TICAM-Rep.* 95-05 (1995).

[Fad00] E.A. Fadlun, R. Verzicco, P. Orlando and J. Moud-Yusof - Combined Immersed-Boundary Finite-Difference Methods for Three-Dimensional Complex Flow Simulations; *J. Comp. Phys.* 161, 33-60 (2000).

[Fen02] Y.T. Feng, K. Han and D.R.J. Owen - An Advancing Front Packing of Polygons, Ellipses and Spheres; pp 93-98 in *Discrete Element Methods* (B.K. Cook and R.P. Jensen eds.), ASCE (2002).

[Fuc98] A. Fuchs - Automatic Grid Generation with Almost Regular Delaunay Tetrahedra; pp. 133-148 in *Proc. 7th Int. Meshing Roundtable* (1998).

[Geo90] P.L. George, F. Hecht and E. Saltel - Fully Automatic Mesh Generation for 3D Domains of any Shape; *Impact of Computing in Science and Engineering* 2, 3, 187-218 (1990).

[Geo91] P.L. George, F. Hecht and E. Saltel - Automatic Mesh Generator With Specified Boundary; *Comp. Meth. Appl. Mech. Eng.* 92, 269-288 (1991).

[Geo98] P.L. George and H. Borouchaki - *Delaunay Triangulation and Meshing*; Editions Hermes, Paris (1998).

[Gil05] A. Gilmanov and F. Sotiropoulos - A Hybrid Cartesian/Immersed Boundary Method for Simulating Flows with 3-D, Geometrically Complex Moving Bodies; *J. Comp. Phys.* 207, 2, 457-492 (2005).

[Gin83] R.A. Gingold and J.J. Monahghan - Shock Simulation by the Particle Method SPH; *J. Comp. Phys.* 52, 374-389 (1983).

[Kal92] Y. Kallinderis and S. Ward - Prismatic Grid Generation with an Efficient Algebraic Method for Aircraft Configurations; *AIAA*-92-2721 (1992).

[Kar95] S.L. Karman - SPLITFLOW: A 3-D Unstructured Cartesian/ Prismatic Grid CFD Code for Complex Geometries; *AIAA*-95-0343 (1995).

[Lan97] A.M. Landsberg and J.P. Boris - The Virtual Cell Embedding Method: A Simple Approach for Gridding Complex Geometries; *AIAA*-97-1982 (1997).

[Lev99] R.J. LeVeque and D. Calhoun - Cartesian Grid Methods for Fluid Flow in Complex Geometries; pp. 117-143 in *Computational Modeling in Biological Fluid Dynamics* (L. J. Fauci and S. Gueron, eds.), IMA Volumes in Mathematics and its Applications 124, Springer-Verlag (2001).

[Liu96] W.K. Liu, Y. Chen, S. Jun, J.S. Chen, T. Belytschko, C. Pan, R.A. Uras and C.T. Chang - Overview and Applications of the Reproducing Kernel Particle Methods; *Archives Comp. Meth. Eng.* 3(1), 3-80 (1996).

[Löh88] R. Löhner and P. Parikh - Three-Dimensional Grid Generation by the Advancing Front Method; *Int. J. Num. Meth. Fluids* 8, 1135-1149 (1988).

[Löh92] R. Löhner and J.D. Baum - Adaptive H-Refinement on 3-D Unstructured Grids for Transient Problems; *Int. J. Num. Meth. Fluids* 14, 1407-1419 (1992).

[Löh96] R. Löhner - Extensions and Improvements of the Advancing Front Grid Generation Technique; *Comm. Num. Meth. Eng.* 12, 683-702 (1996).

[Löh97] R. Löhner - Automatic Unstructured Grid Generators; *Finite Elements in Analysis and Design* 25, 111-134 (1997).

[Löh98] R. Löhner and E. Oñate - An Advancing Point Grid Generation Technique; *Comm. Num. Meth. Eng.* 14, 1097-1108 (1998).

[Löh01a] R. Löhner - *Applied CFD Techniques*; J. Wiley & Sons (2001).

[Löh01b] R. Löhner - A Parallel Advancing Front Grid Generation Scheme; *Int. J. Num. Meth. Eng.* 51, 663-678 (2001).

[Löh02] R. Löhner, C. Sacco, E. Oñate and S. Idelsohn - A Finite Point Method for Compressible Flow; *Int. J. Num. Meth. Eng.* 53, 1765-1779 (2002).

[Löh04a] R. Löhner, J.D. Baum, E. Mestreau, D. Sharov, C. Charman and D. Pelessone - Adaptive Embedded Unstructured Grid Methods; *Int. J. Num. Meth. Eng.* 60, 641-660 (2004).

[Löh04b] R. Löhner and E. Oñate - A General Advancing Front Technique for Filling Space With Arbitrary Objects; *Int. J. Num. Meth. Eng.* 61, 1977-1991 (2004).

[Mel93] J.E. Melton, M.J. Berger and M.J. Aftosmis - 3-D Applications of a Cartesian Grid Euler Method; *AIAA*-93-0853-CP (1993).

[Mur03a] S.M. Murman, M.J. Aftosmis and M.J. Berger - Implicit Approaches for Moving Boundaries in a 3-D Cartesian Method; *AIAA*-03-1119 (2003).

[Mur03b] S.M. Murman, M.J. Aftosmis and M.J. Berger, Simulations of 6-DOF Motion with a Cartesian Method; *AIAA*-03-1246 (2003).

[Nay72] R.A. Nay and S. Utku - An Alternative for the Finite Element Method; in *Variational Methods in Engineering* 1, Univ. of Southampton (1972).

[Ona96a] E. Oñate, S. Idelsohn, O.C. Zienkiewicz and R.L. Taylor - A Finite Point Method in Computational Mechanics. Applications to Convective Transport and Fluid Flow; *Int. J. Num. Meth. Eng.* 39,3839-3866 (1996).

[Ona96b] E. Oñate, S. Idelsohn, O.C. Zienkiewicz, R.L. Taylor and C. Sacco - A Stabilized Finite Point Method for Analysis of Fluid Mechanics Problems; *Comp. Meth. Appl. Mech. Eng.* 139, 315-346 (1996).

[Pem95] R.B. Pember, J.B. Bell, P. Colella, W.Y. Crutchfield and M.L. Welcome - An Adaptive Cartesian Grid Method for Unsteady Compressible Flow in Irregular Regions; *J. Comp. Phys.* 120, 278 (1995).

[Per90] J. Peraire, K. Morgan and J. Peiro - Unstructured Finite Element Mesh Generation and Adaptive Procedures for CFD; *AGARD-CP-464*, 18 (1990).

[Pes02] C.S. Peskin - The Immersed Boundary Method; *Acta Numerica* 11, 479-517 (2002).

[Pin01] S. Del Pino and O. Pironneau - Fictitious Domain Methods and Freefem3d; *Proc. ECCOMAS CFD Conf.* , Swansea, Wales (2001).

[Qui94] J.J. Quirk - A Cartesian Grid Approach with Hierarchical Refinement for Compressible Flows; *NASA CR-194938, ICASE Report No.* 94-51, (1994).

[Sak02] H. Sakaguchi and A. Murakami - Initial Packing in Discrete Element Modeling; pp 104-106 in *Discrete Element Methods* (B.K. Cook and R.P. Jensen eds.), ASCE (2002).

[Sch95] R. Schneiders and R. Bunten - Automatic Generation of Hexahedral Finite Element Meshes; *Computer Aided Geometric Design* 12, 693-707 (1995).

[Set99] J.A. Sethian - *Level Set Methods and Fast Marching Methods*; Cambridge University Press (1999).

[She91] M.S. Shepard and M.K. Georges - Automatic Three-Dimensional Mesh Generation by the Finite Octree Technique; *Int. J. Num. Meth. Eng.* 32, 709-749 (1991).

[Wea92] N.P. Weatherill - Delaunay Triangulation in Computational Fluid Dynamics; *Comp. Math. Appl.* 24, 5/6, 129-150 (1992).

[Wea93] N. Weatherill, O. Hassan, M. Marchant and D. Marcum - Adaptive Inviscid Flow Solutions for Aerospace Geometries on Efficiently Generated Unstructured Tetrahedral Meshes; *AIAA*-93-3390-CP (1993).

[Wie98] M. Wierse, J. Cabello and Y. Mochizuki - Automatic Grid Generation with HEXAR, pp.843-852 in *Numerical Grid Generation in Computational Field Simulations* (M. Cross, B.K. Soni, J.F. Thompson, J. Häuser and P.R. Eiseman eds.) (1998).

[Yer84] M.A. Yerry and M.S. Shepard - Automatic Three-Dimensional Mesh Generation by the Modified-Octree Technique; *Int. J. Num. Meth. Eng.* 20, 1965-1990 (1984).

[Zee91] D. de Zeeuw and K. Powell - An Adaptively-Refined Cartesian Mesh Solver for the Euler Equations; *AIAA*-91-1542 (1991).

CAE SOFTWARE CUSTOMIZATION AND DEVELOPMENT: THE SMARTCAE EXPERIENCE

Francesco Palloni
Business Development Manager

SmartCAE srl,
Piazza della Gualchierina, 9 – 59100 Prato – Italia
e-mail: info@smartcae.com, Url: www.smartcae.com

1: Introduction

Nowadays, the most important players in the CAE market are driving the development of their products towards the seamless integration between CAD and CAE tools, in order to both simplify the data transfer between applications and reducing the modelling time.

This approach, that is generally appreciated by the end-users, sometimes forces the software house to focus mainly on the most attractive market segments (typically automotive and aerospace industries), ignoring small market niches that could demand special features or enhancements.

Sometimes it happens that a commercial "general purpose" analysis software isn't the best tool to solve a very "specific" niche problem. Often these usability issues are not due to limitation of the mathematical foundation of the code, that indeed could be suitable for the application, but principally to the lack of a good "interface" to prepare the input for the software, or to manipulate the output for a specific purpose.

On other cases some "home-made" software is developed inside a company that requires an user friendly GUI to be effectively used by a new engineer that join the workgroup.

Finally, some small automations on the pre-processing or post-processing phase can improve the quality of the analysis, leaving to the end-users more time to focus on the real aim of their work: evaluate the simulation results with their engineering judgement.

The aim of this paper is to summarize the experience of SmartCAE in the field of customer-driven CAE software development, in the form of both plug-ins for existing commercial software and new stand-alone products, that are tailored to specific applications.

2: The need for software customization

Often the end-users of commercial simulation software need some level of customization to simplify the daily work or to cover some of the technical limitation of the used code. Some commercial pre and postprocessors allow some degree of customization via macro languages or API interfaces.

While this approach is helpful for small enhancements, mostly to automate some repetitive pre and post-processing tasks (productivity tools), it couldn't be satisfactory when also some new algorithms must be implemented.

Being at the same time a CAE software end-user and vendor SmartCAE found many limitations of existing FE software and, sometimes, simple and cost effective ways to overcome those limitations. Sometimes a simple Visual Basic application is enough to achieve the goal, while in other cases the situation is more complicated and it requires a graphical application for CAE data handling and manipulation.

The strategy chosen by SmartCAE for the development of graphical applications is to use existing commercial applications as "frameworks" for the software development. This approach leads to many technical advantages for the developers:

- The "framework" database structure is used to handle (create, edit, manipulate) the model entities (geometry, mesh, properties, results)
- The "framework" GUI, often supporting OpenGL hardware, is used for the graphical visualization of entities and results.
- The existing scripting language and/or programming API of the "framework" that allows the customization of the user interface and the development of mathematical algorithms is exploited.
- The customized software may be portable over different OS platforms such as Windows, Linux, Unix (depending on the platforms supported by the "framework") .
- The "framework" licensing tools are used to "lock" the software as a plug-in for the framework (potential revenue source from the developed tool).
- The developer may focus only on the "core" algorithms and procedures, leaving the GUI development to the framework manufacturer.

The last advantage of the list above is probably the most attractive for small engineering companies, such as SmartCAE, that do not have the economical and/or man-work resources needed to develop and maintain a full-featured graphical CAE application.

This paper shows four different applications initially developed by SmartCAE to enhance the productivity of its consulting services, that have also been packaged as commercial software:

- Smart|FRF, a tool for FRF plot generation from Nastran results to Excel;
- Smart|Browser, a productivity plug-in for FEMAP;
- Smart|AISC, an automated post-processing tool to verify structural results according to AISC rules;
- Smart|Coupling, a tool for multi-physics simulation.

3: Smart|FRF: A fast route from Nastran to Excel

One of the most widely methods used to compute Frequency Response Functions is the modal superposition techniques. The most used FE solver for this kind of analysis is Nastran because of its fast and accurate eigenvalue solver. In order to simplify the Nastran FRF analysis setup and post-processing SmartCAE developed Smart|FRF, a software that:

- creates the input file for modal analysis (measurement points, frequency range, number of residual vectors);
- reads the results from the Nastran Punch file and computes the desired FRF response (dynamic stiffness, inertance, ...) ;
- stores all the results in an Excel file of customizable format

Figure 1 shows the Smart|FRF GUI and a typical FRF plot with many design iterations and the given design targets. Smart|FRF is written in Visual Basic.

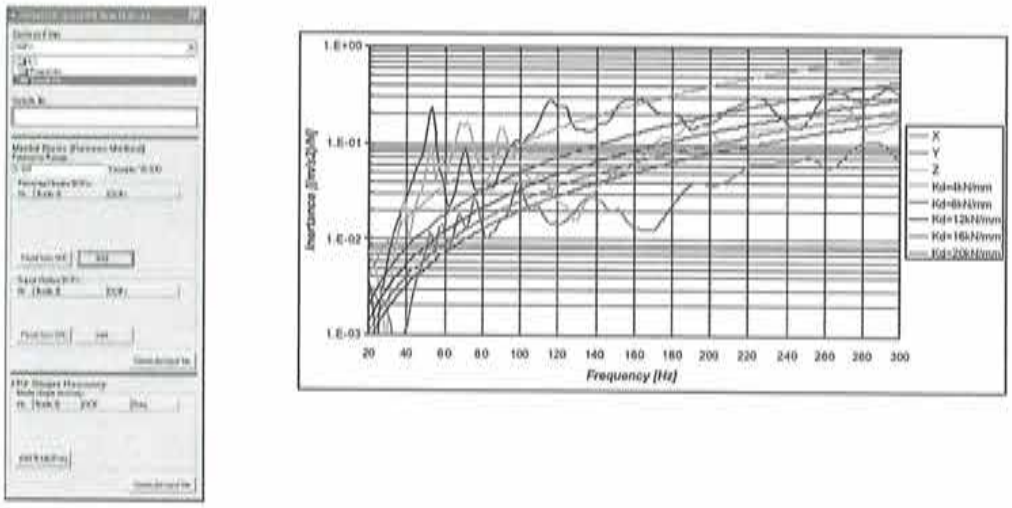

Figure 1: Smart|FRF window and an FRF plot for automatic reporting

4: Smart|Browser: Enhanced pre/post processing in FEMAP

One of the most time consuming task in the CAE process is still the preparation of the analysis model. In some cases, the GUI of the commercially available pre-processors may appear "hostile" for new-to-FEA users, especially if compared to user-friendly tools like popular mid-range 3D CAD systems. Furthermore, some automations of repetitive tasks is sometimes required, especially to simplify the access to advanced post-processing features. This was one of the main reasons behind the development of a productivity plug-in for the popular FE pre-processor FEMAP, Smart|Browser.

Smart|Browser (Figure 2) is a collection of utilities that simplifies the handling of complicated FE models, by using an assembly tree logic, directly derived from modern 3D CAD systems. This program provides an intuitive way to manipulate, create and edit

the FE entities, linking directly the underlying FEMAP database. Smart|Browser not only steeps-up the learning curve for new users, but it also improves the way to use FEMAP for all the other users, because it adds shortcuts to the most common visualization tasks for FE parts and results.

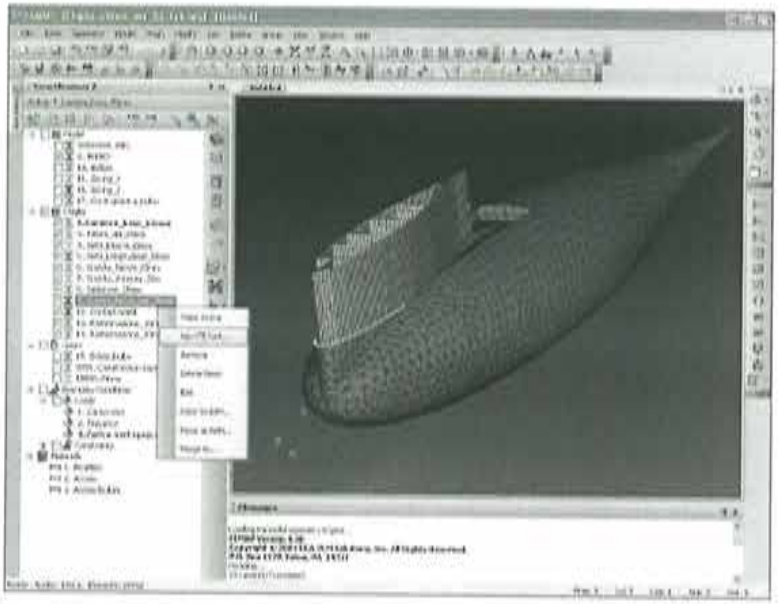

Figure 2: Femap GUI + Smart|Browser tree on left

Together with Smart|Browser comes Smart|Laminate, a specific plug-in for composites pre-processing of laminated composites (Figure 3). This tool simplifies the modelling of complex laminations, providing to the user tools to add multiple plies, automatic computation of the total thickness and the equivalent stiffness properties of the laminate. Smart|Laminate helps the designer to both optimize the lamination and prevent the most common mistakes in the FE modelling of composites with FEMAP.

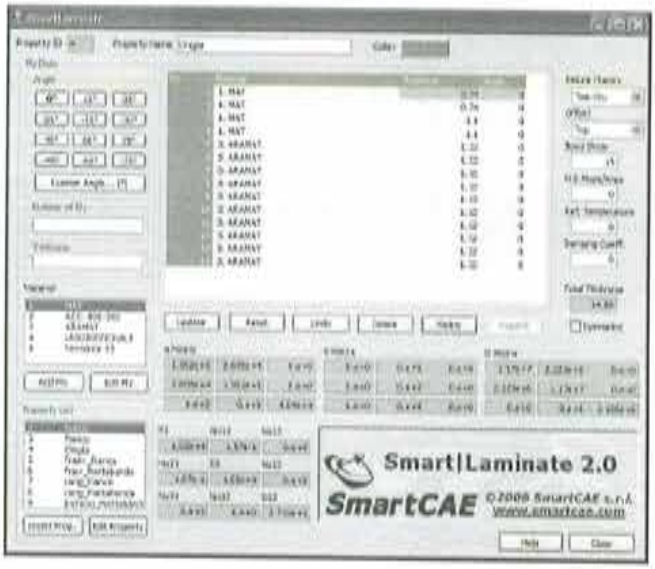

Figure 3: Smart|Laminate window

For the post-processing of FEA results, Smart|Browser provides quick-buttons for filtering the contour map, reverse the contour colour table, or plot vector results such as SPC forces, MPC forces or principal stresses over shells. Please notice that all these functionalities are already available on the FEMAP environment, but they require a relatively long and sometime error-prone sequence of "mouse clicks" to be used.

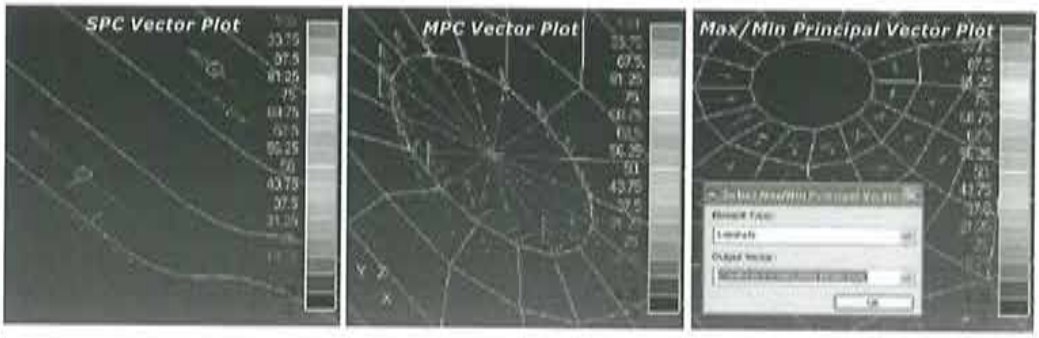

Figure 4: Different kind of vector plots

Smart|Browser and Smart|Laminate are written in Visual Basic. They interact with FEMAP via API, by using the Microsoft COM and .NET paradigms.

5: Smart|AISC: Verification of structures according AISC for FEMAP

Another time consuming task is the post-processing of structural results in order to fit prescribed regulation standards. For framed structures, modelled with beam elements, this purposes, SmartCAE developed Smart|AISC, a software that is able to pre and post-process a FE model within FEMAP in such a way to match the AISC code procedure.

Smart|AISC is able to identify automatically the frame geometry topology, to apply the appropriate verification procedure to each member of the structure. The output is given as a contour map over the FEA model, with the Utilization Factors under the different load components, and as a summary of the relevant results in Excel format.

Smart|AISC is written in Visual Basic. It dialogs with FEMAP via API using the Microsoft COM and .NET paradigms.

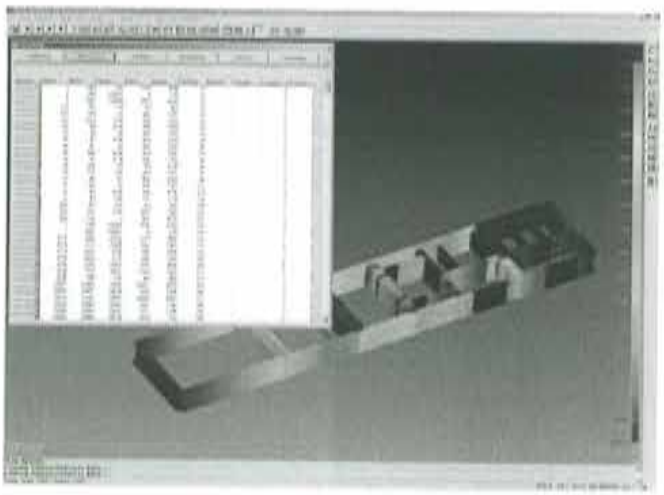

Figure 5: Application of Smart|AISC on a steel baseplate structure

6: Smart|Coupling: A tool for multidisciplinary simulations

One of the most challenging tasks in today's simulations is the Multi Disciplinary Optimization (MDO) of a mechanical system.

The goal of MDO is to make engineers able to analyse and optimise complex physical phenomena, where more than one discipline is involved. This class of problem is very wide and it includes, for example, the Fluid – Structure Interaction (FSI), where the structural response of a body under the action of fluid dynamic boundary conditions, has an influence on the calculation of the thermo-fluid-dynamic field and vice-versa (Figure 6).

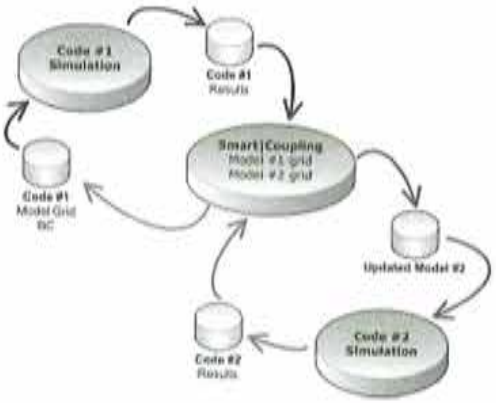

Figure 6: Data flow for MDO: Coupled problem

The main problem for a practical and effective MDO is that, nowadays, only few simulation software are able to handle efficiently a fully coupled simulation, and usually they are applicable only under some modelling restrictions. On the other hand, the engineer can choose between many different good commercial tools, to explore each specific engineering field: CFD, FEA, EMAG, etc.

Practical MDO is then complicated, by the fact that heterogeneous hardware, software and engineering competencies may be involved (Figure 7):

- the hardware / operating system requirements of the codes may be different (RISC, IA32, IA64,Windows, Unix, Linux, etc.);
- the engineering skill and experience required for each discipline may be significantly different;
- different simulation software requires different modelling strategies (grid shape, density) and, in general, one and the same mesh can't actually be used for different disciplines.

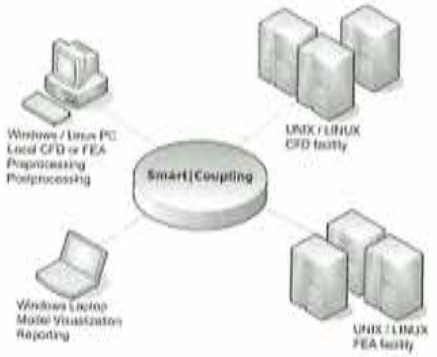

Figure 7: Example of typical CAE environment for MDO

To cover this kind of needs SmartCAE has developed a tool called Smart|Coupling, which enables MDO by interfacing different CAE software. The program provides engineers with many tools for model import/export, multi-model matching, data interpolation, grid transformation and optimization.

The core of Smart|Coupling is its database where two models can be stored, viewed, modified and paired for multi disciplinary simulation. The typical workflow within Smart|Coupling is described in the following steps:

Step #1 - Multiple model import. The software can import two models with their results from different sources (CFD, FEA, Process, EMAG, etc.). During the import phase, the user can select the parts of the whole model that are actually subjected to interaction. Then, the engineer can view the model and check the imported results by means of graphic contour.

Step #2 - Model matching. The engineer can transform (scale, translate, rotate) one or both of the imported models (both grid and results) to fit the two grids in the space, as shown in Figure 8. This is useful because the two models may have different units: typical for FSI is to have the CFD model with length in meters and the FEA in millimetres. Doing the transformation of the model "a posteriori" doesn't require the engineers to change their modelling strategies, thus reducing the impact for the MDO deployment on the existing CAE procedures.

Figure 8: Overlapping between CFD model (yellow) and FEA mesh (blue)

Step #3 - Data interpolation. Once the pairing strategy has been decided, it is possible to transfer the result field from the source grid as a boundary condition to the destination one. This is done trough a 3D interpolation algorithm that allows a smooth transition of the result field across the two grids. The algorithm works on both volumetric grids and surfaces. The quality of the interpolated field can be shown graphically by means of contours (as shown in Figure 9), or quantitatively by means of checksum values and XY plots.

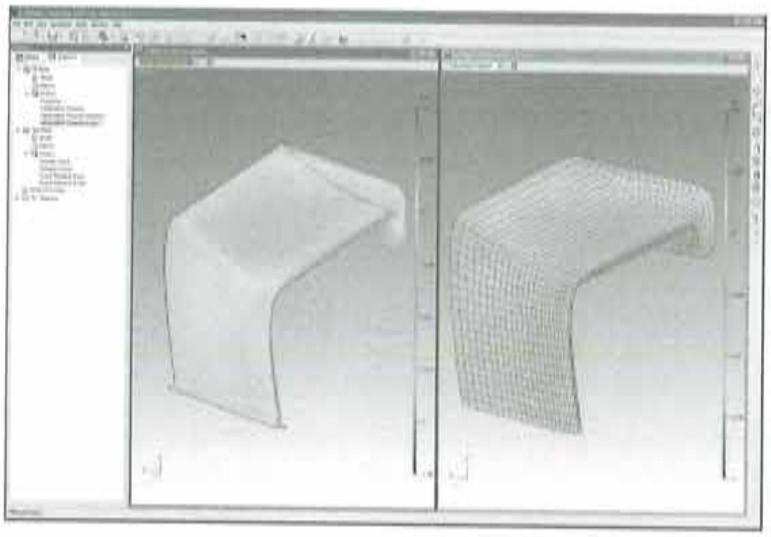

Figure 9: Pressure interpolation result. Left: the source CFD model, Right the destination FE mesh

Step #4 - Updated model export. The interpolated data may be exported and used as a boundary condition for the next simulation software.

Smart|Coupling is developed by using the FEMtools Framework from Dynamic Design Solutions for model data storing and manipulation.

7: GiD: a cost-effective CAE software development toolbox

SmartCAE considers GiD a cost-effective and valuable development platform for mesh-based codes and vertical pre/post processors for existing simulation software. The benefits of GiD for the developer, either software houses or end-users are:

- porting of GiD on different OS;
- availability of all the typical pre/post processing tools, from geometry import, to mesh generation, to result visualization (both structural and CFD);
- interfaces for popular commercial FE software such NASTRAN;
- platform-independent scripting language such as Tcl/Tk that allows the development of custom and portable applications.

Possible toolbox to be developed on the GiD framework could be:

- specialty postprocessors for FE result verification according to international rules (civil engineering, shipping registers, ...);
- specific pre and postprocessors for laminated composites structures (draping of skins over the mesh, custom failure index criteria, ...);
- graphical pre and post processors for automatic Design Optimization routines (sensitivity based, topology, ...).

8: Conclusion

Industry-specific tools that are easy to use and able to automate the every day's CAE tasks are continuously required by the CAE community.

General purpose simulation environments are not always able to cover such specific requirements and there is room for the development of custom programs, which can be in the form of plug-ins for existing software, or brand new vertical applications.

In order to minimize the development efforts, costs and time, an accurate selection of the development framework has to be made, by using, as a preference, software which are well suited to such extensions (i.e. has a scripting language as GiD and/or API interface as FEMAP) or CAE-oriented programming platforms such as FEMtools.

Contributed Papers

1D CROSS SECTIONS FROM A 2D MESH, A FEATURE FOR A HYDRAULIC SIMULATION TOOL.

Georgina Corestein[*], Ernest Bladé[†], Manuel Gómez[†], Josep Dolz[†], Eugenio Oñate[*], Javier Piazzese[*]

[*] International Center for Numerical Methods in Engineering (CIMNE) - UPC
Campus Nord UPC, 08034 Barcelona, Spain
email: geocores@cimne.upc.edu , web page: http://cimne.upc.es/

[†] Department of Hydraulic, Maritime and Environmental Engineering (DEHMA) - UPC
Jordi Girona 3-1, Edifici D1, Campus Nord UPC, 08034 Barcelona, Spain
email: ernest.blade@upc.edu - Web page: http://www.flumen.upc.es

Key words: GiD customization, hydraulic simulation, 1D-2D mesh, flood risk.

Abstract. *A new feature, wrote in tcl and FORTRAN, prepared to obtain 1D meshed cross sections from a 2D mesh of a surface was developed with the idea of improve the existing GiD interface for the hydraulic simulation code CARPA in order to make it able to interact with one of its more useful capabilities, perform 1D-2D coupled simulations.*
The importance of this option is easily explainable by the huge amount of data involved in a hydraulic simulation of real rivers, which is an aim of this code.
These works were developed as part of the RAMFlood-DSS Project an EU granted project finished on February 2005.

1 INTRODUCTION

RAMFLOOD-DSS is a project co-funded by the 5th Framework Program of the European Community - managed by the European Commission - and forms part of the Information Society Technologies (IST) activities. The objective of this project is to develop a web based decision support system to assist public administration and emergency services in the risk assessment and management of floods.

Ramflood uses CARPA [4] hydraulic simulation model to perform flood routing computations in the area of interest. Hydraulic simulation results are then used to train an Artificial Intelligence module based on neural networks which, once trained, can give results of flood risk maps in a few seconds. For neural networks training hundreds of hydraulic simulation results associated to input data are needed, so maximum efficiency of the hydraulic module is sought.

Flood propagation on natural channels is done by numerically solving the Saint Venant equations. This can be done either with a one dimensional or two dimensional approximations, the first one with less computational and information cost, the second one with more precise results when the real flow pattern does not correspond with a 1D domain. CARPA uses a 1D-2D integrated finite volume high resolution numerical scheme.

Ramflood DSS is oriented to different end users profiles, being a crucial one that of a non technical Water Administration or Natural Disasters Manager. For that reason results were represented in terms of risk rather than hydraulic variables to help such administrators in their fast decision taking. The risk criterion of the Catalan Water Agency, which uses a risk classification according to water levels, velocities or a combination of them (partner of the Ramflood Project), was used (Fig. 1 and 2).

2 GENERATION CROSS SECTIONS FROM GIS DATA

Using this tool involve a number of steps; first the geometry -terrain surface- has to be created from the GIS data, that can be done using the DTM import tool [2], and meshed; then the user have to select from the surface mesh, which part will be used to create 1D cross section; next the user have to draw the lines that determine the position of the cross section and assign its number, those steps can be done using the specific GiD window; finally by click the option "Create 1D sections" the tool performs the tasks required to create, store and draw the new 1D cross sections.

The interface for this feature, specifics windows and buttons, was written in tcl language as well as the code that collect and prepare the information needed and call the executable that perform the geometric tasks. The code that actually creates the cross section was written in FORTRAN language and works in the following manner: reads from a file the information, of the mesh and about defined reaches and cross sections (information to create planes); Going through each section, creates the plane; boks for the elements that intersects; over these elements list calculates the scalar product between each side of the element and the normal of the plane to determine if they cross or not, if yes them it is verified if the intersection point is between the two nodes that define the side, this procedure is repeated for all the sides, and the point are stored in a list, then sorted according the global axis, a possible point repetition is checked and corrected and finally the point are sorted according local axis. The information from new cross section, including x and y coordinates and roughness coefficient is exported to the input data file that will be used by CARPA to calculate.

3 RESULTS ADAPTATION TO DISPLAY IN RISK CRITERIA

As one of the aims of the RAMFlood project was to asses risks of flood, was important to enable the software to show result according to Risk Criteria scales. The hydraulic results produced by the simulation model were pre-processed by using the Gidpost library in order to be shown over the cross sections –lines- both in ranged and graded scales. An example of these results can be seen in Figures 3 and 4.

4 APPLICATION CASE: LLOBREGAT RIVER

For the application of the system to the test case area of interest corresponding to the lower reach of Llobregat river, a coupled 1D-2D approximation was used (Fig 5). The topographic information was imported from ArcInfo/Ascii Grid Format (Fig. 6) and discretized using 13480 quadrilaterals in the 2D area and 307 cross sections in the 1D reach (Fig. 7).

Developments made for the 1D cross sections generation from the imported geometry were proved useful in that practical application. After computations results of both the hydraulic simulations and artificial intelligence module the 1D and 2D areas were successfully visualized using GiD (Figures 8 and 9), thus proving the great value of the new interface for coupled 1D-2D free surface flow modelling with great efficiency.

5 CONCLUSIONS

- This work has developed a customization of GiD for the one dimensional hydraulic analysis in order to take advantage of all the capacities of the CARPA code.
- A set of particular results, adapted to show simulation values in Risk scale format were created.
- A fully integrated 1D-2D coupled hydraulic simulation environment combining GiD and CARPA was successfully developed and tested.

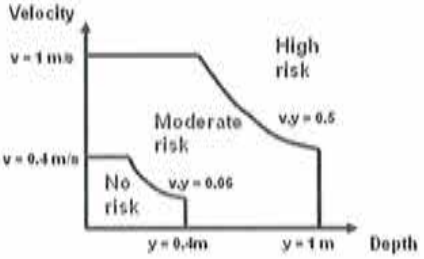

Figure 1: Risk criteria combining water velocities and depths.

Figure 2: Risk Criteria based on flooding time.

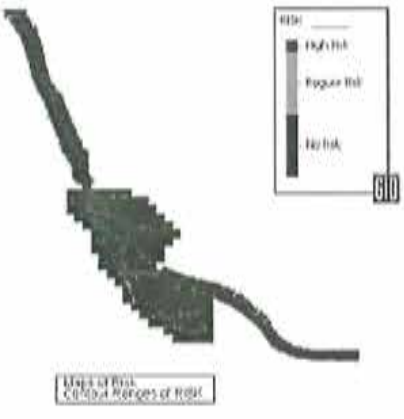

Figure 3: Risk Results, Risk

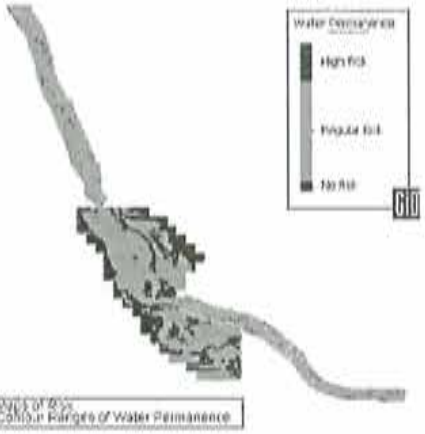

Figure 4: Risk Results, Water Permanence

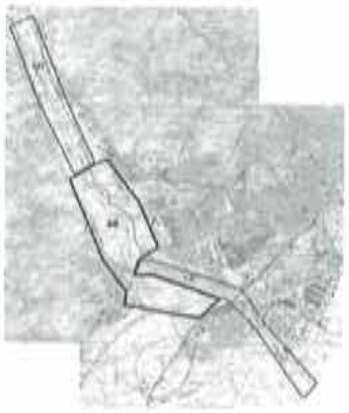

Figure 5: Coupled 1D-2D Model of last reach of Llobregat River

Figure 7: Coupled 1D-2D geometry.

Figure 6: Detail of a rendered image of the topography

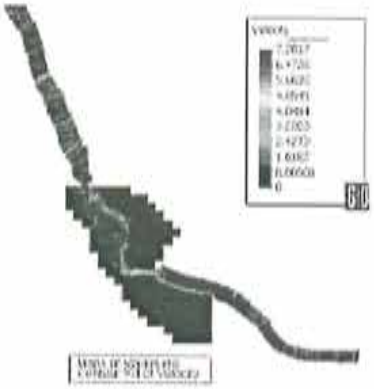

Figure 8: Hydraulic Results, Velocities.

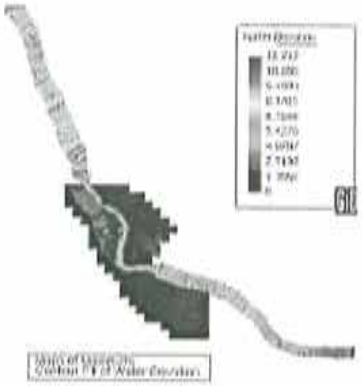

Figure 9: Hydraulic Results, Water Elevation

REFERENCES

[1] RAMFLOOD-DSS, *Decision Support System for Risk Assessment and Management of FLOODS,* IST-2001-37581.

[2] Corestein, G., Bladé, E. & all, *New GiD Interface for RAMFlood-DSS Project Hydraulic Simulation Code,* 2nd Conference on Advances and Application of GiD (2004).

[3] GiD Team, *GiD On-line Manual*, www.gidhome.com/support.

[4] Bladé, E. *Modelación del flujo en lámina libre sobre cauces naturales. Análisis integrado con esquemas en volúmenes finitos en una y dos dimensiones.* Tesis Doctoral. UPC. Barcelona 2005.

APPLICATION OF CODE_BRIGHT – GID TO GEOTECHNICAL PROBLEMS

Sebastià Olivella and Jean Vaunat
Department of Geotechnical Engineering and Geosciences

Abstract: *This paper describes capabilities of CODE_BRIGHT–GiD to analyze geotechnical problems involving unsaturated soils. Customization of GiD for CODE_BRIGHT has been a success task and some aspects related to geotechnical analysis are discussed in the paper. The paper focuses in the construction process of earth dams and related aspects and highlights the complexity of the boundary conditions to be applied in these problems.*

1. INTRODUCTION

We customized GiD for using as pre- and post-process of CODE_BRIGHT (Olivella et al 1996) which is a program that solves coupled THM problems in geological materials using the finite element method. A preliminary version for CODE_BRIGHT - GiD was presented in Vaunat and Olivella (2002).

The program CODE_BRIGHT couples the thermal (multiphase heat transport in porous media), hydraulic (two phase flow of liquid and gas in porous media), mechanical (unsaturated soil mechanics) problems and the solute transport. These problems require a number of constitutive laws and these have been organized accordingly. Since the number of material properties and parameters is large, it is useful to import sets of parameters if they are similar in other applications.

A functionality that has been introduced recently in CODE_BRIGHT is the construction and excavation of geomaterials. This is of especial relevance in geotechnics as most of problems require construction (for example an earth dam or and embankment) or excavation (for example tunneling and diaphragm walls). From the finite element point of view, this facility implies activation and deactivation of elements, typically by layers. Normally, ramp variation of weight application permits to fully smooth this process which is very important for avoiding sharp changes which may lead to numerical difficulties and do not correspond to the actual process in the field. In the case of GiD pre-process this is solved by combination of material definition by layers which activate and deactivate in the different intervals. Yet, construction or excavation implies change of boundary condition position. For instance, the atmospheric conditions (rain and evaporation at soil surface) move as soil layers are constructed in an embankment. Applications of earth dam construction are presented to illustrate the capabilities of the program.

2. GENERAL DESCRIPTION OF CODE_BRIGHT

CODE_BRIGHT is a finite element code for the analysis of THM problems in geological media. A porous medium composed by solid grains, water and gas is considered. Thermal, Hydraulic and Mechanical aspects are taken into account, including coupling between them in all possible directions. As illustrated in Figure 1, the problem is formulated in a multiphase and multispecies approach.

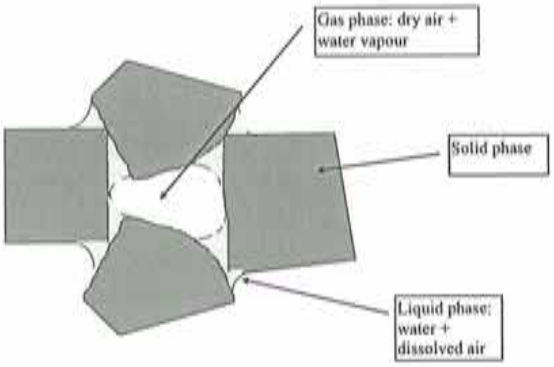

The three phases are

- solid phase (*s*):
- liquid phase (*l*): water + air dissolved + solute
- gas phase (*g*): mixture of dry air and water vapour

The three species are:

- solid (-): mineral
- water (*w*): as liquid or evaporated in the gas phase
- air (*a*): dry air, as gas or dissolved in the liquid phase
- solute (c): in the liquid phase

Figure 1. Schematic representation of an unsaturated porous material

Table 1: Constitutive equations and equilibrium restrictions

EQUATION	VARIABLE NAME
Constitutive equations	
Darcy's law	Liquid and gas advective flux (conductivity depends on porosity, water content and temperature)
Fick's law	Vapour and air non-advective fluxes Solute non-advective fluxes (diffusion + dispersion)
Fourier's law	Conductive heat flux (thermal conductivity depends on porosity, water content and temperature)
Retention curve	Liquid phase degree of saturation
Mechanical constitutive model	Stress tensor. Models for unsaturated geological materials developed using EP and VP approaches
Phase density	Liquid density. Depends on pressure, temperature and solute concentration.
Gases law	Gas density. Ideal gases law for the mixture of vapor and dry air.
Equilibrium restrictions	
Henry's law	Air dissolved mass fraction.
Psychrometric law	Vapor mass fraction as a function of temperature and capillary pressure.

The following assumptions are considered in the formulation of the problem: Dry air is considered a single species and it is the main component of the gaseous phase. Henry's law is used to express equilibrium of dissolved air. Thermal equilibrium between phases is assumed. This means that the three phases are at the same temperature. Vapor

concentration is in equilibrium with the liquid phase, the psychrometric law expresses its concentration. State variables (unknowns) are: solid displacements, $\boldsymbol{u}$ (three spatial directions); liquid pressure, P_l; gas pressure, P_g; and temperature, T. Balance of momentum for the medium as a whole is reduced to the equation of stress equilibrium together with a mechanical constitutive model to relate stresses with strains. Strains are defined in terms of displacements. Small strains and small strain rates are assumed for solid deformation. Advective terms due to solid displacement are neglected after the formulation is transformed in terms of material derivatives (in fact, material derivatives are approximated as eulerian time derivatives). In this way, volumetric strain is properly considered. Balance of momentum for dissolved species and for fluid phases are reduced to constitutive equations (Fick's law and Darcy's law). Physical parameters in constitutive laws are function of pressure and temperature. For example: concentration of vapour under planar surface (in psychrometric law), surface tension (in retention curve), dynamic viscosity (in Darcy's law), are strongly dependent on temperature.

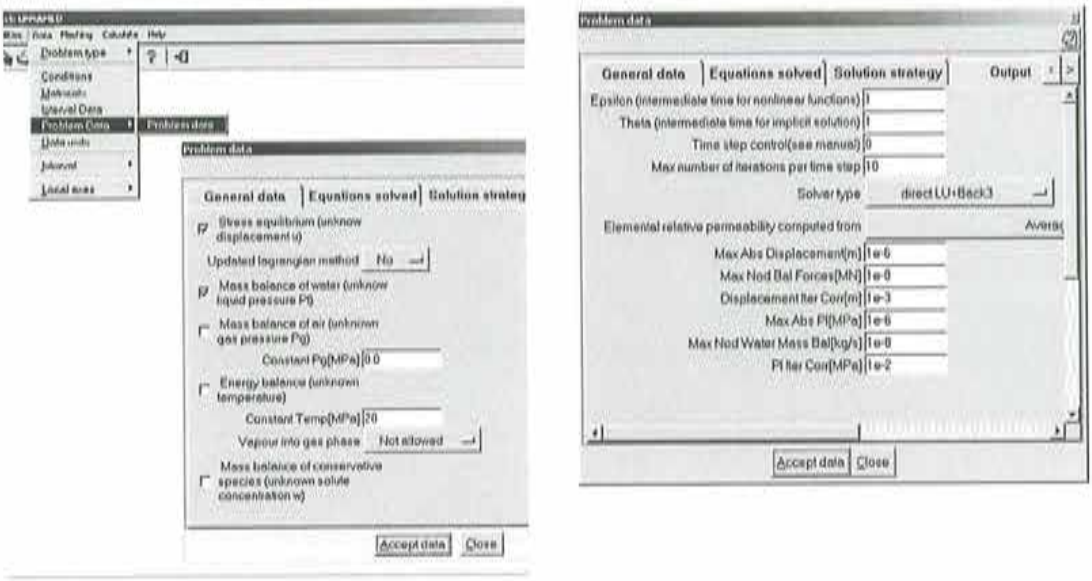

Figure 2. Customized window where the equations to be solved are selected. Dynamic options are used (e.g. **Constant Pg** is only required when air balance is not solved and disappears as the air equation is ticked). **Solution strategy** and **Output** sections contain default values (e.g. for tolerances that control convergence of nonlinear iterations).

The governing equations that CODE_BRIGHT solves are: Mass balance of solid, Mass balance of water, Mass balance of air, Momentum balance for the medium, Internal energy balance for the medium, and Mass balance of solutes. Associated with this formulation there is a set of necessary constitutive and equilibrium laws. Table 1 is a summary of the constitutive laws and equilibrium restrictions that should be incorporated in the general formulation. The dependent variables that are computed using each of the laws are also included.

The constitutive equations establish the link between the independent variables (or unknowns) and the dependent variables. There are several categories of dependent variables depending on the complexity with which they are related to the unknowns.

1The governing equations are finally written in terms of the unknowns when the constitutive equations are substituted in the balance equations.

The resulting system of PDE's (Partial Differential Equations) is solved numerically. The numerical approach can be viewed as divided into two parts: spatial and temporal discretizations. Finite element method is used for the spatial discretization while finite differences are used for the temporal discretization. The discretization in time is linear and the implicit scheme uses two intermediate points, $t^{k+\varepsilon}$ (for nonlinear terms) and $t^{k+\theta}$ (for gradient terms) between the initial t^k and final t^{k+1} times. Finally, since the problems are non-linear, the Newton-Raphson method was adopted to find an iterative scheme.

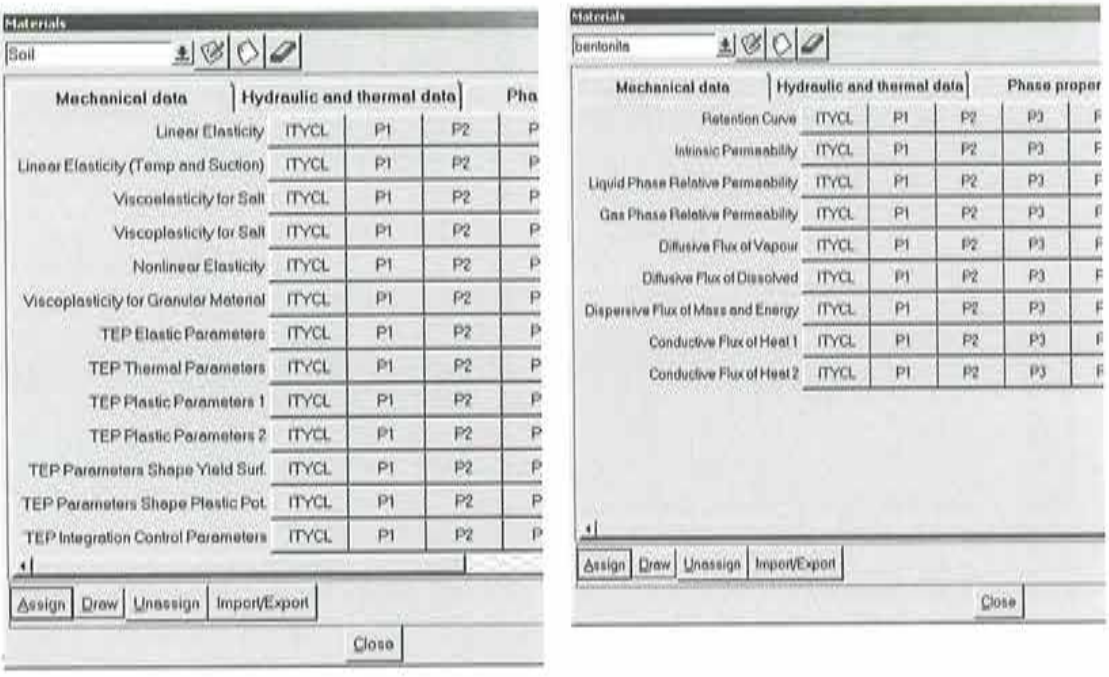

Figure 3. Customized window for material parameter input. Note that Mechanical models, hydraulic/thermal and Phase properties have been grouped.. **ITYCL** is used to decide types of laws inside a constitutive law (e.g. Viscoplasticity for granular materials may have different options of flow rules). Each line contains a maximum of 10 parameters (**P1, P2**, etc) and hence some laws are defined in a series of lines (e.g. **TEP** model).

A number of improvements have been done in the code since its early development, namely: construction/excavation, time step control by error estimates, iterative solver with compressed sparse storage, quadratic elements and new constitutive laws.

3. APPLICATION OF CODE_BRIGHT TO CIVIL ENGINEERING PROBLEMS. LONG TERM BEHAVIOUR OF AN EARTH DAM

Figure 4 shows an earth dam which was constructed in Algarve (Portugal) using rockfill and clay. This earth dam was extensively monitorized in terms of displacements, pressures and stresses. Alonso, Olivella and Pinyol (2005) present a review which includes geotechnical analysis of the dam behaviour taking into account construction stages, water level rise in the reservoir and long term behaviour during different rainfall

events. The constitutive models used in that contribution (Rockfill Model and Barcelona Basic Model) have been integrated using a viscoplastic approach and are the more advanced framework existing in the field of geotechnics of earth dams.

Beliche dam (Algarve, Portugal)

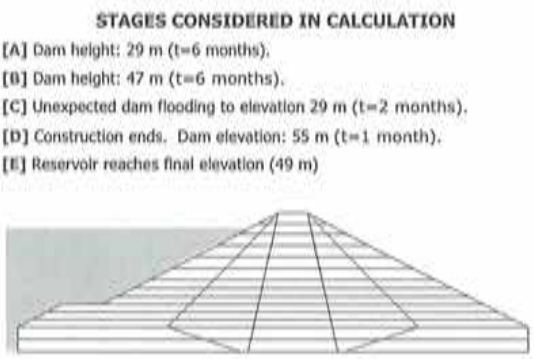

Intervals included during the analysis

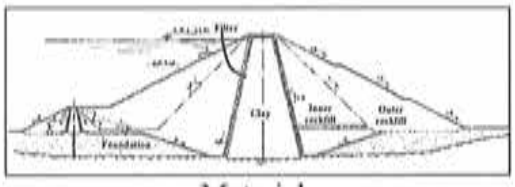

Materials

Finite element mesh made of quadratic triangles

Figure 4. Modelling an earth dam (rockfill shoulders + clay core). (from Alonso, Pinyol and Olivella, 2005).

This problem is used in this paper to discuss different aspects that are related to the modelling performed.

Material Parameters

The material parameters in this problem consist in hydraulic parameters and mechanical parameters. The hydraulic parameters are hydraulic conductivity, retention curve (water content versus capillary pressure) and relative permeability. All are nonlinear functions. The mechanical parameters correspond to a generalized viscoplastic model for unsaturated soils and rockfills, based on Perzyna theory. Flow rule, failure envelope and compression parameters are different for the clay core and for the rockfill shoulders. A total of 15 parameters are required for each material (clay core, inner rockfill, outer rockfill). Hence, the existing possibility in GiD to import and export a material is obviously extremely useful as permits to transfer sets of parameters from one problem to another. In principle, history variables (such as preconsolidation stress) are required as a function of space, however if construction is simulated, these history variables can be set constant by surfaces or volumes, or by materials.

Construction intervals

The stress state in a geotechnical structure such as an earth dam can only be determined if the construction is simulated realistically. In this problem, construction was simulated by layers (these are indicated in Figure 4). In CODE_BRIGHT, materials and construction layers are identified, and therefore a number of materials have to be defined in this case. However, any new material can be defined as having the same

properties as an existing one. For instance, any new layer of soil has the same properties as the ones already constructed but the material is still in its soft state (hardening history variables have not yet changed because they are element dependent). Even construction using thin layers may be a numerical problem if the loading is instantaneous. Therefore, in order to smooth the construction process, the final weight of each layer is achieved in a ramp way during the time interval. Since the material is soft during construction, the self weight and the progressive construction of subsequent layers implies a hardening of the material which is realistic. In CODE_BRIGHT, a material may have 3 states: (a) active, (b) is constructed during the interval and (2) not active (has been excavated or not yet constructed). Construction of each layer is done during specified time periods (intervals).

Excavation of soil layers is also possible but does not happen in this example. Excavation in a smooth way is not a straight forward question. For instance, excavation of a tunnel requires not only to deactivate the material but also to decrease the pressure that is exerting on the wall surface of the tunnel.

Boundary conditions

Boundary conditions are quite standard for the mechanical problem. They are prepared for loads (**nodal**) or stresses (**boundary**) and permit to prescribe displacement rates or force/stress constant values or increments (for instance a ramp loading during a given interval). Flux boundary conditions can be **nodal**, **boundary** or **volume** and permit to represent, for instance: a well in an aquifer (**nodal**), a constant pressure at a boundary (**boundary**) or a rain on a surface (**volume**), among other cases. **Boundary** and **Volume** apply to line-surface or surface-volume, respectively, depending if the problem is in 2 or 3 dimensions.

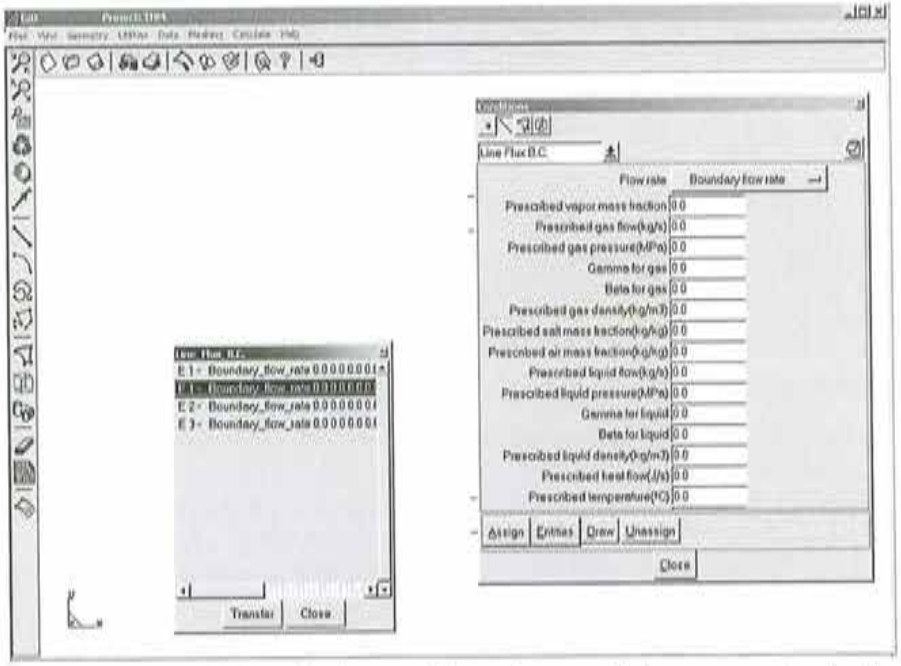

Figure 5. Customized window for input of boundary condition parameters in the case of **Flux** type boundary condition.

Boundary conditions of **Flux** type include all the parameters required for the boundary conditions related for Water, Air, Energy and Solute conservation. For instance, if only temperature is to be prescribed at a boundary, only the prescribed value (T_o) and a constant (γ) have to be introduced (heat flow rate is calculated as: $Q_h = \gamma(T-T_o)$). But the **Flux** condition includes terms to prescribe vapor concentration, water infiltration (e.g. rain), atmospheric pressure prescription, etc. The parameters of boundary conditions, in general, change with time and for this reason increments can also be input. An increment is applied during a time interval, and for the next time interval the new achieved values should be input in the boundary conditions.

The problem of the earth dam described in figure 4 requires several boundary conditions. The earth layers that are constructed are exposed to the atmosphere and hence, rain and relative humidity (suction in this case) should be prescribed during time. Since the exposed surface to the atmosphere in the earth dam changes with time, the boundary condition should change with space and time. The boundary conditions applied to unconstructed layers are not active until the layers are constructed. As a new layer is constructed the boundary conditions should disappear. Figure 6 shows the rainfall evolution and dam water level in the reservoir that were applied as boundary conditions. The response in terms of water pressure in the dam (time evolution plot and contour field plots) shows that transient conditions prevail due to continuous changes in boundary conditions. Upstream and downstream points undergo different response due to water level in the reservoir, but the downstream points are reach liquid pressures close to zero.

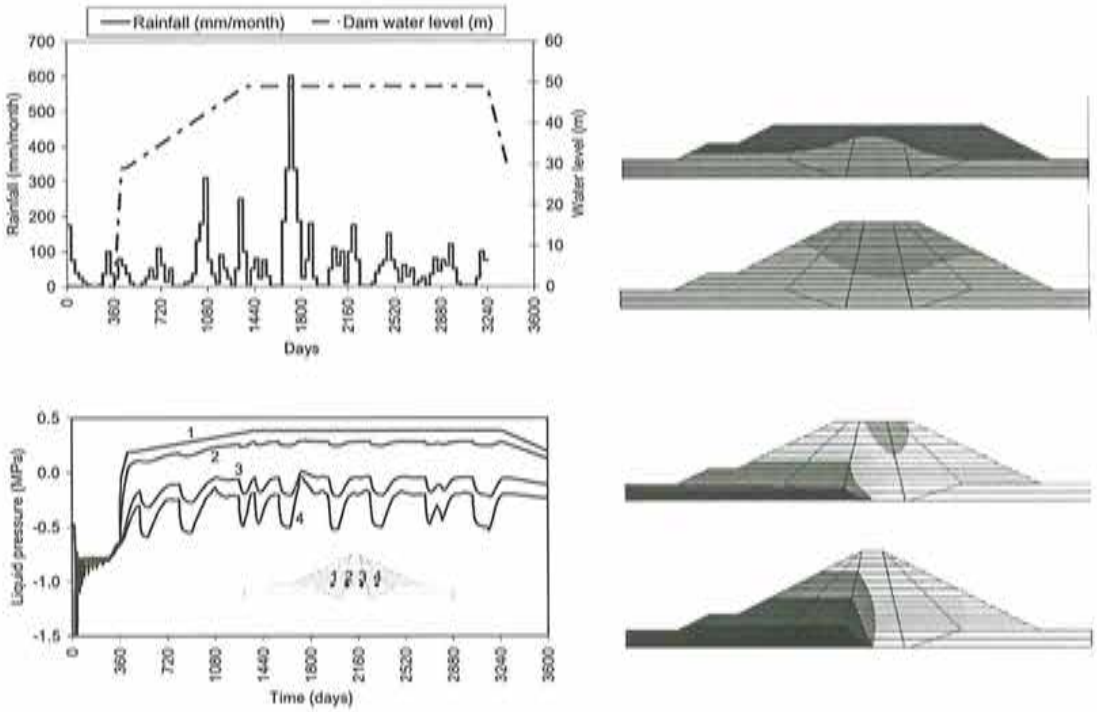

Figure 6. Evolution of rainfall and water level in the reservoir and response of liquid pressure in the dam (Alonso, Olivella and Pinyol, 2005).

The impounding history of the reservoir is simulated by means of a set of periods in which the water level changes linearly between the two extreme times (t_a, t_b) considered. To this end, the auxiliary function:

$$p(t) = \frac{t - t_b}{t_a - t_b} \quad \text{for} \quad t_a < t \leq t_b \tag{1}$$

is introduced. Water pressure at a point of the boundary having a vertical height, y, above the reference level, is given by:

$$p_w = \gamma_w h(t) \tag{2}$$

where

$$h(t) = H \times p(t) - y \qquad \text{if} \quad H \times p(t) > y$$

$$h(t) = 0 \qquad \text{if} \quad H \times p(t) \leq y \tag{3}$$

where H is the maximum reservoir level in the period considered. Normal stresses on the upstream boundary are specified equal to the liquid water pressure:

$$\sigma_n = p_w \tag{4}$$

Alternatively, the water in the reservoir can be represented explicitly as a material with appropriate parameters equivalent to water properties. If this material can undergo the two states, namely dry and fully saturated, then the water level variations can be represented adequately.

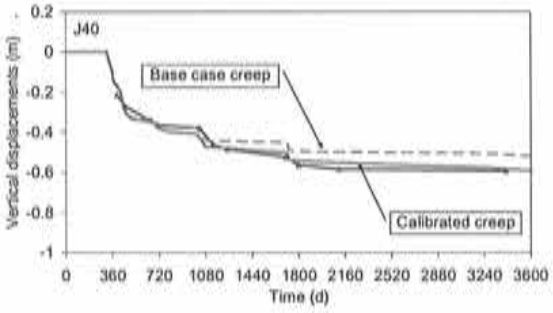

Displacements measured and calculated at a point near the crest of the dam.

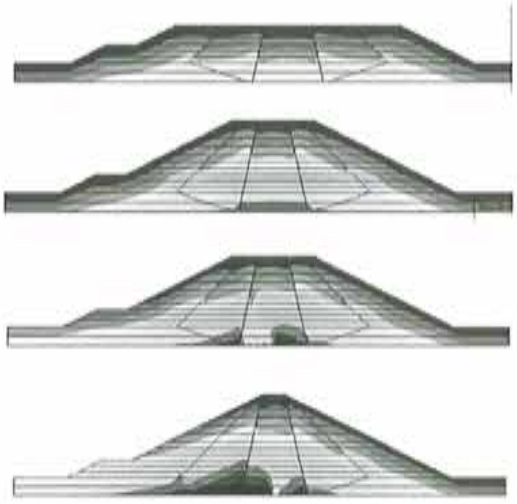

Figure 7. Evolution of displacements and vertical stress distribution (Alonso, Olivella and Pinyol, 2005).

Finally, Figure 7 shows the results of displacements (evolutions) and stresses (distribution at different stages of the model) in the earth dam. The displacements are compared with measurements that were recorded during several years. Note that the displacement increase around 1800 days is related with a peak in the water pressure curve (Figure 6). This is due to a collapse deformation induced by impoundment that

takes place in the clay core and the rockfill shoulders. Intensity and duration of rainfall events play a major role in the earth dam long term behavior. Stress distribution is quite sensitive to collapse, as the collapsing zones undergo unloading while the zones that remain more stiff undergo loading.

Intervals in time

As mentioned above, intervals in time are important in geotechnical applications. For instance, in the described case there are several intervals for which different actions take place. For instance, construction of each layer requires a time interval. Change in boundary conditions also requires a time interval. When GiD is used, an initial interval is defined and all the information is introduced. As new intervals are introduced, some information should be modified. A table *time-value* can also be incorporated if required for a given parameter.

4. APPLICATION OF CODE_BRIGHT TO CIVIL ENGINEERING PROBLEMS. STABILITY OF TAILING DAMS

Figure 8 and figure 9 show another example of geotechnical analysis. The model represents the construction of a dam made of mine tailings (Lloret y Olivella, 2005). An old waste fill which is similar to a clay material and that has low shear strength under undrained conditions is filling a valley where a salt tailing dam should be constructed. The model was used to predict the safety factor to failure using the shear strength reduction method. Accurate simulation of the construction of the layers that form the new dam is important as failure may take place during this process.

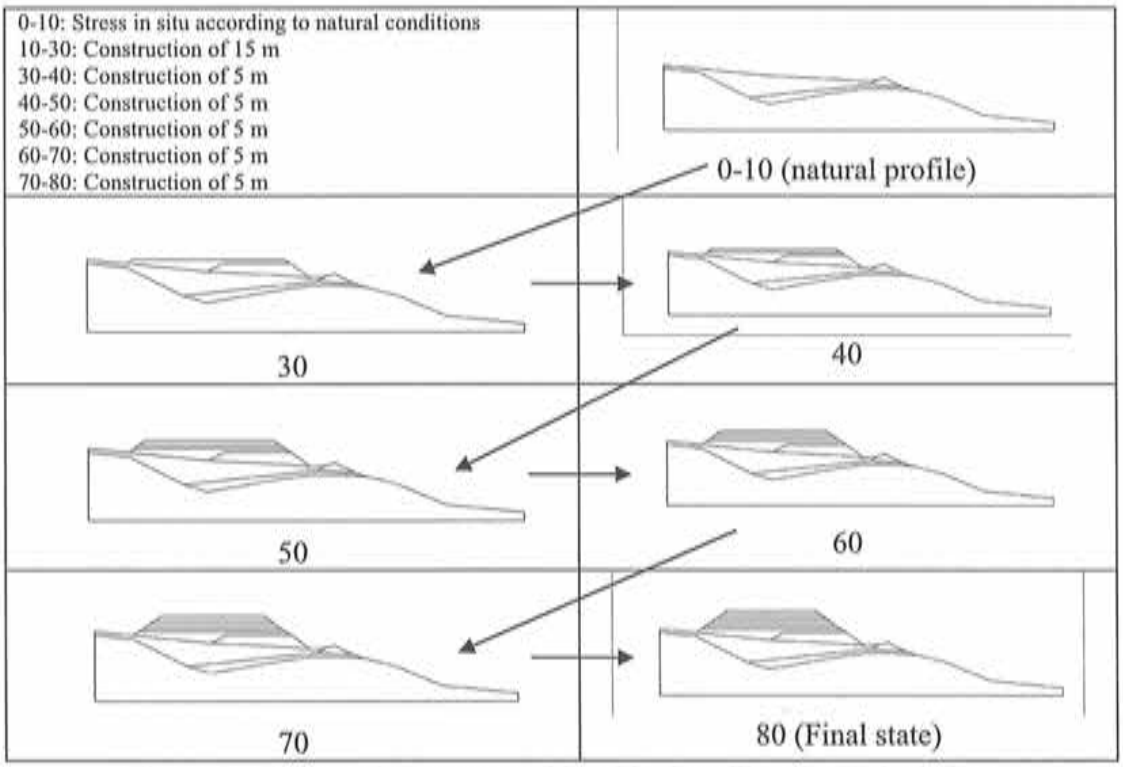

Figure 8: Construction steps considered in the tailing dam calculation.

Figure 9. Displacement field at failure (undrained shear strength: 30 kPa).

5. CONCLUDING REMARKS

The customization of GiD for CODE_BRIGHT pre- and post- processing has been a successful task and we have available a user-friendly tool for advanced geotechnical analysis. Post process has been a relatively straight forward task. After some preliminary steps in the customization of the pre-process, CODE_BRIGHT was modified in some aspects related to boundary condition assignation to boundaries because the original development was not adequate for graphical introduction of boundary conditions. The success of the customization can be demonstrated by evaluating the capacity of solving problems directly through GiD. Several things can be improved including new capabilities but the steady state regime has been achieved.

Geotechnical applications for unsaturated soils including thermal effects are probably the problems that make the difference of CODE_BRIGHT-GiD in comparison to other existing codes. CODE_BRIGHT was developed originally for analysis of radioactive waste disposal schemes that contain engineered barriers (made of compacted impermeable soils). Several utilities that were not foreseen in the original program development, such as structural elements, geotextiles and geomembranes, anchors, etc; should be developed in the future.

6. REFERENCES

Alonso, E., S. Olivella, N-M. Pinyol (2005). A review of Beliche dam. *Géotechnique*, 55(4): 267-285.

Lloret, A. y S. Olivella (2005). Propuesta de análisis de estabilidad para la construcción de una presa de sal granulada en las minas potásicas de Sallent. Informe Departamento de Ingeniería del Terreno, UPC.

Olivella, S., A. Gens, J. Carrera & E. E. Alonso (1996). Numerical formulation for simulator (CODE_BRIGHT) for coupled analysis of saline media. *Engineering computations*, 13(7): 87-112.

Vaunat J and S. Olivella (2002). CODE_BRIGHT-GiD. A 3-D program for Thermo – Hydro – Mechanical Analysis in Geological Media. 1st Conference on Advances and Applications of GiD. 20, 21 and 22 February 2002. Barcelona, Spain

APPLICATION OF GID ON THE MODEL OF ONE TEMPLE OF THE HISTORICAL CENTER OF PUEBLA'S CITY

J. Lozano

Facultad de Ingeniería, BUAP
Puebla, México
dlozano@siu.buap.mx

Key words: unreinforced, masonry, modeling, meshing

Abstract: *The historical center of Puebla's city is part of the list of the world patrimony of the UNESCO since 1987, because Puebla's city was the second more important city in the Nueva España; the majority of the constructions were made with unreinforced masonry, on the other hand the Mexican Republic is frequently affected by earthquakes with epicenters near to the pacific coast where exist subduction zones. The finite element method requires the elaboration of models that take in account the problems relational with the geometry, the material's behavior and the boundary conditions. In the document is presented the complete model of the temple and also two and three dimensional models in which were divide the structure to realize the partial studies. The models were processed with the use of the SAP2000 software obtaining the vibration modes, the deformation and the stresses diagrams for gravitational and seismic loads.*

1 INTRODUCTION

Puebla's city was founded in 1531 and its historical center was included by the UNESCO (1987) in the list of the world-wide Patrimony with 2619 classified historical buildings. The construction of the historical buildings is located between centuries XVI and XIX, the majority of them built with unreinforced masonry, formed by units of stone or brick and meetings of mortar, that's why the material is a heterogeneous compound with a nonlinear behavior.

The conservation of the historical patrimony of the city implies the study of vulnerability of buildings built with masonry; in special form, the study of the ancient temples of the city that are in use is required and which they showed vulnerability in the seismic events of 1973 and 1999; both of them with epicenters distances less than 170 km of the Puebla's city and with mechanisms of normal fault. It is worth noting that the problem of damages in ancient constructions of unreinforced masonry and in particular in the case of temples, is not circumscribed to the urban area of the Puebla's city, since in relation to the earthquakes of 15 and 21 of June and of the 30 of September of 1999, the FONDEN[i] reported damages in one thousand three hundred ancient constructions in seven states of the Republic.

The evaluation of the seismic vulnerability of an ancient construction implies the study of the answer of the structure and the estimation of damages before on one important seismic demand, presenting diverse challenges:

- The elaboration of the structural model.
- To consider the history of the construction with additions or retirement of elements.
- The quantitative evaluation of the resistance of the structure it's more difficult because it's not easy to get experimental results of the structural elements and from the materials that constitute them.
- The dynamic behavior is complex to be modeled with the models of concentrated masses employees in skeletal structures.
- The behavior obtained in a linear elastic analysis only represents the departure point for a study that considers the behavior nonlinear of the material.

2 STRUCTURAL MODELS

Is required to establish a mathematical model that represents of the best possible form the real problem but at the same time the model must be simple and easy to analyze. The model definition implies to take in account the geometry, the material's behavior and seismic actions that could act on the structure.

The damages after one earthquake help to define the collapse mechanisms that must be considered to know the answer in a limit analysis, this is also applied to the temples, since the absence of one continuity cause frequently partial collapses in weak zones, that may be were not known.

In the case of ancient buildings not always the most advisable is to work with complete three-dimensional models that include all the elements that constitution the structure[ii]. Two-dimensional models can be used to obtain satisfactory results of the structural behavior of the macro element in the plane.

The location, the dimensions, aspect ratio, the continuity or not of the different structural elements are the departure point for the elaboration of the structural model. For the modeled one of the material two options exist, the micro and the macro modeled, using the homogenization technique. The analysis methods depend on the target, on the information successfully obtained in relation to the materials and to the degree of deterioration of such, of the costs, the complexity, the importance and the size of the structure.

With relation to the analysis, Croci indicates the convenience of making a first elastic analysis to detect the zones of tension where the cracking based on the loads will appear later and an analysis nonlinear, step by step, increasing the loads to locate the border of the

resistance dominion and to determine the rigidity of the structure in each stage, eliminating the participation of the elements that have reached a state limit[iii].

3 MODELS AND ANALYSIS

After the topographical survey, were done the drawings in AutoCAD, considering the simpler geometric characteristics without modifying the structural concept; the files exported to the GID[iv] for their discretation using plate elements with nodes on its three apexes and linear approximation and with the aid of this preprocessor the meshing one was made having in account the thickness of the walls; later the meshing model was returned to the AutoCAD to operate it and to be able to import it from the SAP2000, where is assign the material information, the conditions of border and the loads for the required analysis (figures 1 to 5). The complete model have more of 60 000 elements.

4 CONCLUSIONS

The GID is a very useful tool to make the meshing one of models with complex geometries allowing the engineer to dedicate more time to the revision and to the interpretation of the results obtained after a finite element analysis.

REFERENCES

[i] Memoria FONDEN 2000. Rehabilitación de inmuebles históricos dañados por los sismos de junio y septiembre de 1999 en los estados de Guerrero, México, Morelos, Oaxaca, Puebla, Tlaxcala y Veracruz

[ii] P. B. Lourenço, "Historical Analysis of constructions: From thrust-lines to advanced simulations ", Historical Constructions, P. B. Lourenço, P. Roca (Eds.), Guimarães

[iii] G. Croci G, "Conservazione e restauro strutturale dei beni architttonici", 2001 UTET Libreria Srl

[iv] GID reference manual. "Pre and post processing system for F.E.M. calculations". International Center For Numerical Methods In Engineering (CIMNE)

Figure 1: Plane models (GID)

Figure 2: Two-Dimensional Masonry Wall

Figure 3: Complete Model

Figure 4: First Natural Mode

Figure 5: Third Natural Mode

Finite Element Modelling of Porosity during Solidification

Abbass Dabiransari*, Jordi Tartera†, Eugenio Onate‡

*Islamic Azad University, Karaj Unit, Iran.
† E.T.S. Inginieria Metalurgica Industriales, UPC, Barcelona, Espana.
‡ CIMNE, Universidad Polytecnica de Catalunya, Barcelona, Espana.

Key words: FEM, solidification, thermo-mechanical, damage, porosity

Abstract: *The present paper describes the computational framework for a fully coupelled macroscopic thermomechanical damage model which can predict the nucleation and growth of shrinkage porosity in a casting during its solidification.*
The numerical analysis results obtained from the model indicate that the combination of an apropriate thermal nucleation criteria and a Gurson's compressible growth model provide a reliable tool for the prediction of shrinkage cavities in geometrically complex castings.

1 INTRODUCTION

Casting may be defined as a classic metal forming process in which, a definite volume of the melt conformed to the shape of the mold cavity, hardens by losing its heat content to the environment, producing a stable solid part. This definition leaves behind in time history the melting and filling operations performed in the foundary practice, and only considers reflecting their effects in the initial and boundary value conditions of the thermo-mechanically coupelled solidification problem[i]. For which the application of the finite element approximate solutions of the problem, to describe the plastic and viscoplastic behaviour of the phase transformation are generally considered appropriate[ii,iii].

Despite successful continuous single crystal growth from the melt of some slow growth rate pure materials, in practice, even during the filling of the cold mold with the melt of a pure metal, many dendritic crystallites will form initially, and then the growth will generally proceed inwards from the wall, as heat is extracted. For an alloy it is even more complicated because the dendritic structure depends on the coupelled diffusion of heat and a competitive diffusion of chemical elements[iv].

Within the solidification body, because of the thermal and phase change contraction and/or expansions, once a solid skin is formed, porosity occurs because of the inability of the melt to feed localized regions in the casting[v,vi], and presence of the dissolved gases trapped in the melt[vi]. Cavitation can also occur when there is a negative pressure in the melt[iii]. Coalecense and pore diffusion can easily occur at these high temperatures of solidification[vii].

2 THERMAL NUCLEATION CRITERION

During the solidification phase transfer, thermal contractions and expansions, morphological evolution, and mechanical properties are all strongly temperature dependent. Consequently, after detailed careful analytical evaluation of the existing

thermal criteria functions in the literature[iii,ix,x], the following thermal porosity function was formulated to be used in the damage model;

$$TPC = \wp = 1 - \exp(-\alpha.\sqrt{t}\left(\frac{Rate}{\sqrt{GradT}}\right))$$

Here, $\wp$ is the Thermal Porosity Criterion function, in which t is the solidification time, $GradT$ is the temperature gradient and $Rate$ is the rate of cooling for an element of material. This function combines the Niyama[ix] thermal criteria variables and Lee's[x] local solidification time. In this function α is an adjustable parameter which depends on the material. The value of α taken in the present analysis is $\alpha = 0.005$.

$\wp$ can vary within the range of $0 \le \wp \le 1$. And the probability of shrinkage cavity formation increases with the increase of this variable, reaching the maximum when $\wp = 1$. It is considered that the total fraction of porosity for each element will be;

$$f_{tot} = f_n + f_g$$

Where, sub-indices tot, n and g indicate total, nucleation and growth respectively.

3 GURSON VOID MODEL

Gurson formulated the following mathematical expression of the yield surface for a Vom Mises perfectly plastic material;

$$\Phi(J_2(s), tr\sigma, \sigma_M, f) := J_2(s) - \frac{1}{3}\left\{1 + f^2 - 2f \cdot Cosh\left(\frac{3p}{2\sigma_M}\right)\right\}\sigma^2{}_M$$

Where, f is the porosity fraction and the damage variable, p is the pressure, σ_M is the actual uniaxial yield stress of the material matrix in tension , and $\sigma_M = \sigma_0 + K(R)$ in which σ_0 s the initial yield stress, $K(R)$ is a hardening function depending only on a single parameter R .

This yield surface allows the desired expansion and contraction of the matrix material.

Details of the theory and its implementation within a general framework of the plasticity, are given in previous references[3].

It can be seen from the form of the yield function that when the fraction of porosity is at zero percent, then the Gurson yield criteria returns to its original Von Mises condition. Also, we assume that the softening effect of the porosity growth is independent from the thermal hardening during each time step.

Figure 1. The 2D and 3D Sections of the meshed sreel bar in the sand mold.

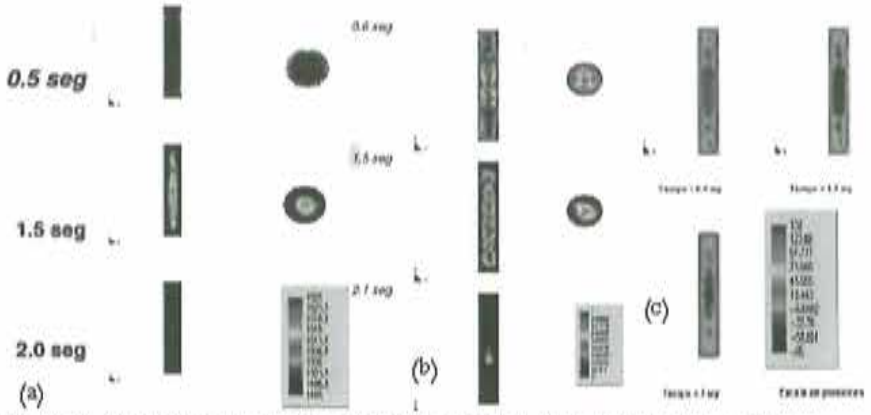

Figure 2. (a)Mushy zone evolution. (b) TSC evolution. (c) Local pressure evolutions.

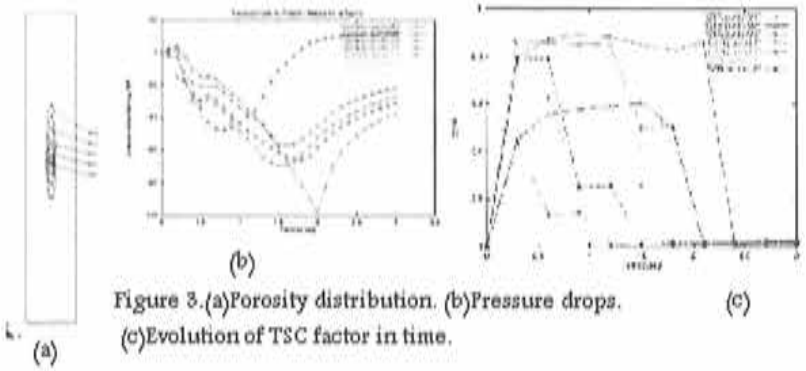

Figure 3.(a)Porosity distribution. (b)Pressure drops. (c)Evolution of TSC factor in time.

4 ALYSIS and RESULTS

Solidification process of a simple cylindrical, low carbon steel bar in a sand mold has been analysed employing the Vulcan thermo-mechanical code in which the present gurson damage model has been implemented[iii].

In Figure 1, sections of the meshed geometry of the solidification analysis sample has been shown. The diameter of the bar is 10 mm and its length is 60 mm, cast in a cylindrical sand mold.

A further meshing sub-structure, that is cylinders within cylinders inside the 10 by 60 mm steel bar has been imposed, to help with the iniciation and propogation of porosity nucleation during the course of the analysis. The right hand side image shows the meshing sub-structure of cylinders in the steel bar, and identifies three points across the mid-height section of the bar. These points have been used to follow the evolution of the variables during the analysis. The solidification temperature range for this steel bar has been taken to be between 1525 (solidification starts) and 1495 degrees centigrade (ends). More complete details of the thermal and mechanical properties used in the present work can be found in references available at cimne[iii].

In Figure 2, three time evolution results obtained from the analysis have been shown, (a) shows the advancing mushy zone at different times of the solidification analysis. (b) shows the evolution of the Thermal Porosity Criterion (TPC) values, which have been used here to indicate the starting time and location of nucleation in a material element in the bar, by triggering the damge growth model. (c) shows the average pressure

distributions in the bar at different times during the solidification. The concentration of the negative hydrostatic pressures at the center of the bar can be observed.

Figure 3, (b) and (c) show the relative evolution graphs of TPC values and mean pressure values, at identified points on the axis of the bar (note the maximum pressure drop to approximately -20 MP at the center of the bar). Figure 3, (a) shows the distribution of the porosity within the solidifying steel bar.

5 DISCUSSIONS and CONCLUSSIONS

The results presented here in this paper demonstrate that:

A) The thermal criteria function, based only on the thermal results of the solidification analysis, indicates an experimentally acceptable "hot spot" at the thermal center of the cylindrical specimen as the most probable point at which the initial nucleation of the porosity can occur.

B) Demonstrate how the implementation of the Gurson damage model within the framework of the finite element formulation of thermo-plastic hardening model can produce expansion or contraction of porosity in response to the local hydrostatic pressure in the volume element material matrix. In the present context this local growth of the porosity is a consequence of the thermally confirmed TPC signal, and the propagation gradient created through the cylindrical sub-structured meshing.

We can conclude that, the nucleation followed by the porosity growth of the Gurson model, has simulated the physically logical response of the sample to the negative hydrostatic pressures in the solidifying steel bar. Considering the physical importance of the pressure terms as far as the thermodynamics of the closed and open material bodies are concerned, many useful applications of this damage model can be devised, of which casting porosity is one of the traditionally complex ones, presented in this work.

REFERENCES

[i] E. Onate, D. Celentano, R. Codina, S. Oller, O. Soto, A.D. Ansari and G. Duffett, "Avances en la Simulacion del llenado del Moldes y del Proceso de Solidificacion y Enfriamiento en Fundicion", *Proc. II Congresso Iberico de Fundiciones*, Oporto, Portugal, 1996.

[ii] D. Celentano, A. Dabiransari, J.Tartera "*Un Modelo Viscoplastico para Simular la Solidificacion y el Enfriamiento de la fundicion de Hierro*", Proc.ENIEF95: 9th Congress on Numerical Methods and Their Applications, S.C.de Bariloche, Argentina, 6-10 Nov.1995.

[iii] A. Dabiransari, "*Simulacion Termomecanica de la Solidificacion en Fundicion Ferrea*", Tesis Doctoral, UPC, Barcelona, Espana, 1997.

[iv] B. Chalmers, "*Principles of Solidification*", Jhon Wiley & Sons, inc., New York, 1964.

[v] J. Campbell, "*Casting*", Ed. Butterworth-Heinemann Ltd., Oxford, 1991.

[vi] V.K.Suri, Nagy El-kaddeh, and J.T. Berry,"*Control of Macrostructure in Aluminium Casting* ", Trans. AFS, vol. 70, 1991, pp 187-191.

[vii] A. Dabiransari, "*Nitrosintering and physical properties of Stainless Steel Strip*", M.Eng. Thesis, Liverpool University, England, 1980.

[viii] A.L. Gurson, "*Continuum Theory of Ductile Rupture by Void Nucleation and Growth: Part I , Yield Criteria and Flow Rules for Porous Ductile Media*", J. of Eng. Materials and Technology 99, 2-15,1977.

[ix] E. Niyama, T. Uchida, M. Morikawa, M. Saito, "*Predicting Shrinkage in large Steel Castings from Temperature Gradient Calculations*", AFS Int. Cast Metals Institute Jnl., 6,pp. 16-22,1981.

[x] Y.W. Lee, E. Chang, C.F.Chieu, "*Modelling of Feeder Behaviour of Solidifying Al-7Si-0.3Mg Alloy Plate Casting*", Met. Trans. 21B,pp. 715-722,1990.

GID INTERFACE TO A 3D TOPOLOGY OPTIMIZATION TOOL

Iuliana Matei[*], Inga Shklyar[*] and Emanuel Teichmann[*]

[*] Fraunhofer Institut für Techno- und Wirtschaftsmathematik (ITWM)
Fraunhofer-Platz 1, 67633 Kaiserslautern, Germany
e-mail: {matei, shklyar, teichmann}@itwm.fraunhofer.de, web page: www.itwm.fhg.de

Key words: Topology Optimization, Level Set Methods, Topological Gradient

Abstract. *In the framework of the project "MIDPAG – Innovative Methods for Integrated Dimensioning and Process Design for Cast Parts", an environment for a complete topology optimization simulation has been created under the GiD graphical user interface. The optimization algorithm (TopLevel) is based on level set methods and the topological gradient and includes a fast iterative and parallelized structural analysis solver (DDFEM). Various modules for data definition, automatic start of the optimization process on a remote parallel computer, and post-processing of the optimization results are fully integrated into the presented GiD-TopLevel interface.*

1 INTRODUCTION

The aim of the project "MIDPAG - Innovative Methods for Integrated Dimensioning and Process Design for Cast Parts" is twofold:

On one hand, an algorithm for iterative solution of topology optimization problems has to be developed. Starting from as few data as possible, i.e., a specification of the design space (maximal admissible volume of a structure) and a description of the applied boundary conditions, the optimal shape and topology (material distribution within the design space) of the structure have to be determined. At this, optimality can be defined in different ways. One example is maximization of stiffness combined with a prescribed volume reduction. More general objective functions can be chosen.

On the other hand, the handling of the resulting software has to be simple and intuitive and should not require special knowledge in topology optimization or FEM computations.

The solution to the first problem is the topology optimization software TopLevel. It is based on level set methods and the topological gradient, which is computed from the results of a structural analysis being performed in each iteration on the remeshed structure under consideration. Therefore it includes modules for initialization of the level set function and contouring (LevelDict[i]), a fast iterative and parallelized FE solver (DDFEM[ii]), and a tetrahedral volume mesh generator (TetMesh[iii]). A graphical representation of the software chain is given in Figure 1.

For the solution of the second problem we aimed at unification of the software packages

mentioned above under a common graphical user interface (GUI). This GUI had to be as intuitive and simple as possible but powerful enough to handle the complexity of the structures and load cases under consideration.

We chose the GUI of GiD as the basic component for the solution of the second problem since it provides tools for pre- and post-processing, i.e., designing the structure and visualization of results of a topology optimization or FE computations. Moreover, it is possible to program user-defined modules for data definition, especially boundary conditions and material data. This data can be assigned graphically to surface patches or volumes. Menu items can be used to automatically start external processes via script files.

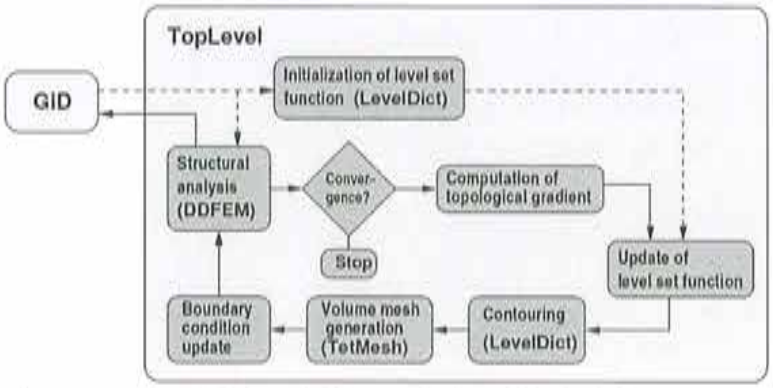

Figure 1: Graphical representation of TopLevel. The steps indicated by dashed lines are performed only once.

Therefore, the entire optimization process can be conveniently set up, triggered, and evaluated under one and the same graphical user interface.

Section 2 of this paper describes the GiD interface to the topology optimization software TopLevel. In section 3, TopLevel is presented in greater detail. The main ideas of the topological gradient and the level set function approach we used are given. Conclusions, acknowledgements, and a list of references finish the paper.

2 INTERFACE

In order to represent real-life load cases as realistically as possible, interfaces for specification of several types of boundary conditions had to be implemented. Using the GiD-TopLevel interface, it is now possible to define displacement constraints for nodes, edges, and geometric surfaces. Furthermore, loads can be applied to nodes and geometric surfaces. For surfaces, we distinguish between normal surface load, pressure surface load, and bearing pressure load. In the first case the load acts in direction of the normal of the surface, whereas in the second case an arbitrary direction can be prescribed. Bearing pressure loads approximate the force exerted on the surrounding cylinder by a rigid bolt (axle, rivet, ...) which is positioned in a drill hole. Momentum boundary conditions can be assigned to surfaces by specification of a neutral axis and the values of a momentum with respect to the coordinate axes. Finally, body forces in terms of acceleration vectors along coordinate axes can be assigned to the entire structure.

Boundary conditions are assigned to surfaces by graphically selecting the respective surface. It is possible to display boundary conditions. These functionalities are provided by GiD. The optimization parameters required by TopLevel, such as target volume, maximal number of iterations, or choice of stopping criterion, can be comfortably entered under the

same interface. This is an alternative to the more error-prone use of text files.

3 TOPLEVEL

As shown in Figure 1, the 3D topology optimization tool TopLevel incorporates a FE solver, a tetrahedral mesh generator, and level set function modules. Starting point for the topology optimization is a CAD description of the structure to be optimized together with a description of the applied boundary conditions. This data is set up using the GiD-TopLevel interface. The initialization module of LevelDict transforms a surface triangulation of the geometry into a level set function representation, which is the basis for alteration of the structure during the optimization process. After meshing the structure with TetMesh, the boundary conditions are transferred automatically to the new volume mesh. The results of the subsequent structural analysis being performed by DDFEM are used to compute the topological gradient, i.e. a criterion for alteration of the level set function describing the structure. The optimization loop is closed by generation of a new surface description in stl format by the contouring module of LevelDict.

To keep computation times low, it is extremely important to solve the elasticity problems occurring in the optimization iterations fast. We use DDFEM, which is a parallel 3D linear elasticity solver for steady-state problems. It scales very well to large numbers of CPUs and performs much better than many other elasticity solvers, even commercial ones. More information on DDFEM can be found in[ii,iv].

The main idea of the level set function approach is to represent the structure's boundary as the zero level set of a function $\varphi: \mathbb{R}^3 \rightarrow \mathbb{R}$. Negative function values indicate the interior of the structure, positive values the outside. The usage of a level set function for representation of the structure has important advantages, especially if boundaries have to be moved, as it is the case during the iterations of the optimization process. Creation, merging, and deletion of holes come absolutely naturally and trouble-free. The precision of the boundary representation and the resolution of the finite element mesh are decoupled, which allows for higher flexibility. Remeshing and update of the boundary conditions in each iteration automatically build a complete FE model of the structure. The structural analysis is performed in each step, such that the quality of the optimization results can be evaluated immediately. Compared to methods operating on a fixed mesh, our method is more accurate due to adaptive remeshing.

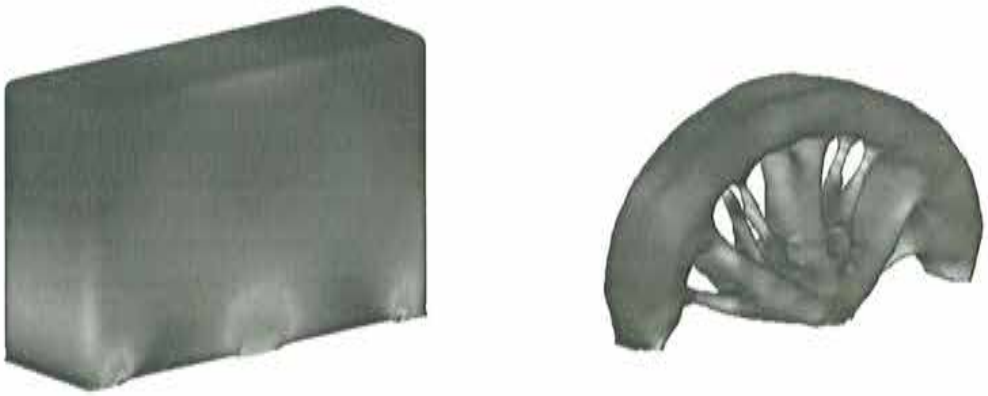

Figure 2: Results of a topology optimization with TopLevel.

As a mathematical (in contrast to heuristic) criterion for the placement of holes we chose the topological gradient and thereby followed an approach presented in[v], which has been further developed in, e.g., [vi]. The topological gradient is a scalar quantity measuring the effect of creation of a hole on the objective function in every point of the structure. It is computed by the solution of a single adjoint problem. If the compliance is to be minimized, the problem is self-adjoint and one finite element computation per iteration is sufficient.

Figure 2 shows some simple results of a topology optimization with TopLevel (Left: Original configuration. The bar is supported at both ends. In the middle, a vertical load is applied. Right: Optimized structure after 24 iterations. The volume has been reduced to 35 % of the original volume). For visualization, the post-processing functionalities of GiD are used. More details about TopLevel can be found in[vii].

4 CONCLUSIONS

An interface between the FE pre- and post-processor GiD and the topology optimization software TopLevel has been introduced. It has been shown how the interface has been adapted to fit with the requirements of the project, namely ability to handle complex problems and at the same time simple and intuitive handling of the graphical user interface. The main ideas of the topological gradient and the level set approach, which are the main components of TopLevel, have been presented.

5 ACKNOWLEDGEMENTS

We would like to thank H. Andrä and D. Stoyanov for their constructive cooperation and advice in numerous questions of detail.

The project "MIDPAG - Innovative Methods for Integrated Dimensioning and Process Design for Cast Parts" is financially supported by the European Regional Development Fund, ERDF, and the Ministry of Economic Affairs, Transport, Agriculture, and Viniculture of Rhineland-Palatinate.

REFERENCES

[i] LevelDict: Simulation of three-dimensional moving surfaces by the level set method. Developed at Fraunhofer ITWM by A. Wiegmann and A. K. Vaikuntam. http://www.itwm.fhg.de/en/sks__projects__sks_algorithms__levelset/levelset/

[ii] DDFEM - parallel code for three-dimensional structure mechanics http://www.itwm.fhg.de/en/hpc__parallelisierung__ddfem/ddfem/

[iii] TetMesh-GHS3D V3.1 The fast, reliable, high quality tetrahedral mesh generator and optimiser; White paper. http://www.simulog.fr/mesh

[iv] H. Andrä, D. Stoyanov. DDFEM: a parallel finite element solver for linear elasticity. Fraunhofer Institut für Techno- und Wirtschaftsmathematik, Kaiserslautern, 2005.

[v] A. Schumacher. Topologieoptimierung von Bauteilstrukturen unter Verwendung von Lochpositionierungskriterien. Universität-Gesamthochschule-Siegen, 1995.

[vi] S. Garreau, P. Guillaume, and M. Masmoudi. The topological asymptotic for PDE systems: the elasticity case.

[vii] E. Teichmann. Numerical Solution of Three-Dimensional Topology Optimization Problems in Elasticity. Diploma Thesis. University of Kaiserslautern, Department of Mathematics. August 2004.

IMPLEMENTATION OF AN INTERFACE FOR ELECTROMAGNETIC ANALYSIS USING UTD

R. Fernández-Recio[1], L.E. García-Castillo[1] and E. Escolano[2]

[1] Departamento de Teoría de la Señal y Comunicaciones, Universidad de Alcalá
Escuela Politécnica, Campus Universitario, Ctra. Madrid-Barcelona Km. 33.600
28806 Alcalá de Henares (Madrid), Spain. Email: luise.garcia@uah.es

[2]Centro Internacional de Métodos Numéricos en Ingeniería (CIMNE)
Universidad Politécnica de Catalunya (Barcelona), Spain

Key words: Uniform Theory of Diffraction (UTD), TCL-TK, OpenGL, canvas, RamDebugger

Abstract. *A user interface oriented to the analysis of electromagnetic problems based on the Uniform Theory of Diffraction (UTD) has been implemented using GiD. The UTD is a high frequency technique based on ray-tracing where the electric and magnetic field in an observation point are obtained as the sum of the different rays that arrives to that point. The UTD kernel uses the NURBS surfaces generated by GiD. The TCL-TK and the TKWidget have been used to improve the functionality and the quality of the interface. The RamDebugger has been used to debug the TCL-TK codes. The interface allows to draw the different rays (direct, reflected, diffracted ..) using OpenGL. The user can get the different parameters of the rays (reflected and diffracted points, angles, coefficients ..) just selecting with the mouse on the desired ray or rays. The interface allows to plot, either the total field, or the different contributions from the different rays for the desired polarizations using a package based on the* widget canvas *from TCL-TK.*

1 INTRODUCTION

A user interface oriented to the analysis of electromagnetic problems based on the Uniform Theory of Diffraction (UTD) has been implemented using GiD. The UTD [1] predicts the electric and magnetic fields using a ray tracing scheme from the source point to the observation point (or observation direction). The electric field in the observation point is calculated as the sum of the contributions of the different rays that arrives to that point. Different kinds of rays can be found depending on the geometry of the problem under consideration such as direct, reflected, diffracted, and high order effects involving different objects such as double reflected, reflected-diffracted . . .. The UTD is an asymptotic technique or high frequency technique that only can be apply when the objects of the problem are electrically large and do not have small features. Because of the fact that it is an asymptotic technique the solution tends to the correct solution when the electric size of objects tends to infinity.

[1]This work has been supported by the Ministerio de Educacion y Ciencia, Spain, under projects TIC2001-1019 and TEC2004-06252

The Reseach Group, which the authors belong to, has developed a program based on the UTD written in FORTRAN. The UTD codes have been successfully hybridized with the Finite Element Method (FEM) [2]. Actually, the developments of the UTD interface are planned to be used on the interface for the hybrid FEM-UTD method. The decision of using GiD as the pre- and post- processor for the interface with the UTD kernel has been taken due to several reasons:

1. GiD supports NURBS surfaces, which are the base of the UTD geometrical modelling for arbitrary objects.
2. It is very easy to adapt to any numerical simulation code.
3. Portable in *Linux* and *Windows*.
4. GiD features such as TKWidget and its extension to TCL-TK allows the possibility of a hihg quality interface [3]-[4].

The interaction of the UTD kernel with GiD is in the pre and postprocessing stages.

2 PREPROCESS

Two aspects can be pointed out in the preprocess stage. On one hand, the general data related to the UTD (antenna position, frequency ...) is presented using a facility of GiD called TKWidget that allows to communicate the information got in the graphical user interfaces (GUI) with the internal data of GiD and also attends some events related to the window and its data.

On the other hand, the user can draw the geometry in GiD or export from another format supported by GiD. Finally, the geometry is exported to IGES format, which is the geometrical input data to the UTD kernel. It is very important to highlight that the geometry is described using NURBS surfaces for arbitrary objects, which are directly used in the minimization/maximization process to find the critical points of the UTD kernel (e.g. reflected, diffracted points ...). The geometry may also be given in terms of planar facets and some canonical objects. In this case, the critical points can be calculated analytically.

3 POSTPROCESS

A UTD interface requires two main kinds of postprocesses:

1. To visualize the ray tracing problem.
2. To plot the radiation pattern of the problem.

The ray visualization has been implemented using OpenGL. The user can draw any of the contributions independently (see Figure 1). Moreover, the user can select with the mouse one or several rays and see the characteristics of the selected rays. A lot of information related to the UTD kernel such as the type of ray, critical points, general data of the problem, UTD coefficients, angles of the ray with the surfaces and auxiliary system of vectors in the critical

points is shown in the information window. This information is very useful for debugging purposes with the UTD kernel or being used by experienced users or students to understand the problem under consideration.

The radiation pattern is visualized in terms of two-dimensional (2D) cuts in the three-dimensional radiation pattern describing the amplitude of the electric or magnetic far-field in given directions. At the moment, GiD does not have a powerful tool to represent this kind of information in the postprocess stage. Nevertheless, the flexibility of GiD and its extension to the TCL-TK language allows to find solutions to this problem. In this context, the authors have developed a powerful tool to draw 2D curves based on a widget of TCL-TK called *canvas* (see Figure 2). The starting point of the developmet of the facility has come from the free package *plotchart* at [5] where the features of the tool has been extended to the requirements of the interface. The actual package allows to draw for the desired contribution independently or at the same time the electric and magnetic fields for different polarizations in magnitude or in phase. It allows to edit the features of the curves such as color, type of line, width, type of mark ... using an option table generated using the widget *TableList*. Moreover, a postcript file can be generated to print the information depicted in the *canvas*. Other features are being developed at the present time. Finally, it is important to note that the debugging of the interface has been carried out with the help of the tool RamDebugger [6].

4 CONCLUSIONS

A graphical interface for UTD has been developed using GiD. The two main aspects of a postprocess of a UTD program have been successfully implemented making use of OpenGL routines and the TCL-TK language.

REFERENCES

[1] R.G. Kouyoumjian and P.H. Pathak, *A Uniform Geometrical Theory of Diffraction for an Edge in a Perfectly Conducting Planes*, Proceedings of the IEEE, pp. 1448-1461, Nov. 1974

[2] R. Fernandez-Recio, I. Gomez-Revuelto and L.E. Garcia-Castillo, *A Hybrid FEM-UTD Method for the Analysis of Radiation Problems in Complex Environments*, in International Conference on Electromagnetics in Advanced Applications (ICEAA'05), Torino, (Italy), pp. 465-462, Sept. 2005

[3] J. Suit Perez, E. Escolano and M. Pasenau, *Advanced Problem Type Development: Data Dependencies and GUI Customization (TKWIDGET)*, 2nd Conference on Advances and Applications of GiD, Barcelona, 2004

[4] A. Valls, *GiD-NASTRAN Interface: Guideline for Development of a High Quality Interface*, 2nd Conference on Advances and Applications of GiD, Barcelona, 2004

[5] http://tcllib.sourceforge.net/

[6] http://www.gidhome.com/RamDebugger/RamDebugger_toc.html

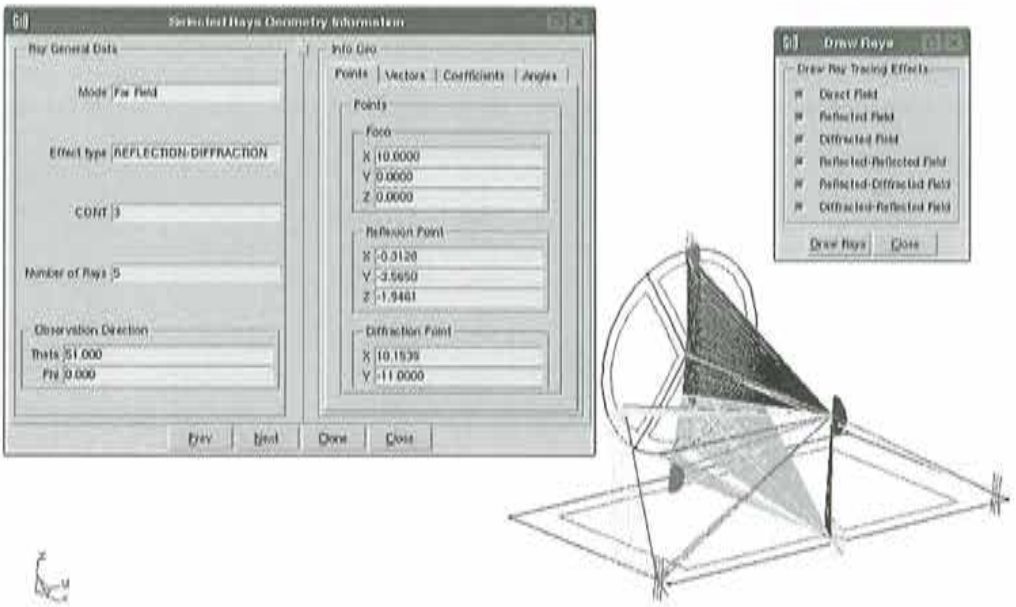

Figure 1: Postprocess related to the ray tracing visualization

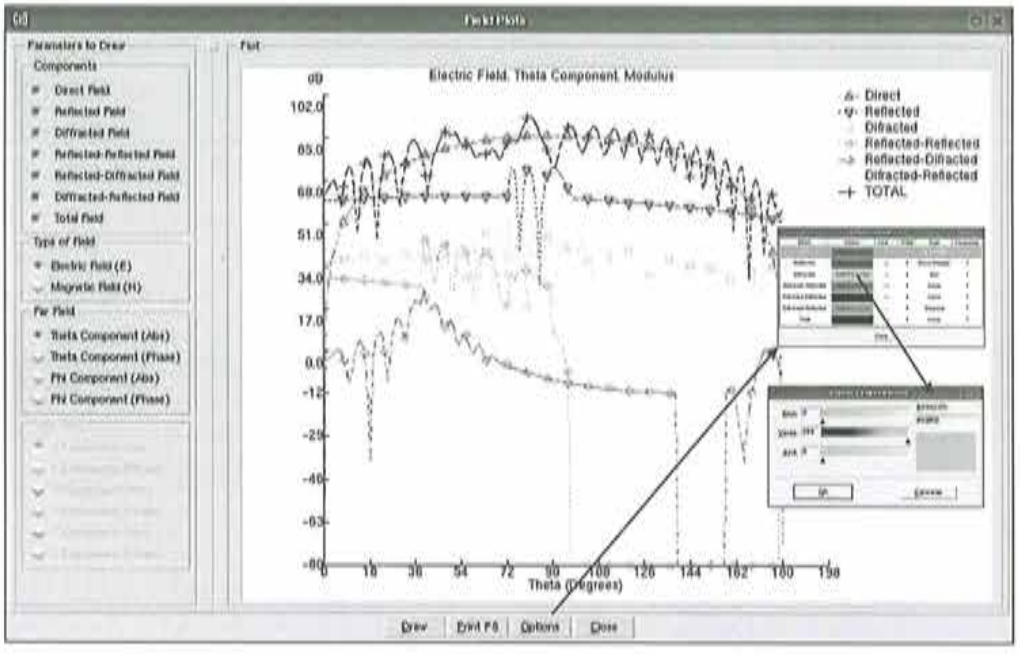

Figure 2: Postprocess related to the Representation of the radiation pattern using the widget *Canvas*

LARGE DISPLACEMENT OF IN-ELASTIC ANALYSIS OF CONCRETE CABLE STAYED BRIDGE USING XFINAS-3 FEM SYSTEM AND GID

Ki-Du Kim* **and Seong-Tae Cho†**

* **Department of Civil and Environmental System Engineering, Konkuk University, Seoul, Korea ()**

e-mail: kimkd@konkuk.ac.kr , web page: http://www.xfinas.com

† Samsung Corporation, Seoul, Korea

Email: hellotae@samsung.com

Key words: *Large displacement, in-elastic, Cable Stayed Bridge*

Abstract. *With increasing emphasis on the use of the ultimate design of steel and reinforced concrete structures, attention has inevitably turned to the consideration of non-linearity with large displacement of elasto-plastic behaviour. The solutions of both geometrical and material non-linearity problems have been greatly facilitated by the development of powerful and efficient finite element formulation using XFINAS. The XFINAS structural analysis system has been developed for the static and dynamic solution of elastic and elasto-plastic frames, shells and solids. The beam formulation includes large displacement effects and elasto-plastic material behavior for the steel structures and fiber model for 3-D reinforced concrete structures. The concrete cable stayed bridge example using XFINAS showed the good performance in fully 3-D nonlinear behavior.*

1 INTRODUCTION

The program based on the nonlinear finite element method, FINAS which is capable of the elasto-plastic stability assessment of thin walled structures, was developed on a CDC-Main frame and UNIX environment, at Imperial College, London by Trueb (1984), Bates (1987) and Kim (1992). The **XFINAS** which is an e**X**tended version of **FINAS** has been developed for the general purpose software in Konkuk University (2006). XFINAS to be introduced enables a powerful nonlinear dynamic structural analysis, taking into account of

material and geometric nonlinearity. Thus, the nonlinear dynamic algorithm in XFINAS can be used for the research and design of the steel and concrete structures under the static, dynamic and seismic loading. A large number of numerical testing has been carried out for the validation of **XFINAS** elements, which shows the good agreement with the references. The pre- and post processing of **XFINAS** can be carried out by using **GiD**. Thus, the new program will be efficient and powerful tool in design and research of the steel structures.

2 XFINAS FINITE ELEMENT SYSTEM

The window based **XFINAS** software having in-core solution scheme and no limitation of array allocation will be the most powerful analysis tool for any type of problem to be analyzed. **XFINAS** provides a series of solution strategies for nonlinear analysis. An automatic selection of constraint equation and arc-length control are available for highly nonlinear problems. The solution procedure uses either full or modified Newton-Raphson method. In compared with XFINAS version by Kim (2004), the present version is improved on the nonlinear concrete model (Mander model and general concrete), parabolic cable element and Gap model for support and nonlinear concrete shell (Plasticity and Elasto-plastic fracture model).

TABLE 1 : XFINAS SOLUTION FEATURES

1	Linear Static, buckling, natural frequency, linear dynamic, nonlinear static and nonlinear dynamic analysis, Heat Transfer
2	Time-history analysis using explicit and implicit methods: Central difference, Newmark-beta, Wilson-theta and HHT Methods
3	Mode superposition method for linear dynamic analysis (with damped and undamped system) by using eigenvector and load dependent Ritz vector
4	Seismic analysis using time integration, mode superposition method and response spectrum methods
5	2-D and 3-D Heat Transfer analysis
5	Co-rotational method for nonlinear beam and shell element
6	Nonlinear control algorithm: load control, displacement control, constant arc-length, and automatic arc-length control method for highly nonlinear problems
7	Geometrical nonlinearity: Updated Lagrangian Method
8	Elasto-plastic material : Von-Mises with strain hardening, Ivanov-Ilyusin with strain hardening, Mohre-Column , Drecker-Prager , Tresca
9	Concrete Creep and shrinkage according to the CEB-FIP Model Code 90 and ACI
10	Fiber-reinforced composite materials with the progressive failure analysis (Maximum stress, Tsai-Wu, Tsai-Hill and Modified Puck Criterion Theory)
11	Postbuckling analysis of frame, plate and shell
12	Eigenvalue analysis using inverse iteration, subspace iteration method and Lanczos vector
13	Buckling and natural frequency analysis
14	Vibration control using viscous damper
15	Base-isolation of framed structures
16	Loss of prestressing in pre-tensioned and post-tensioned frame element due to elastic shortening, friction, anchor slip, creep, shrinkage and relaxation using 3-D frame element
17	Parabolic cable element for cable supported bridge

18	Boundary spring element, gap element, hook element and gap-hook element for support model
19	Offset in the beam and frame element
20	Automatic analysis of 2-D and 3-D Bridge moving load based on AASHTO
21	Displacement loading
22	Standard steel section property: Korean-code, Euro-code

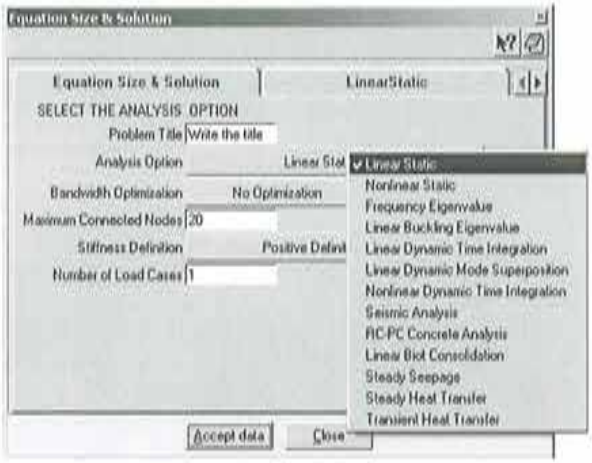

Figure 1 Various solution options of XFINAS system

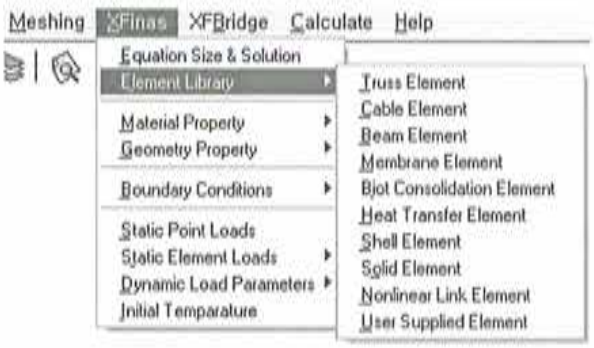

Figure 2 XFINAS Element Library Menu

3 TITLE, AUTHORS, AFFILIATION, KEY WORDS

The new elements in XFINAS are very efficient, accurate and robust as can be seen in an example manual (2006). In the following, the features of the XFINAS elements are briefly summarized in the appendix. A three dimensional 2-noded frame (**XFRAME**) and 2& 3 noded beam element (**XBEAM2** and **XBEAM3**) can be used for the nonlinear dynamic analysis of 3-D framed structures. The **XFRAME** has a semi-rigid and offset for easy and efficient modeling. Nonlinear 2-noded straight and 3-noded curved beam elements are based on the thin walled Vlasov beam theory and include transverse shear deformation. The elements are capable of representing any open and closed sections. The beam element can be used either in stand-alone form or as a stiffener element.

4 NUMERICAL EXAMPLE

In the following, the example of 3 dimensional analysis of the cable stayed bridge is suggested. The bridge has a total 520 m length and 2 towers with unsymmetric cable shapes. Using the fiber model of frame element and nonlinear cable element in XFINAS, the large displacement of in-elastic analysis of the cable stayed bridge is carried out. The supports in abutment are modeled using Gap-spring model in XFINAS The ultimate behaviour of the result is used to check the safety of the critical point in the design.

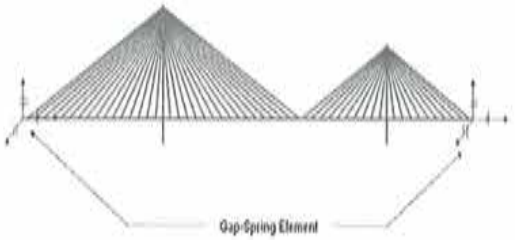

Figure 3 Bridge Model using frame, cable and gap element

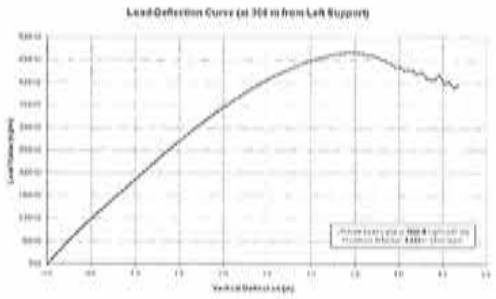

Figure 4 Load-deflection curve

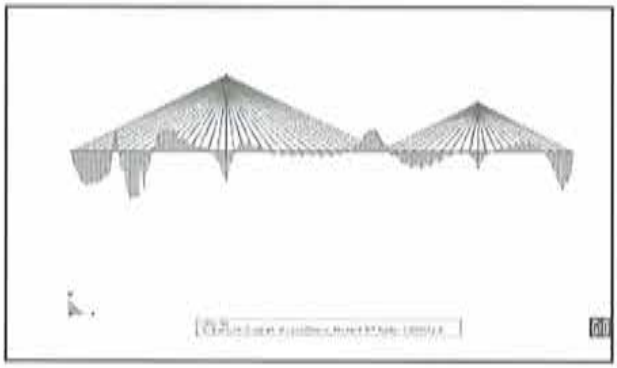

Figure 5 Bending moment at the ultimate load

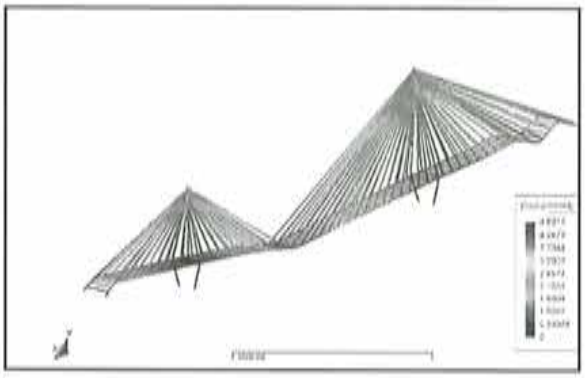

Figure 6 Deformed shape at the ultimate load

4. CONCLUDING REMARKS

Although a lot of general purpose softwares are available for the bridge design and research, there are still rooms to improve the solution with design purpose. For this purpose, XFINAS system is developed based on the most efficient formulation. All the XFINAS elements are fully tested and validated. Based on the XFINAS element, the nonlinear RC fiber beam-column element has developed and implemented for the advanced concrete bridge analysis. Using the RC fiber model, 3-D analysis of the concrete cable stayed bridge is carried out to get the ultimate load analysis. The results are used in the design of Hwapo Bridge in Turn-key project of Korea.

REFERENCES

[1] **XFINAS** 2.0 (2006) Theory, Example, Reference and User Manual, April 2003 (www.xfinas.com)
GiD 7.2 (2002) CIMNE, Barcelona, Spain, 2002

[2] Urs Trueb (1983) Stability Problems of Elasto-plastic Plates and shells by Finite Elements, Ph.D. Thesis , Dept. of Civil Engineering, Imperial College, London, 1983

[3] Agelidis, N. (1984) Buckling of stringer stiffened shells under axial and pressure loading, Ph.D. Thesis, Dept. of Civil Engineering, Imperial College, London.

[4] Bates D.N. (1987) The Mechanics of Thin Walled Structures with Special Reference to Finite Rotations", Ph.D. Thesis, Dept. of Civil Engineering, Imperial College, London

[5] Bathe K.J. and Dvorkin E. N. (1986) A Formulation of General Shell Elements-The use of Mixed Interpolation of Tensorial Components, Int. J. Numer. Meth. Engng., 22, 697-722.

[6] Kim K.D. (1992) Non-linear Analysis of Fibre-Reinforced Composite Structures Using Finite Elements', Ph.D. Thesis, Dept. of Civil Engineering, Imperial College, London, 1992

[7] Kim K.D., Lomboy G. R. and Han S.C. (2003)" A Co-rotational 8-Node Assumed Strain Shell Element for Postbuckling

[8] Analysis of Laminated Composite Plates and Shells", in printing, "Computational Mechanics", Volume 30 Issue 4 , pp 330-342.

[9] Kim K.D. (2003), Large Displacement of Elasto-Plastic Analysis of Stiffened Plates and Shells using Corotational 8-Node Assumed Strain Element, Structural Engineering and Mechanics, An International Journal, Vol. 15, No.2, (199-223)

[10] Kim K.D., Lomboy G.R. and Voyiadjis G.Z. (2003) A 4-Node Assumed Strain Quasi-Conforming Shell Element with 6 D.O.F., , International Journal for Numerical Methods in Engineering, Volume 58, Issue 14, p2177-2200, December

TABLE 2 :XFINAS element library

Geometrically nonlinear Elements		Material library
Shell element	(1)**XSHELL41**: 4 nodes quasi-conforming element (2)**XSHELL42**: 4 nodes assumed natural strain element (3)**XSHELL82**: 8 nodes element with a penalty function (4)**XSHELL83**: 8 nodes assumed natural strain element	Laminated Composite materials Von-Mises, Ilyusin-Ivanov: Small Strain Elasto-plasticity with straining hardening Von-Mises, Ilyusin-Ivanov: Large Strain Elasto-plasticity with straining hardening Concrete Plasticity Elast-plastic Fracture Model Creep and Shrinkage (ACI, CEB/FIP 90)
Frame & Beam element	(1) **XFRAME**: 2 nodes frame element (2)**XBEAM2Q**: 2-nodes Valsov beam element with 7th D.O.F. (Warping) (3) **XBEAM31:** 3 nodes Vlasoc beam element with 7th D.O.F.	Elasto-plasticity (Von-Mises) Loss of Pestressing Offset, Semi-rigid, Hinge option Mander and General concrete model Fiber Model
3-D Solid element	(1) **XSOLID81:EAS,** Assumed Natural Strain Method (2) **XSOLID4**: 4-node Tetrahedral element	2-D Plasticity Von-Mises, Drucker-Prager, Mohr-Coulomb, Tresca
Plane element (plane stress, strain, axi-symmetric)	(1)**XPLANE4**:4-nodes EAS element (2)**XMEMB8:** 8-nodes plane element	2-D Plasticity Von-Mises, Drucker-Prager, Mohr-Coulomb, Tresca
Truss element	**XTRUSS**: Three dimensional 2-nodes element	Nonlinear elastic
Cable Element	Nonlinear parabolic element (Cable sag effects)	5 point nonlinear material model
Spring element	**XSPRING**: Three dimensional element (Three translations and Rotations)	Linear elastic
Non-linear Link element	**Gap element, Hook Element and Gap-Hook Element**	* bridge support and expansion joint model

MULTIPHYSICAL SIMULATIONS WITH ELMER FINITE ELEMENT SOFTWARE IN COMBINATION WITH GID

Antti Pursula, Mikko Lyly, Esko Järvinen, Thomas Zwinger and Juha Ruokolainen

CSC – Scientific Computing Ltd
Keilaranta 14, P.O.Box 405, 02101 Espoo, Finland
e-mail: antti.pursula@csc.fi , web page: http://www.csc.fi/elmer

Key words: Open Source, Multiphysics, Simulation, Finite Element Analysis, GiD Interface

Abstract. *We present the interface between GiD and the Finite Element software Elmer. GiD can be used in both pre-processing and post-processing of Elmer simulations. Elmer is an open source software capable of simulating a diverse selection of multiphysical phenomena. Examples of GiD usage in combination with Elmer simulations are presented.*

1 INTRODUCTION

This paper introduces the Elmer software and describes the interface which has been developed to import data from GiD into Elmer, and vice versa. The interface has gained popularity among the Elmer users both in academic organizations and among industry.

Elmer is a multiphysical simulation software that is developed by CSC, the governmental funded Finnish IT center for science. Elmer uses Finite Element Method (FEM) to discretize partial differential equations and the resulting matrix equations can be solved with various efficient methods, including direct, iterative and multigrid solvers. Elmer has been developed since 1995 and it includes modules for simulating a large range of physical phenomena, such as fluid dynamics, heat and mass transfer, electromagnetics, acoustics and elasticity[i]. The strength of the software is in its modular structure which allows almost arbitrary coupling between the physical models. This is reflected by the publications on many application areas in which coupling of equations is essential: microsystem modeling[ii], ice-sheet modeling[iii], hemodynamics[iv], acoustics[v], and silicon crystal growth[vi].

Recently, CSC has published Elmer under an open source license, the GNU Public License (GPL). The source code can be downloaded from the Elmer website, http://www.csc.fi/elmer. A public source code gives scientists interested in advanced mathematical modeling a possibility to review the algorithms of the software and to apply own changes to them.

2 ELMER – GID INTERFACE

The interface between GiD and Elmer includes both the transfer of element mesh created in GiD into Elmer and the transfer of simulation results from Elmer into GiD for post-processing. The interface uses the advanced features of GiD that allow smooth linking with other software. Basically, the functionality is achieved by two separate file type conversions. First, the conversion of GiD meshes into Elmer mesh files has been implemented as GiD template. The conversion of Elmer results into GiD post-processing format, on the other hand, has been implemented as a module in Elmer software. Together these tools provide a powerful and efficient method for computational science and engineering.

2.1 Benefits of the GiD – Elmer interface

The emphasis of Elmer development has long been in the inclusion of physical models and in the improvement of numerical methods. Also, a powerful postprocessor, ElmerPost, has been developed. For pre-processing Elmer offers a Delaunay mesh generator for 2D meshes, including adaptive meshing, and structured mesh generator for simple 3D meshes. Elmer has also been made available for most operating systems, such as Windows, Linux, Mac, Solaris, etc. and it can perform parallel simulations on clusters and supercomputers.

The need for advanced 3D pre-processing has been satisfied by implementing interfaces to various academic or commercially available programs, such as Ansys, Gambit, or Comsol multiphysics (previously known as FemLab). There are many reasons why GiD is an excellent addition to the selection of available pre-processors: GiD provides a graphical user interface, includes advanced meshing capabilities, supports importing various CAD formats and is relatively inexpensive. This makes GiD a very attractive choice as a pre-processor for Elmer simulations.

Elmer contains its own post-processor, as stated earlier. There are, nevertheless, certain advantages in using GiD post-processing for Elmer simulation results. Obviously, if one is already familiar with GiD it is convenient that the post-processing can be done with the same software. Also users of ElmerPost may find GiD post-processing attractive in some cases, since, e.g., producing mpeg-animations is more straightforward with GiD than with ElmerPost.

3 EXAMPLES

GiD – Elmer interface has been used in simulations in the fields of hemodynamics and glacier dynamics, for example. In hemodynamics, the blood flow inside a carotid artery with flexible walls has been modeled. The geometry data for this simulation is taken from medical CT (computed tomography) scans of human head. The scans have subsequently been processed with segmentation tools to produce the geometry of the artery and its walls. The geometry has been imported into GiD as STL format for meshing. The simulations were performed with Elmer and, in this case, also post-processed within Elmer software. Figure 1 shows the imported geometry and the generated element mesh in GiD as well as a snapshot of the simulation results in ElmerPost.

Figure 1: Modeling of blood flow in the bifurcation of carotid artery. Geometry (left), the element mesh (middle), and a snapshot of the simulation results (right). The colors of the artery surface and the vectors indicate the displacements of the artery and the velocity of the blood, respectively. The geometry is meshed in GiD and the results are computed and visualized with Elmer.

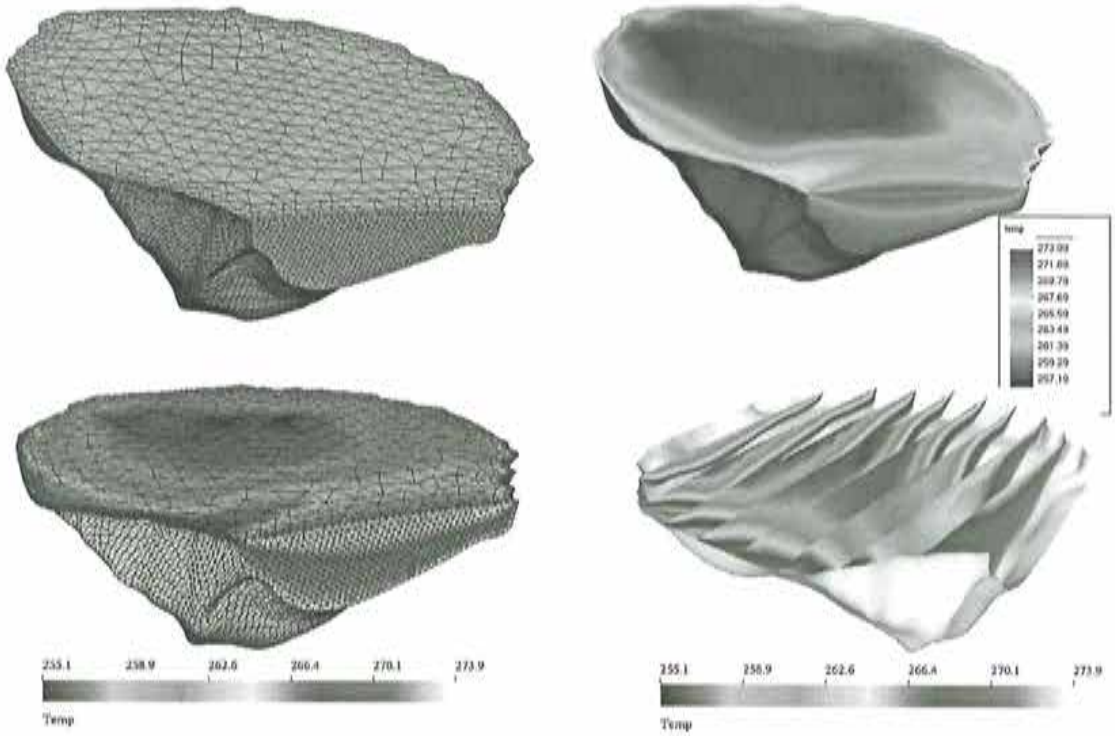

Figure 2: Modeled temperature distributions in a crater glacier. Element mesh in GiD (top left), results in GiD postprocessor (top right), and results in ElmerPost (bottom left and right). The mesh was generated in GiD, the simulations were performed with Elmer and the results have been visualized both with GiD and with ElmerPost. The temperatures above are given in Kelvin.

The interface has been successfully utilized also in modeling of glacier dynamics. As an example the heat transfer inside a crater glacier in the Ushkovsky volcano in Russia is presented. The measured glacier surface extent and bedrock data was converted into an IGES file which was imported into GiD. The tetrahedral element mesh was created with GiD. The simulations were performed with Elmer and the results have been visualized with both GiD and ElmerPost, see Figure 2. The glacier is heated from below by geothermal heating which melts the ice gradually at the bottom. The precipitation, however, gradually accumulates new ice on top of the glacier.

4 CONCLUSIONS

The interface between GiD and Elmer software has been presented. Elmer as an open source software is perfectly suited for academic model development and supports cooperation among computational scientists. There is a clear advantage of using GiD as a pre-processor for Elmer simulations, since the advanced functionality of GiD complement well the features of Elmer package. The interface also increases the target audience of the simulation software by bringing available more pre-processing choices, especially for academic users. Also the post-processor features of GiD may well be applied to Elmer simulations. As demonstrated by the presented examples, the combination of GiD and Elmer forms an advanced simulation package for multiphysical modeling.

REFERENCES

[i] *Elmer Models Manual*, http://www.csc.fi/download/ElmerModelsManual.pdf, Jan 2006.

[ii] T. Veijola, A. Pursula and P. Råback, "Extending the Validity of Squeezed-Film Damper Models with Elongations of Surface Dimensions", *J. Micromech. Microeng.*, **15**, 1624-1636 (2005).

[iii] E. Le Meur, O. Gagliardini, T. Zwinger and J. Ruokolainen, "Glacier flow modelling: a comparison of the Shallow Ice Approximation and the full-Stokes equation", *C. R. Physique*, **5**, 709-722 (2004).

[iv] E. Järvinen, M. Lyly, J. Ruokolainen and P. Råback, "Three-dimensional fluid-structure interaction modeling of blood flow in elastic arteries", *Proc. ECCOMAS CFD*, Swansea (2001).

[v] M. Malinen, M. Lyly, P. Råback, A. Kärkkäinen and L. Kärkkäinen, "A finite element method for the modeling of thermo-viscous effects in acoustics", *Proc. ECCOMAS*, Jyväskylä, Finland (2004).

[vi] V. Savolainen, J. Heikonen, J. Ruokolainen, O. Anttila, M. Laakso and J. Paloheimo, "Simulation of large-scale silicon melt flow in magnetic Czochralski growth", *J. Crystal Growth*, **243/2**, 243-260 (2002).

THE USE OF GID IN THE STATIC MODELLING OF CARBON FIBRE FISHING RODS UNDERGOING LARGE DISPLACEMENTS.

Colin Skene

Hardy Advanced Composites (HAC)
Hardy & Greys Ltd
Willowburn, Alnwick, Northumberland, England, UK
Email: cskene@hardygreys.com Web page: www.hardyfishing.com

Key words: COMET, Interface, Collaboration, Secondment, Mixing Theory

Abstract: *This document details the collaborative activities between CIMNE and Hardy Advanced Composites as part of the UK's Department of Trade and Industry's Global Watch Secondment scheme. New, large displacement elements were developed for use in the CIMNE developed FE code, "COMET" to allow the simulation of static loading on carbon fibre fishing rod geometries undergoing large displacements. A spreadsheet based interface for rapid geometry generation in GiD was used in conjunction with an Advanced Serial Parallel Mixing Theory developed by Rastellini et al [1] of CIMNE. Details of the secondment and further collaboration between CIMNE and Hardy Advanced Composites are presented along with an overview of techniques employed in the use of GiD during this project.*

1. INTRODUCTION

Hardy Advanced Composites is the technical division of Hardy & Greys Ltd based in the North East of England. Hardy & Greys Ltd, manufacture, distribute and sell fishing rods and tackle with the Hardy brand catering for the premium game angler. The Hardy brothers established the business in 1872 and the company has enjoyed a history of innovation and success including Royal Warrants and export awards. Both companies are part of the Harris & Sheldon Group.

In 1969 the Fibatube division was formed to manufacture industrial tubes using the same composite materials employed in the glass fibre and carbon fibre fishing rods, which Hardy were manufacturing at that time. Customers include military and aerospace companies along with automotive, marine and space technology organisations.

The ability to accurately model the static and dynamic performance of composite tubes, particularly fishing rods was identified by Hardy Advanced Composites more than 5 years ago as a critical area for research and development. Since then several projects have been carried out in conjunction with various academic and commercial bodies in an attempt to offer an effective design and analysis tool for the Hardy Rod design team. On each occasion the projects were confronted by a "technological barrier" leading to an oversimplified and non practical outcome. The Global Watch

Secondment scheme run by the UK Department of Trade and Industry has allowed Hardy Advanced Composites to breach this barrier by introducing a cutting edge system developed by experts in numerical techniques at CIMNE based in Barcelona, Spain.

2. OVERVIEW OF MODELLING PROCEDURE

Figure 1 below shows the general procedure employed in the modelling of fishing rods at Hardy Advanced Composites. The following sections detail the methods for each of the steps.

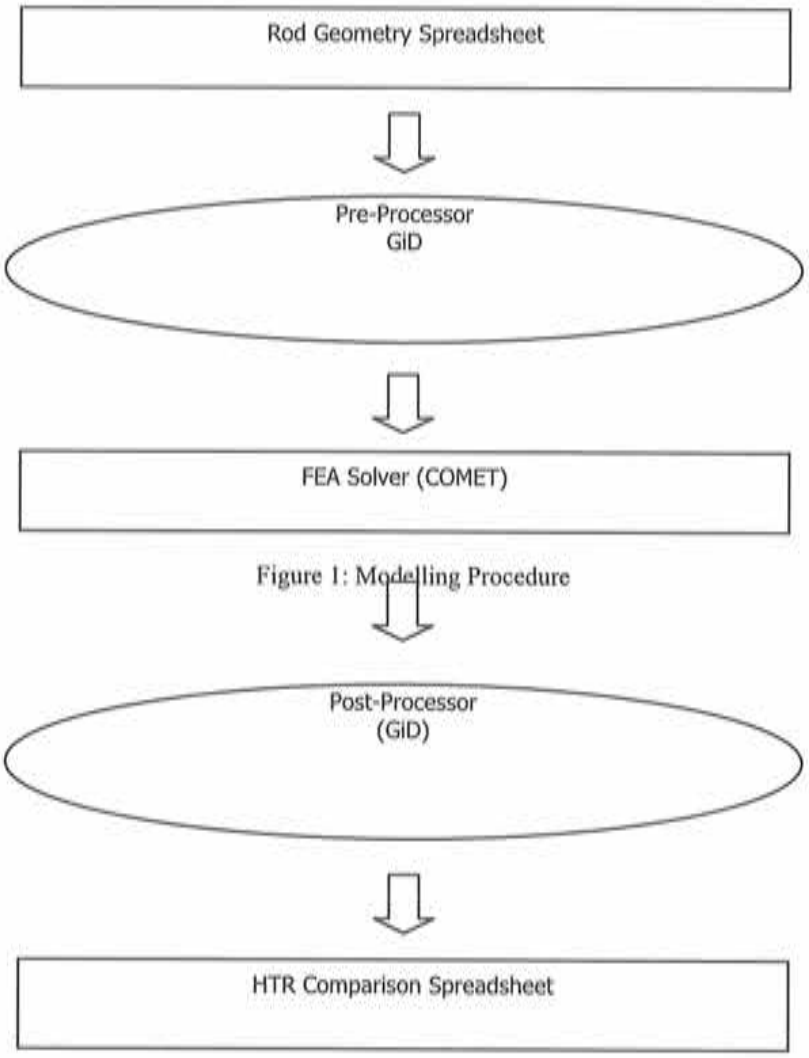

Figure 1: Modelling Procedure

2. SPREADSHEET INTERFACE FOR GID

At first glance, a fishing rod section geometry may seem very simple but on closer inspection it can be seen that the rods' make up is in fact quite complicated and varies considerably from section to section.

Figure 2 below right shows a cross sectional view through a 3 piece fishing rod complete with spigot joints. Consideration must be given during geometry creation for the following.

- Inside / Outside diameters
- Lengths and taper ratios
- Position and length of spigots
- Boundary / loading conditions

The problem is further complicated when consideration is given to the lay-up and configuration of the carbon fibre pre-preg which makes up the rod sections. Figure 3 below shows a cross section through a section showing the layers of carbon fibre.

Figure 2: Rod geometry (rendered)

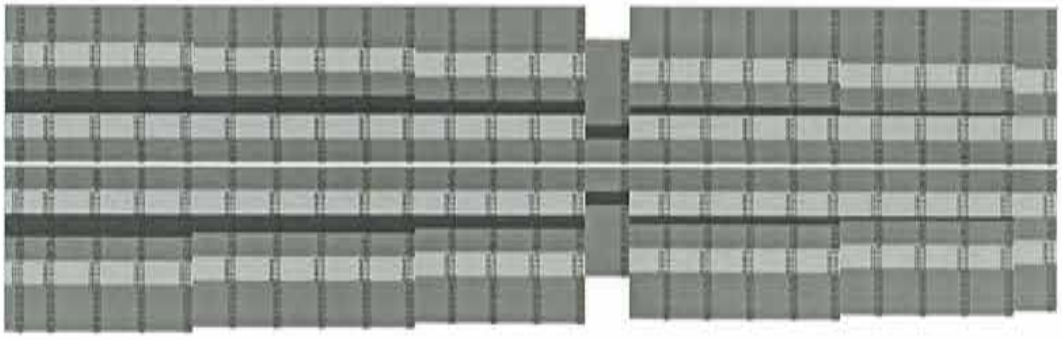

Figure 3: Rod Cross Section

Here we can see that the section is made up of different layers of different materials in different areas of the rod section. The information required to generate such geometry was already held in a raw form within the HAC production spreadsheets which have been in use for years. It seemed sensible to allow the rod designer to continue using this format so an interface was written using Microsoft Excel to transfer the required information into GiD for rapid geometry generation. This also allows for relatively rapid modifications to be made to the modelling using visual basic rather than using Tcl/ Tk used in GiD. The spreadsheet exports a GiD batch file which is then easily imported into GiD. The ability to produce rapid changes in geometry for analysis has proved to be a very powerful tool in this application.

The batch file instructs GiD to do the following;

Figure 4: Basic Geometry

The basic geometry is created, with regions defined for spigots, reinforcements etc. Material, loading and boundary conditions are also applied.

Next a mesh is generated using Quadratic, Hexagonal elements developed at CIMNE for analysing large displacements.

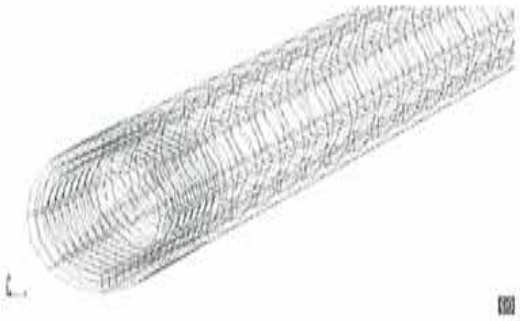

Figure 5: Hexahedral Mesh

Once the geometric, loading, boundary conditions and problem data has been imported, COMET is then run from within GiD. Once completed, GiD is then employed in Post-Process mode to analyse the results as required. A typical rod deflection analysis is shown below.

Figure 6: GiD Post-Process visualisation

In order to compare several rod profiles at once it was necessary to write an interface within the GiD menus to automatically generate and export the profile data for viewing in Microsoft Excel. This work was carried out by Fernando Rastellini of CIMNE during his time spent on a secondment to Hardy Advanced Composites in the UK. Figure 7 overleaf shows a screen shot of the interface in use within GiD together with the rod profiles ready for comparison in Excel.

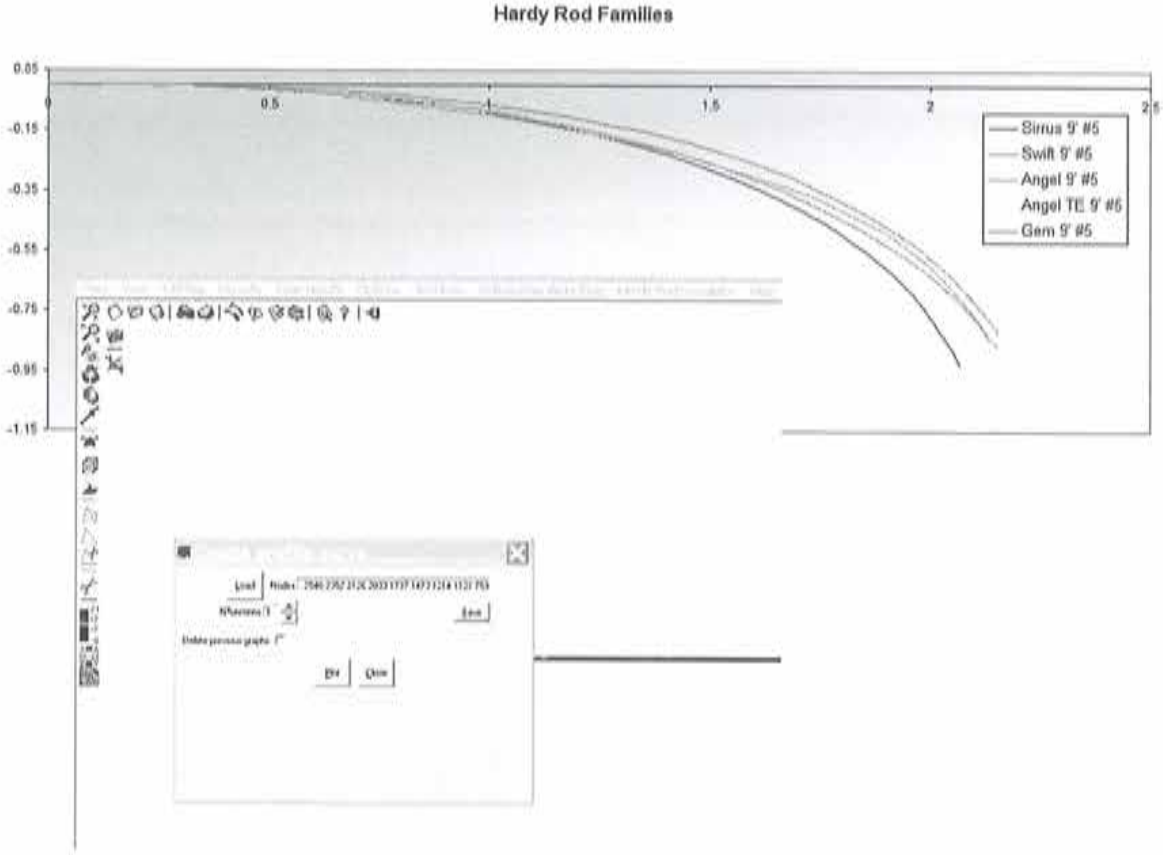

Figure 7: GiD Profile Curve Interface

3. FUTURE DEVELOPMENTS

Hardy Advanced Composites has embarked on further collaborative projects with CIMNE. A large displacement natural frequency analysis code has been developed specifically for the analysis of Hardy fishing rods. Hardy Advanced Composites are also actively partner CIMNE in the search for funding for future projects involving computational methods.

4. CONCLUSIONS

The use of GiD along with COMET has offered Hardy Advanced Composites a new dimension in fishing rod design and analysis capabilities. The number of prototypes required has been reduced and investigations into the use of alternative materials are currently underway. Hardy Advanced Composites intends to continue collaboration with CIMNE on various projects all involving the use of GiD.

5. REFERENCES

[i] Advanced Serial-Parallel Mixing Theory for Composite Materials Analysis. Continuum Basis and Finite Element Applications. (Fernando Rastellini, Sergio Oller, Omar Salomon and Eugenio Oñate.) 2003 CIMNE.

TWO-SCALE MODELLING OF METAL MATRIX COMPOSITES' THERMOMECHANICAL BEHAVIOUR USING GID

J. Pinho-da-Cruz*, J.A. Oliveira, A. Andrade-Campos and F. Teixeira-Dias

Departamento de Engenharia Mecânica
Universidade de Aveiro, Campus Universitário de Santiago
3810-193 Aveiro, Portugal

Keywords: Thermomechanical Behaviour, Asymptotic Expansion Homogenization, Metal Matrix Composite Material, Representative Unit-Cells, Periodicity.

Abstract. *The thermomechanical modelling of the behaviour of Metal Matrix Composites (MMCs) requires a deep understanding of the physical phenomena that span two or more spatial length scales. The Asymptotic Expansion Homogenisation (AEH) method appears to be a highly suitable technique to address this multiscale dependence. In this context, this methodology is applied to the two-scale modelling of the thermomecanical behaviour of metal matrix composites, focusing mainly on engineering issues related to its finite element implementation and applications. Geometrical models are built using GiD's pre-processor. All the process data are introduced in a dedicated problem type with a graphical user-friendly interface (GUI) developed within GiD. The problem type was implemented with the use of Tcl/Tk. Post-processing is also carried out with GiD. This fact enables the straightforward simulation of linear/non-linear and stationary/transient thermomechanical behaviour of metal matrix composites. An illustrative example of the simulation of linear thermoelastic homogenised behaviour of an aluminium matrix composite reinforced with spherical SiC particles (AlSiCp MMC) is presented.*

1 INTRODUCTION

Several physical processes exhibit coupling between mechanical and thermal phenomena. In general terms, due to the thermal expansion of the material, an increase in temperature induces deformations on the body. This, in turn, may contribute to an increase in the temperature. Therefore, the mechanical response of the solid medium generally depends on its thermal behaviour and *vice versa*. On the other hand, the thermomechanical modelling of the

*Corresponding author: Tel.: +351.234.370830; Fax: +351.234.370953; *e-mail*: jpc@mec.ua.pt

behaviour of Metal Matrix Composites (MMCs) requires a deep understanding of the physical phenomena that span two or more spatial length scales. In fact, constituent thermoelastic properties of metal matrix composites are generally temperature dependent, which affects the effective overall behaviour of the composite material. In this context, the Asymptotic Expansion Homogenisation (AEH) method[i,ii] appears to be a highly suitable technique to address this multiscale dependence. With this approach it is possible to estimate the effective thermoelastic properties of complex microstructures. Several AEH frameworks have been applied to the solution of linear and non-linear structural problems[iii,iv]. Moreover, in contrast to other homogenisation approaches, this methodology is useful due to its inherent capability to seamlessly perform both homogenisation and localisation within a single method by considering the microstructural details on a macrolevel analysis. Following previously developed work by the authors, the AEH methodology is applied to the two-scale modelling of the thermomecanical behaviour of an $AlSiC_p$ MMC, focusing mainly on engineering issues related to its finite element implementation and applications[v,vi]. To adequately simulate this kind of processes it is essential to have an intuitive graphical user interface in order to solve the problem and to analyse results properly. The simulation of an AEH thermomechanical problem requires the definition of the (i) thermomechanical properties of the material and (ii) boundary conditions (both mechanical and thermal). Although trivial, this procedure can be time consuming. In this context, GiD was used as pre- and post-processor together with the developed AEH thermoelastic finite element code.

The expansion of an $AlSiC_p$ MMC bar due to a prescribed temperature in one of its edges is used to exemplify an application of the two-scale AEH methodology. All geometrical models are built and discretised with GiD's pre-processor. The results are subsequently analysed with GiD's built-in post-processor. A dedicated problem type was developed in order to collect all the process input data – geometry and discretisation included – and to write it into an AEH thermoelastic finite element code input data file.

2 GiD IMPLEMENTATION AND APPLICATION ASPECTS

All the process data are introduced in GiD's dedicated problem type with a graphical user-friendly interface (GUI) developed within GiD. The problem type was implemented using Tcl/Tk. Both the thermal and mechanical boundary conditions are assigned to entities in the problem type. 8-node hexahedral and 4-node tetrahedral elements were used in the macro- and microscale meshes, respectively. While the macroscale finite element coarse mesh was automatically generated with GiD, the microscale mesh was generated within GiD using SphereCell. This automatic unit-cell generation code[v] allows the generation of reinforcement particles in order to guarantee cell-to-cell continuity and periodicity, *i.e.* ensuring the existence of periodic boundary conditions. In this analysis, a 40% reinforcement unit-cell was automatically generated. The considered macro- and microscale finite element meshes can be seen in figures 1 and 2a, respectively. In the analysis, a prescribed temperature of 393 K was imposed on one edge of a metallic bar, initially at room temperature (293 K). Constant thermoelastic material properties where considered, leading to a transient linear numerical analysis. Reinforcement particles distribution is illustrated in figure 2b, in which cell-to-cell continuity and periodicity can be observed. The original/deformed geometry and an intermedi-

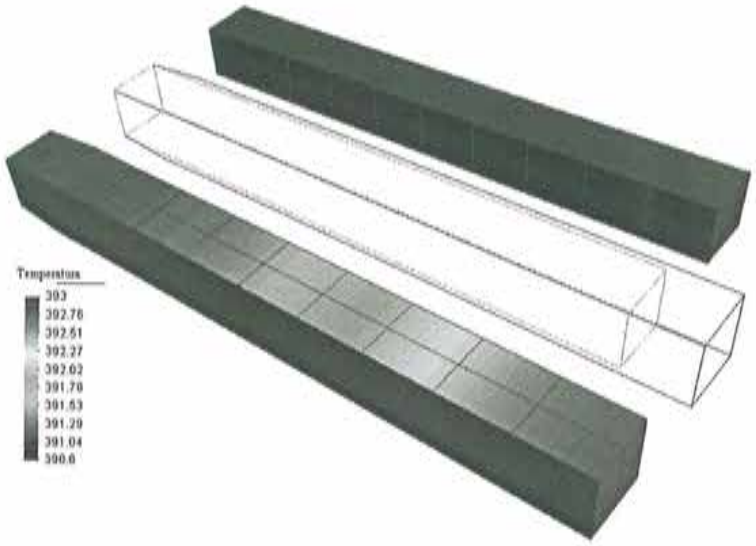

Figure 1: Macroscale mesh, original/deformed geometry and intermediate temperature field

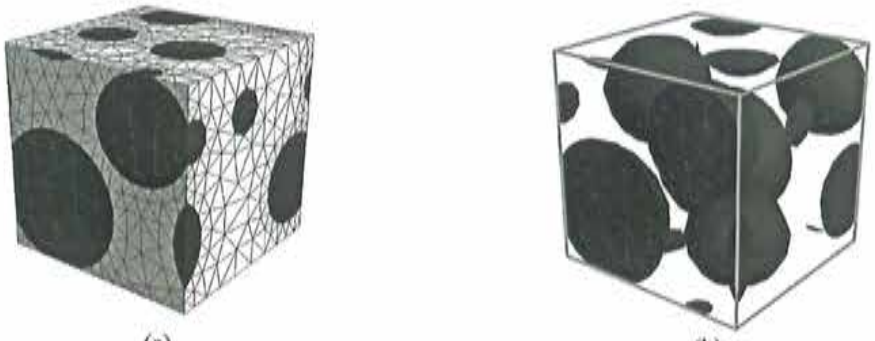

(a) (b)

Figure 2: (a) Microscale mesh and (b) reinforcement particles distribution

ate temperature field are shown in figure 1. As it can be seen, the macroscale behaves like a homogenous material. This macroscale behaviour is defined on microscale eigendeformation information, which is generated by the AEH methodology. As an example, two of the six microscale unit-cell eigendeformation elasticity fields are shown in figure 3. The gradients of these fields are used to define the homogenised elastic coefficient values.

4 CONCLUDING REMARKS

An example of the application of GiD in the numerical simulation of two-scale homogenised linear thermoelastic behaviour of an $AlSiC_p$ MMC was presented. It can be stated that GiD's pre- and post-processor are highly useful tools for science and engineering applications, providing an efficient interface for the modelling of two-scale AEH thermomechanical problems.

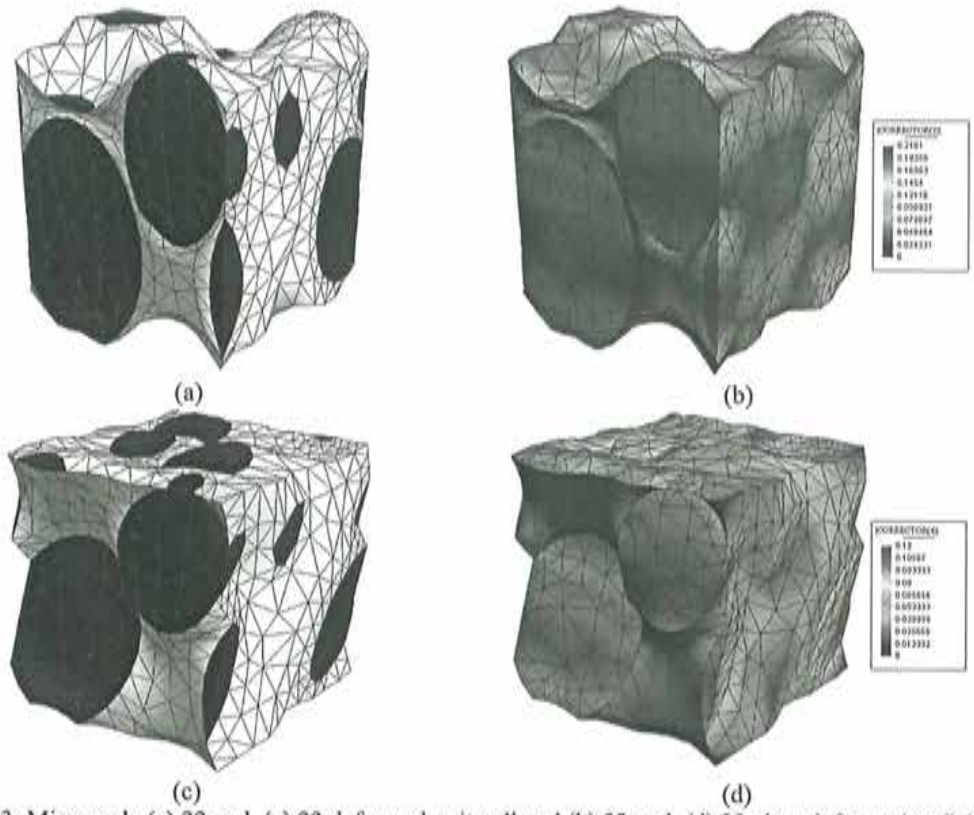

Figure 3: Microscale (a) 22 and (c) 23 deformed unit-cell and (b) 22 and (d) 23 eigendeformation fields

REFERENCES

[i] A. Bensoussan, J.-L. Lions and G. Papanicolaou, *Asymptotic analysis for periodic structures*, North-Holland, Amsterdam, Holland, (1978).

[ii] J.M. Guedes and N. Kikuchi, "Preprocessing and postprocessing for materials based on the homogenization method with adaptive finite element methods", *Computer Methods in Applied Mechanics and Engineering*, **83**, 143-198 (1990).

[iii] P.W. Chung, K.K. Tamma and R.R. Namburu, "Asymptotic expansion homogenization for heterogenous media: computational issues and applications", *Composites Part A*, **32**, 1291-1301 (2001).

[iv] P.W. Chung, K.K. Tamma and R.R. Namburu, *On the homogenization of temperature dependent thermal conductivity in composite materials*, AIAA-1999-878, 37th Aerospace Sciences Meeting and Exhibit, (1999).

[v] J.A. Oliveira, J. Pinho-da-Cruz, A. Andrade-Campos and F. Teixeira-Dias, *On the modelling of representative unit-cell geometries with GiD*, 2nd Conference on Advances and Applications of GiD, UPC, Barcelona, Spain, (2004).

[vi] A. Andrade-Campos, J. Pinho-da-Cruz, J.A. Oliveira and F. Teixeira-Dias, *Using GiD in the finite element analysis of thermomechanical coupled problems*, 2nd Conference on Advances and Applications of GiD, UPC, Barcelona, Spain, (2004).